

**TWO-LAYERED POLYPROPYLENE AND POLYETHYLENE PRODUCT
BY ONE-STEP ROTATIONAL MOLDING**



EKTINAI JANSRI

**A DISSERTATION SUBMITTED IN PARTIAL FULFILLMENT OF THE
REQUIREMENTS FOR THE DEGREE OF DOCTOR OF ENGINEERING
PROGRAM IN ENERGY AND MATERIALS ENGINEERING
(INTERNATIONAL PROGRAM)**

FACULTY OF ENGINEERING

RAJAMANGALA UNIVERSITY OF TECHNOLOGY THANYABURI

ACADEMIC YEAR 2017

**COPYRIGHT OF RAJAMANGALA UNIVERSITY
OF TECHNOLOGY THANYABURI**

**TWO-LAYERED POLYPROPYLENE AND POLYETHYLENE PRODUCT
BY ONE-STEP ROTATIONAL MOLDING**



EKTINAI JANSRI

**A DISSERTATION SUBMITTED IN PARTIAL FULFILLMENT OF THE
REQUIREMENTS FOR THE DEGREE OF DOCTOR OF ENGINEERING
PROGRAM IN ENERGY AND MATERIALS ENGINEERING
(INTERNATIONAL PROGRAM)**

FACULTY OF ENGINEERING

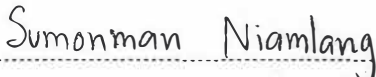
RAJAMANGALA UNIVERSITY OF TECHNOLOGY THANYABURI


ACADEMIC YEAR 2017


**COPYRIGHT OF RAJAMANGALA UNIVERSITY
OF TECHNOLOGY THANYABURI**


Dissertation Title Two-Layered Polypropylene and Polyethylene Product
by One-Step Rotational Molding
Name-Surname Mr. Ektinai Jansri
Program Energy and Materials Engineering
Dissertation Advisor Mr. Narongchai O-charoen, Ph.D.
Academic Year 2017

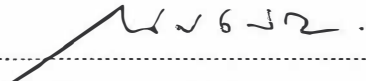
DISSERTATION COMMITTEE


..... Chairman
(Miss Sumonman Niamlang, Ph.D.)



..... Committee
(Professor Hamada Hiroyuki, D.Eng.)


..... Committee
(Mr. Anin memon, Ph.D.)


..... Committee
(Mr. Natee Srisawat, Ph.D.)


..... Committee
(Mr. Narongchai O-Charoen, Ph.D.)

Approved by the Faculty of Engineering, Rajamangala University of
Technology Thanyaburi in Partial Fulfillment of the Requirement for the Degree of
Doctor of Engineering


..... Dean of Faculty of Engineering
(Assistant Professor Sivakorn Anghong, Ph.D.)

May 18, 2018

Dissertation Title	Two-Layered Polypropylene and Polyethylene Product by One-Step Rotational Molding
Name-Surname	Mr. Ektinai Jansri
Program	Energy and Materials Engineering
Dissertation Advisor	Mr. Narongchai O-Charoen, Ph.D.
Academic Year	2017

ABSTRACT

A two-layered product can be molded through various processes. Rotational molding is a useful process used to produce a two-layered thermoplastic product. However, the rotational molding requires a complicated technique as well as special and expensive equipment. The particle size and size distribution of plastic are one of the process criteria. In this research we studied the possibility of using the one-step rotational molding technique to produce a two-layered molding of polypropylene (PP) and polyethylene (PE) by focusing on the effects of different particle shapes, sizes of PP and the rotational speed.

The axial powder flow apparatus was used for molding study. The particle sizes of PP were determined as equal as, 2 and 4 times as large than those of PE. PP particles were determined to be a spherical and non-spherical shape, and the rotational speed was compared for 7 and 60 rpm. The two materials were mixed in a ratio of 50:50 (wt%) by a dry blending method. The phenomenon happening during the molding was observed and recorded in real time by a high-resolution camera. After molding, the specimens were investigated in terms of their layer separation, thermal property, surface quality, thickness distribution and mechanical property.

The results of the experiment indicated that the two-layered molding of PP and PE using an uncomplicated technique for rotational molding had a high probability of success. Particularly, in the case of PP with a spherical shape, it was 4 times as large as that of PE at the rotational speed of 7 rpm. It was also found that an increase in rotational speed resulted in a more chance of two-layered separation.

Keywords: two-layered, polypropylene, polyethylene, rotational molding, one-step process

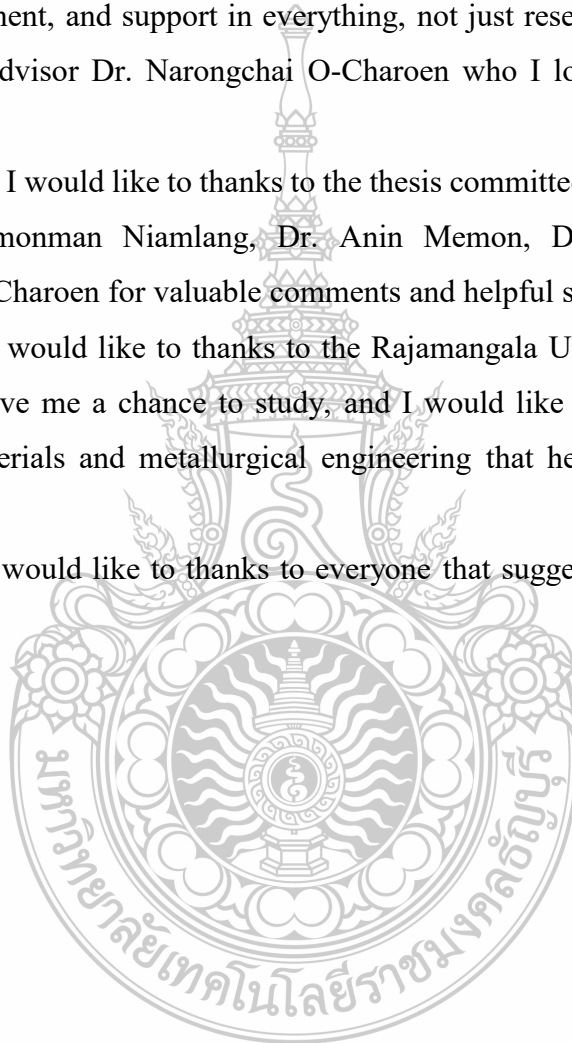
Acknowledgements

This thesis will not be successful without the support of these important individuals. So, firstly, I would like to thank my dad and mom for giving me life, encouragement and everything support. And thanks to the brother who passed away that is an inspiration for doing things to accomplish. And indispensable, I am grateful for the advice, encouragement, and support in everything, not just research, but also the social life of my thesis advisor Dr. Narongchai O-Charoen who I love and respect like my family.

Secondly, I would like to thanks to the thesis committees, Professor HAMADA Hiroyuki, Dr. Sumonman Niamlang, Dr. Anin Memon, Dr. Natee Srisawat and Dr. Narongchai O-Charoen for valuable comments and helpful suggestions.

Thirdly, I would like to thanks to the Rajamangala University of Technology Thanyaburi that gave me a chance to study, and I would like to thank all staff of the department of materials and metallurgical engineering that helped and supported me everything.

Finally, I would like to thanks to everyone that suggested and encouraged all the time.



Ektinai Jansri

Table of Contents

	Page
Abstract.....	(3)
Acknowledgements.....	(4)
Table of Contents.....	(5)
List of Tables.....	(7)
List of Figures.....	(8)
CHAPTER 1 INTRODUCTION	
1.1 Background and Statement of the Problems.....	13
1.2 Purpose of the Study.....	14
1.3 Scope of the Study.....	14
1.4 Contribution to Knowledge.....	15
1.5 Thesis Outline.....	15
CHAPTER 2 BACKGROUNDS AND THORETICAL	
2.1 Rotational Molding Process.....	17
2.2 Types of Rotational Machine.....	24
2.3 The Multi-Layer in Rotational Molding Process.....	27
2.4 Powder Properties.....	30
2.5 Polyethylene and Polypropylene.....	37
CHAPTER 3 RESEARCH METHODOLOGY	
3.1 Materials.....	41
3.2 Generation and Characterization of PP and PE Powders.....	41
3.3 Rheological Characterization.....	44
3.4 The Axial Powder Flow Apparatus.....	48
3.5 Mechanical and Morphology Properties.....	53
CHAPTER 4 RESULTS AND DISCUSSION	
4.1 The Effect of Particles Size of Polypropylene on Two-Layered Process.....	64
4.2 The Effect of Particles Shape of Polypropylene on Two-Layered Process.....	82

Table of Contents (Continued)

	Page
4.3 The Effect of Rotational Speed on Two-Layered Process.....	98
CHAPTER 5 CONCLUSIONS AND RECOMMENDATION	111
List of Bibliography.....	115
Appendices (List of Publications).....	121
Biography.....	123



List of Tables

	Page
Table 3.1	Flow characteristic 45
Table 3.2	The Axial powder flow apparatus technical data 52
Table 4.1	Powder properties of a pure and mixed polymer (different the size of PP)..... 67
Table 4.2	The arithmetic mean of surface roughness of a mixed polymer (different the size of PP)..... 78
Table 4.3	The initial modulus of pure and mixed polymer (different the size of PP)..... 80
Table 4.4	Powder properties of a pure and mixed polymer (different the shape of PP).. 84
Table 4.5	Arithmetic mean of surface roughness of a pure and mixed polymer (different the shape of PP)..... 95
Table 4.6	The initial modulus of a mixed polymer (different the shape of PP)..... 97
Table 4.7	Powder properties of a pure and mixed polymer..... 99
Table 4.8	Arithmetic mean of surface roughness of specimen at rotation speed 60 rpm... 107
Table 4.9	The initial modulus at rotation speed 7 and 60 rpm..... 110
Table 5.1	Processing window..... 114



List of Figures

	Page
Figure 2.1	Rotational molding products..... 17
Figure 2.2	Principle of rotational molding..... 18
Figure 2.3	The processing of rock and roll machine..... 19
Figure 2.4	Oven heating..... 20
Figure 2.5	Oil heating system..... 21
Figure 2.6	Recommended speed ratios for various mold shapes..... 21
Figure 2.7	The temperature profile..... 22
Figure 2.8	Batch type machine..... 24
Figure 2.9	Fixed-arm type machine..... 25
Figure 2.10	Independent arm type machine..... 26
Figure 2.11	Straight line machine..... 27
Figure 2.12	Drop-box equipment and multi-layer products..... 30
Figure 2.13	Classification of particle shape..... 32
Figure 2.14	Relation of dry flow rate with bulk density flow..... 33
Figure 2.15	Three types of powder bed..... 34
Figure 2.16	Schematic of particle sintering..... 37
Figure 2.17	PE chemical formulas..... 38
Figure 2.18	LDPE branch structure..... 38
Figure 2.19	LLDPE branch structure..... 39
Figure 2.20	HDPE branch structure..... 39
Figure 2.21	PP chemical formulas..... 40
Figure 3.1	Pulverize (hammer mill) machine..... 42
Figure 3.2	Grinder (blade mill) machine..... 43
Figure 3.3	The differential scanning calorimetry (DSC)..... 44
Figure 3.4	Bulk density apparatus..... 45
Figure 3.5	Melt flow indexers..... 46

List of Figures (Continued)

		Page
Figure 3.6	Schematic sintering sequence for two particles, where a , a_0 , a_f and y are the particle radius, initial particle radius, final particle radius, and neck radius.....	47
Figure 3.7	The sintering tester; where A is the processing system consists of a computer and image analysis program. B is temperature measurement and recording instrument. C is a heater plate, adjusts six level of heating. D is digital microscope, maximum zooms in 600X.....	47
Figure 3.8	The axial powder flow apparatus.....	48
Figure 3.9	The high-temperature resistant glass.....	49
Figure 3.10	The mold and heating system.....	49
Figure 3.11	A slip ring component.....	50
Figure 3.12	Cooling system.....	51
Figure 3.13	A VDO captured system.....	51
Figure 3.14	Temperature profile at freezing and boiling point; T1 = connecting cable signal passes to slip ring, T2 = connecting cable signal not passes slip ring.....	53
Figure 3.15	The digital microscope.....	54
Figure 3.16	Image analysis step 1.....	55
Figure 3.17	Image analysis step 2.....	56
Figure 3.18	Image analysis step 3.....	56
Figure 3.19	Image analysis step 4.....	57
Figure 3.20	Image analysis step 5.....	58
Figure 3.21	Image analysis step 6.....	58
Figure 3.22	Image analysis step 7.....	59
Figure 3.23	Image analysis step 8.....	59
Figure 3.24	Image analysis step 9.....	60

List of Figures (Continued)

	Page
Figure 3.25	Image analysis step 10..... 60
Figure 3.26	Surface roughness analysis step 1..... 62
Figure 3.27	Surface roughness analysis step 2..... 63
Figure 3.28	Surface roughness analysis step 3..... 63
Figure 4.1	The particle shape and size of LLDPE, PP-L, PP-M, and PP-S..... 68
Figure 4.2	Schematic of the neck growth ratio (particles sintering)..... 69
Figure 4.3	The sintering rate of LLDPE, PP-L, PP-M, and PP-S..... 69
Figure 4.4	Internal air temperature of (A) pure polymer, (B) mixed polymer and (C) amount of powder charged to the mold..... 71
Figure 4.5	The distribution of PP particles at free surface area; A is PP-L/LLDPE, B is PP-M/LLDPE and C is PP-S/LLDPE; where white colors are LLDPE particles..... 73
Figure 4.6	Schematic of the melting deposition of PP/LLDPE at the different PP particle size..... 74
Figure 4.7	Separation phase in specimens; A= PP-L/LLDPE, B = PP-M/LLDPE and PP-S/LLDPE..... 75
Figure 4.8	DSC specimen preparation in (A) and (B) melt transition temperature (T_m) thermograms..... 76
Figure 4.9	Surface roughness; the left hand is an inner surface and the right hand is an outer surface..... 78
Figure 4.10	The specimen preparation is A and the standard deviations of thickness is B.....81
Figure 4.11	The stress-strain curve of pure and mixed polymer (different the size of PP)..... 82
Figure 4.12	The particle characteristics of LLDPE, PPC, and PPH..... 85
Figure 4.13	Sintering rate of LLDPE, PPC, and PPH..... 87
Figure 4.14	Internal air temperature of (A) pure polymer and (B) mixed polymer (different the shape of PP)..... 88

List of Figures (Continued)

		Page
Figure 4.15	Characteristics of powder formation in radial segregation: (A) particle segregation diagram; particles segregation patterns of (B) PPC/LLDPE and (C) PPH/LLDPE; (D) and (E) are the percolation of particles during avalanche of PPC/LLDPE and PPH/LLDPE respectively; where gray color indicates PPC and PPH, and black color indicates LLDPE.....	90
Figure 4.16	Separation phase in (A) PPC/LLDPE and (B) PPH/LLDPE specimens; the surface of specimens: (C, D) outer surface, (E, F) inner surface, and (G, H) appearance of defects on the inner surface of PPC/LLDPE and PPH/LLDPE, respectively.....	92
Figure 4.17	DSC thermograms of a pure and mixed polymer (different the shape of PP).....	94
Figure 4.18	The standard deviation of thickness of pure and mixed polymer	96
Figure 4.19	Stress-strain curves and initial modulus of a pure and mixed polymer (different the shape of PP).....	97
Figure 4.20	The particle characteristics of LLDPE, PPH-M, PPH-L, and PPC-L.....	100
Figure 4.21	The sintering rate of PPH-M, PPH-L, and PPC-L.....	101
Figure 4.22	Internal air temperature of the mixed polymer at rotational speed 60 rpm.....	102
Figure 4.23	Internal air temperature of the mixed polymer at rotational speed 7 and 60 rpm. . .	102
Figure 4.24	The flow characteristic; A is PP-L/LLDPE, B is PP-M /LLDPE and C is PP-S/LLDPE; where the white color is LLDPE particles.....	103
Figure 4.25	The distribution of PP particles at free surface area; A is PP-L/LLDPE, B is PP-M /LLDPE and C is PP-S/LLDPE; where the white color is LLDPE particles.....	104
Figure 4.26	Separation phase in specimens of PPH-M/LLDPE, PPH-L/LLDPE and PCC-L/LLDPE.....	105
Figure 4.27	The DSC thermograms of a mixed polymer at rotational speed 60 rpm.....	106

List of Figures (Continued)

	Page
Figure 4.28	Surface roughness with different rotational speed..... 107
Figure 4.29	The standard deviation of thickness at rotational speed 7 and 60 rpm..... 108
Figure 4.30	The stress-strain curve of the mixed polymer at rotational speed 60 rpm..... 110
Figure 4.31	The stress-strain curve with different rotational speed..... 110



CHAPTER 1

INTRODUCTION

1.1 Background and Statement of the Problems

Rotational molding or roto-molding is one of the plastic processing for producing big and hollow parts with not complicated of geometry, such as a water tank, septic tank, small boat, canoe, kayak, ice boxes, automotive parts and so on [1]. The advantages of this process have a variety, e.g., the product has a balanced or symmetry and has a stress-free, and the machine is inexpensive and easy to make multi-layer products. However, an important problem affects the processing and quality of the products, which is the limit of the choice of materials [2]. Normally, more than 90% of rotational molding products are made from polyethylene, especially linear low-density polyethylene (LLDPE) in a fine particle form [3] due to it suitable rheological characteristics, as well as it has an easy sintering and coalescence procedure under zero shear conditions [4]. However, although LLDPE has several remarkable properties, it also has major disadvantages that remain significant challenges for the researchers to conquer such as the limit of using in high-temperature conditions or the development of a stiffness etc.

There are many researchers who study on the development of LLDPE properties by using materials with higher stiff, and can use in high temperature, which is polypropylene (PP), it is widely used in the world owing to its variety of molding capabilities and many desirable properties such as a high impact resistance, heat resistance, stiffness, scratch resistance, excellent chemical resistance, and environment stress-cracking resistance, and also PP is a polymer in the polyolefin family similar to polyethylene.

However, in the rotational molding process, there are a few of the researchers that focus on the polymer blends between PP and PE because it was quite difficult to achieve and the results have not been satisfactory. Most of the experiments have used a melt blending method for mixing prior to the molding. The results show that the materials can be molded, but their mechanical properties decrease with increasing PE content. Moreover, a large number of bubbles appear

in the specimens [5, 6]. These reports demonstrate the incompatibility of PP and PE, which this made the idea of improving the properties of a polymer blend between PP and PE by using different methods. One way that expected to help improve the properties of the product is using a multi-layer molding method.

For the multi-layered molding method in the rotational molding can be done by a sorting of the materials were added to the mold. There are many methods typically used for adding or sorting materials into a mold, such as the use of special equipment, called drop boxes, thermoplastic bags containing secondary materials, or even opening the mold during the heating step to add such secondary materials into the mold [7–9]. The above method operates on a simple principle but requires expensive equipment, as well as a place in the mold for installation. In addition, some additional steps may be needed, which increases the production time. However, there is another simpler and uncomplicated method that does not require special equipment, and only requires considering the basic properties of the material, such as the melting point, flow characteristics, size, and shape of the particles [10–12].

Thus, the main aim of this research is to examine the possibility of using two-layered PP/PE in the rotational molding process using such an uncomplicated technique. The phenomenon that happens during molding from the effects of the rotation speed, the particles size and shape of PP on the PP/PE two-layered has been observed. Furthermore, the surface roughness, thermal properties and mechanical properties of the specimens are investigated.

1.2 Purpose of the Study

- 1.2.1 To study the effects of the particles size of PP on PP/LLDPE two-layered.
- 1.2.2 To study the effects of the particles shape of PP on PP/LLDPE two-layered.
- 1.2.3 To study the effect of the rotation speed on PP/ LLDPE two-layered

1.3 Scope of the Study

This research study on the possibility PP/PE two-layered in the rotational molding by using techniques uncomplicated. The effects of the particles shape and

size of PP on PP/PE two-layered was early considered as followed by the consideration of the effect of the rotation speed. The materials as uses were consists of LLDPE commercial grade and PP with various the particles size and shape, with the mixing ratio between PP/LLDPE fixed at ratio 50-50 using dry blend method, rotating speed 7 rpm. The specimen will be analyzed and compared properties, the powder properties, the morphology, thermal properties, the wall thickness distribution, surface quality and mechanical properties.

1.4 Contribution to Knowledge

The benefit should be gained from this research, could be molding the products as two-layered of PP/PE in a single process no need to use a special tool and no have to stop the process. It would help to understand the behavior of plastic powder and phenomena taking place within the mold, and also added the alternative to using the material in this process to more. The processing condition could be molding in the real industry. Finally, these could guide the development of new material and technique for molding multi-layered in the rotational molding process.

1.5 Thesis Outline

Since the objective of the thesis is to develop new techniques of producing multi-layered in rotational molding. The research was focused on the parameter with affecting the possibility of PP/PE in the rotational molding such as the deference of particles shape and size of PP, and rotation speed. Comparative analysis of the experimental results and conclusions are presented in the thesis.

Chapter 2, provides the theoretical background of related subjects including the rotational molding process, powder properties, and the fundamental of PP and PE in rotational molding.

Chapter 3, the details consist of the analysis of polymer materials, Generation and Characterization of PP and PE Powders, description of the axial powder flow apparatus and methods for observing and testing.

Chapter 4, the results of experiments and the phenomenon occurring from the effect the particles shape and size of PP, and including the effect of the rotation speed on PP/PE two-layered are exposed and explained.

Chapter 5, the conclusion, the recommendations, and the future work were exposed in this chapter.



CHAPTER 2

BACKGROUNDS AND THORETICAL

2.1 Rotational Molding Process

Rotational molding, also called rotomolding or rotational casting, is a thermoplastic processing method for producing big size products with shaped hollow for example boats, kayaks, ice boxes, canoes, truck defender, storage tanks, golf car, septic tanks etc. The rotational molding has many types of machines such as clamshell machine, rock-and-roll machines, turret machine, shuttle machine, swing machine, vertical wheel machines and open-flame machine etc. In selecting the type of rotational molding machine depend on product features, installation space and the value of the investment. Although the rotational molding machines have many types, the principle of molding no different, the process of molding are consists of 4 basic steps loading, heating, cooling and de-molding as shown in Figure 2.1 rotational molding products.



Figure 2.1 Rotational molding products.

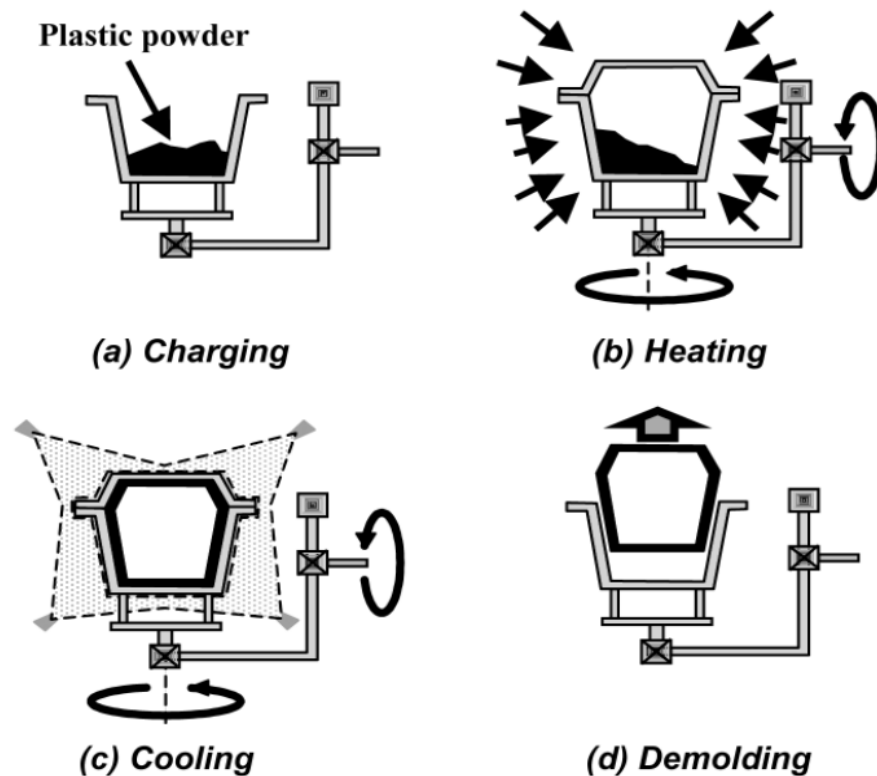


Figure 2.2 Principle of rotational molding [2].

Stage 1 – The mold charging or loading step

In the first step of the process, materials powders were loaded into the mold. The mold parts are locked by clamps or bolts, and the mold part mounted in the rotational machine ready for the molding stage. The vent hole must check to make sure that air can enter or escape the mold during operation. The amount of powder used determines the wall thickness of the molded part. Loading the mold with too much powder results in unnecessarily thick walls, and the cycle will have to be extended to make sure complete melt. Too little powder leads to localized thin areas in the molding wall, with the risk of subsequent product failure. The rotational molding process can achieve easily for parts with wall thickness starting from 1.5 up to 25 mm.

Stage 2 – Mold heating cycle

The mold was mounted on the machine axis and rotated two directions in an oven heated. There are three main ways to heat a mold in a production process:

(A) Direct flame heating

It is found in the system to heat the mold in the rock and roll machine type as shown in Figure 2.3, the flame has been used directly to the mold. The heat is fast transferred to the mold until the plastic inside the mold melting. It is a great way to heat a large mold, save on the price of a machine building, but it also has the disadvantage that is some heat loss to the environment around machine area causes loss of energy and fuel consumption.

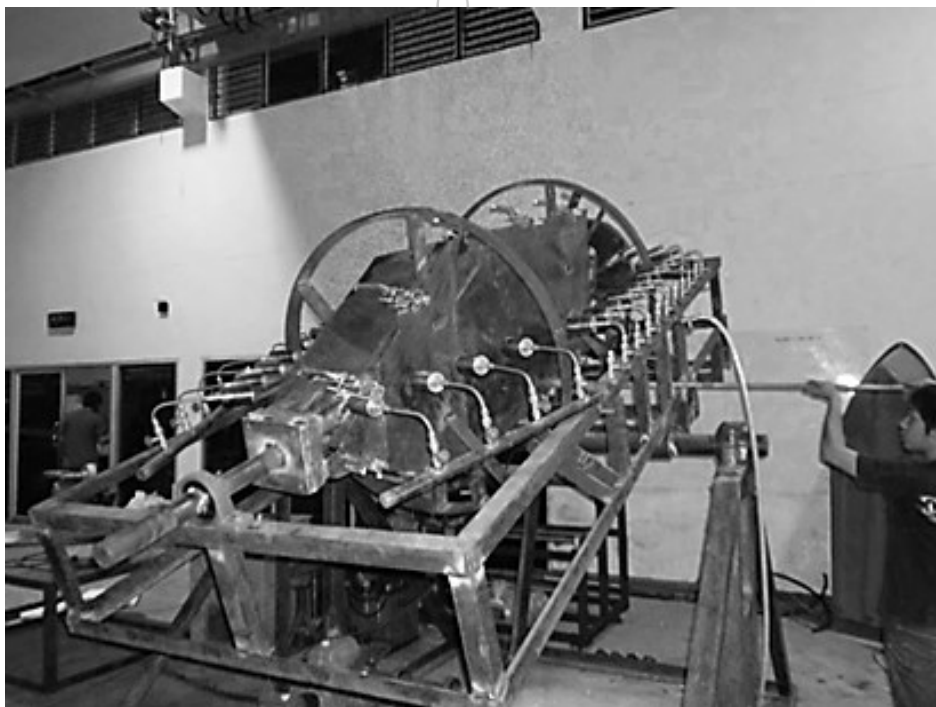


Figure 2.3 The processing of rock and roll machine.

(B) Oven heating

This method provides heat to the molds inside the oven as shown in Figure 2.4, which can control the temperature and heat dissipation in the oven easier. In addition, the heat generated in the system comes from a variety of energy sources such as gas, oil or even from electricity etc. This method of heating has little heat loss and is easy to operate and control the processing, but requires a lot of space to install an oven, and requires the electronic control system to control the temperature, which results in high costs.

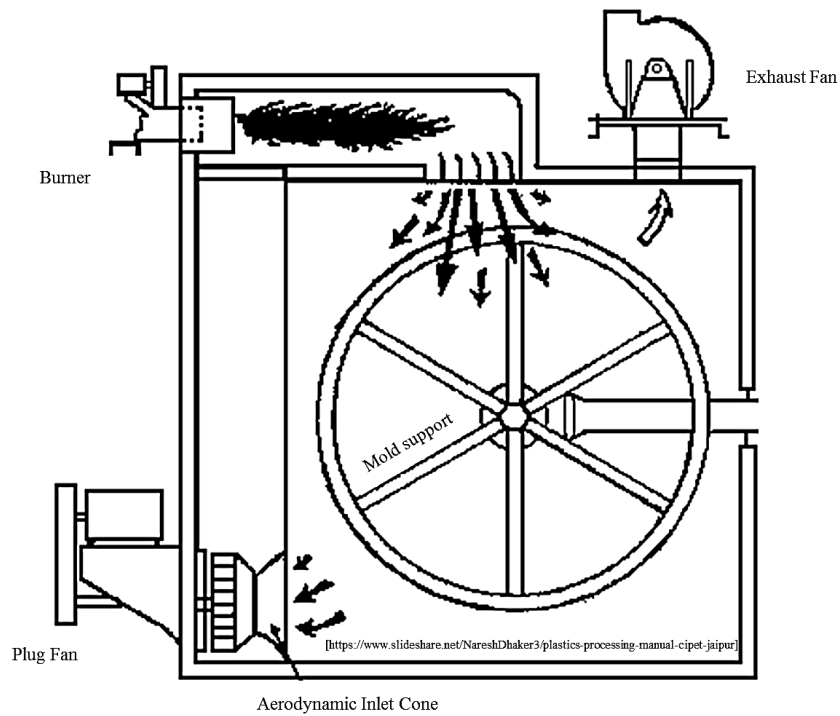


Figure 2.4 Oven heating.

(c) Circulation oil heating

This method is a method of heating the best, which is providing the heat to the mold directly (as shown in Figure 2.5), and it has higher performance than previous two methods. The advantage of this method is not losing heat to the external environment, the principle is used circulation of hot oil for heating to direct on the outer surface of the mold, which makes transferring of the heat occurs quickly. Thus, this method is using a lower molding temperature than other methods, but it also has the disadvantage, the mold quite complex, difficult to design and only use for a specific or special product causes the mold is very expensive.

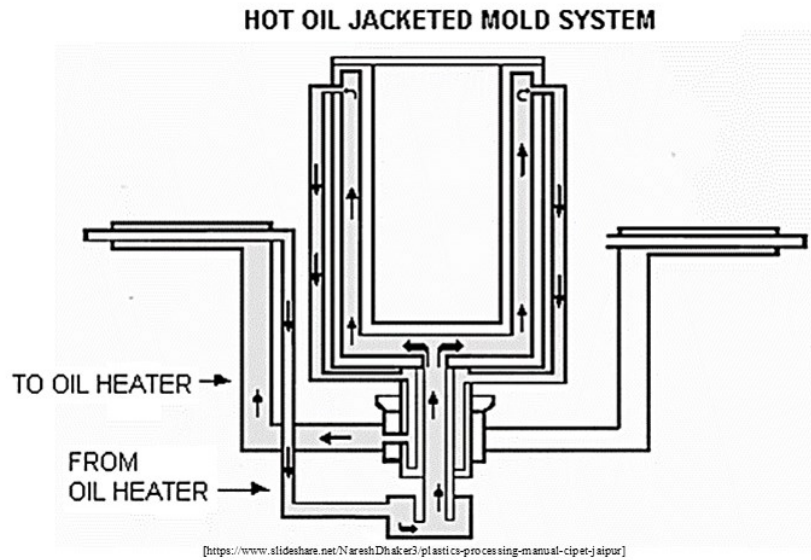


Figure 2.5 Oil heating system.

The speeds of rotation are slow approximately 5 to 20 rounds per minute. Figure 2.6 shows typical values of speed ratios. It should be noted that the speed of rotation in a biaxial rotation machine, the speeds ratio in the two axes have a major influence on the thickness distribution of the plastic on the mold and in addition, the temperature inside the mold was very important in processing control.

Speed Ratio	Shapes
8:1	Oblongs, straight tubes (mounted horizontally)
5:1	Ducts
4:1	Cubes, balls, rectangular boxes, most regular 3-D shapes
2:1	Rings, tires, mannequins, flat shapes
1:2	Parts that show thinning when run at 2:1
1:3	Flat rectangles, suitcase shapes
1:4	Curved ducts, pipe angles, parts that show thinning at 4:1
1:5	Vertically mounted cylinders

Figure 2.6 Recommended speed ratios for various mold shapes.

The temperature profile in Figure 2.7, at point A, the heat through the mold wall, the tumbling powder particles started to melts. The temperature at which

powder particle start to melt and stick with mold surfaces and the neighbor particle is called the tack temperature, the heating rate rise slowly until point B. At point B, the graph shows that there is abruptly changed called the kink temperature, it means that the final particles stick together completely. Which this period the phenomena of coalescence and densification are proceeding. This can be seen from point B to C take longer time due to the thick layer of polymer increases became too insulator, causing the heat transfer is difficult. When the temperature air inside the mold is close to the temperature setpoint C, the heating rate is decreased because the mold is cooled [2].

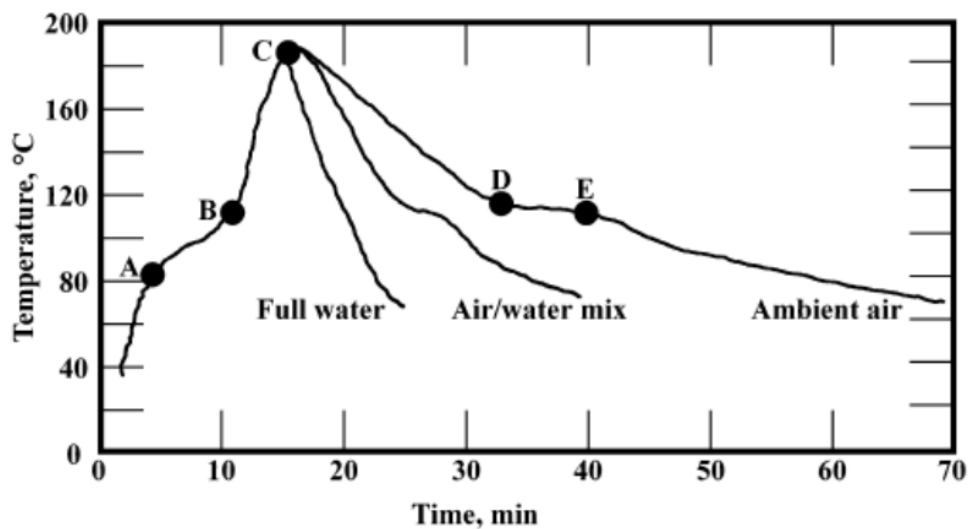


Figure 2.7 The temperature profile [2].

Stage 3 – Cooling

While the mold was cooled, the temperature of polymer that coated at the mold surface decrease rapidly than the polymer inside layer. At D point is abruptly a change of temperature again. That shows crystallization is occurring. When the temperature decreasing to point of temperature glass transition, Point E, That means the specimen will change (shrinkage) very little, the chain molecules arranged quite successfully. It should be noted that in a cooling station if the mold gets air or water not thoroughly all area in the mold, the products will distort.

Stage 4 – De-moulding

In this station, the rotation is stopped, the mold is opened and the finished molding removed. Removal is difficult or easy depending on the shrinkage of the polymer including the shape and complexity of the mold.

The advantages and disadvantages of rotational molding

The advantages

1. The mold is a simple geometry and inexpensive because the rotational molding is a low-pressure process, the mold is not required to be high strength and can be produced within 2-3 weeks.
2. The molds of different sizes and shapes can be molded simultaneously in the production process, and also can molding the product with a multi-layered wall.
3. The waste generated by the production process is minimal.
4. The products have a uniform thickness throughout the plane as well as blow molding or thermoforming process.
5. The product has no internal stress (Free stress) is equally strong because of no piece of welding or no weld line.

The disadvantage

1. Raw material prices are high because they must be in powder form.
2. Not suitable for producing high-resolution products such as edges or corners too large.
3. The raw materials used in the rotational molding are still limited, most of which are used by the polymers of the PE family.
4. Wasting human labor, due to the instep of material loading to the mold and removing the product from the mold, as well as heating the mold in some cases, have still to use the human for the operated.
5. Take a long time for molding make a low of production per day.

2.2 Types of Rotational Machine

2.2.1 Rotational molding batch type machine

Batch type is the cheapest because they are the least complicated, but they require a lot of labor to produce. The mold rotates inside the oven until the heating time is reached, it will be removed from the oven and the new mold will be replaced. The molds that exit the oven will be moved to the cooling station then the sample is removed from the mold.



Figure 2.8 Batch type machine [1].

2.2.2 Rotational molding fixed-arm type machine

This type was invented in the late 50's until the 60's, there is smallest swing diameter 40-inch to 150 inches. It is one of most very popular machines type due to effective higher production and convenient to maintenance. The machine has many different types such as three arms, four arms etc. It may also be different in the placement of the number of stations. In the case of 3 arms, individual arms are attached to the turret in the middle, with each arm having a 120-degree angle with each arm moving at the same time. The movement of the arms tend to have problems such as time of heating and cooling are not equal, It can be solved with four arms type by add one station may be part

of a heating or cooling as appropriate by each arm has angles 90 degrees. For the case of vinyl-plastisol should be used with four arms type with two ovens station due to the need to gradually increase temperature appropriately. For inside the mold, it may contain inert gas to reduce the pressure, prevent shrinkage of a sample, or add nitrogen to remove the oxygen from the mold to prevent oxidation, which effect on the rheology of a polymer. And remember that the rotation reverse of the mold inside the oven can help the polymer flow well within the mold in the case of very complicated parts.



Figure 2.9 Fixed-arm type machine [1].

2.2.3 Rotational molding independent arm type machine

Not so long ago, the rotational molding independent-arm machines type was developed to improve the performance to meets the needs of users. Typically, the machine consists of 5 stations, which may have 2, 3, 4 arms. The important point is that it has fewer arms than the station, meaning that there is an empty station available as a supplementary station that improves productivity. The operator can determine whether it will be a backup station for heating or cooling. The configuration independent-arm machines type shown in Figure 2. 10, it is a four-arm machine with the backup cooling station. Although it is a machine with high performance and productivity, it is very expensive compared to other types of machines mentioned above. On the other hand, in the industrial sector or in the investor sector, it is expected to be a very popular and cost-

effective alternative due to its high production rate and easy quality of product control, and also easy operation of the operator.



Figure 2.10 Independent arm type machine [1].

2.2.4 Rotational molding shuttle type machine

It was developed for installation in limited spaces, the designs have a various type, one of which is easiest to mount the mold with the carriage on the rails, where the end of the rails ends at the oven station. When the heating process is completed, the mold will move out of the oven station then go to the cooling station. In other cases, the oven station is in the middle position between carriage A and B, which are the stations loading/cooling. When the heating process was completed, the carriage A was moved out of the oven station to cooling station, while the carriage B was moving into the oven station for heating.



Figure 2.11 Straight line machine [1].

2.2.5 Rotational molding rock and roll type machine

Most of this type is the open flame method no need the oven as shown in Figure 2.3, it is a relatively low-cost machine suitable for large or long products such as canoe, water tanks, and electric posts etc. the mold is rotated parallel to the ground and tilted up and down at the same time, which the rotating rate will always faster than tilting. Another interesting rock and roll machine called the Rocking oven machine, it still has a very similar working principle; the mold is rotated in the oven, which reduces the amount of loss thermal energy of the production. the rock and roll machine type has the advantage of low cost for large product scale production, but it has some disadvantage, the slow rate of production and it is quite tricky because the most of the process is not automatic also still rely on the labor for operation.

2.3 The Multi-Layer in the Rotational Molding Process

Presently, the multi-layer was used widely in many sections. The most products were found in a barrier film, electronics part and some part of automotive. The multilayer

process in rotational molding can be divided into 2 methods. The first method called one-step process or sometimes called one-shot forming. The general principle in the one-step process, the different kind of polymer were loaded into the mold in the same time, the first polymer with a lower melting point will be melted and coated with the mold wall become to skin layer or first layer. The second polymer with a higher melting point will be melted and coated on skin layer become core layer or second layer. However, it should be noted that for selecting the skin and core polymer should be considered from thermal, rheological, and physical characteristics. The second method called two-step process, the outer skin or first layer polymer was loaded and heating until as liquid state while normal rotational molding. Then the process stopped, the mold was opened for loading the second polymer, the mold was closed and reheated until the second polymer melting completely. In addition, there is another way that can be done without stopping the process using special equipment called drop-box.

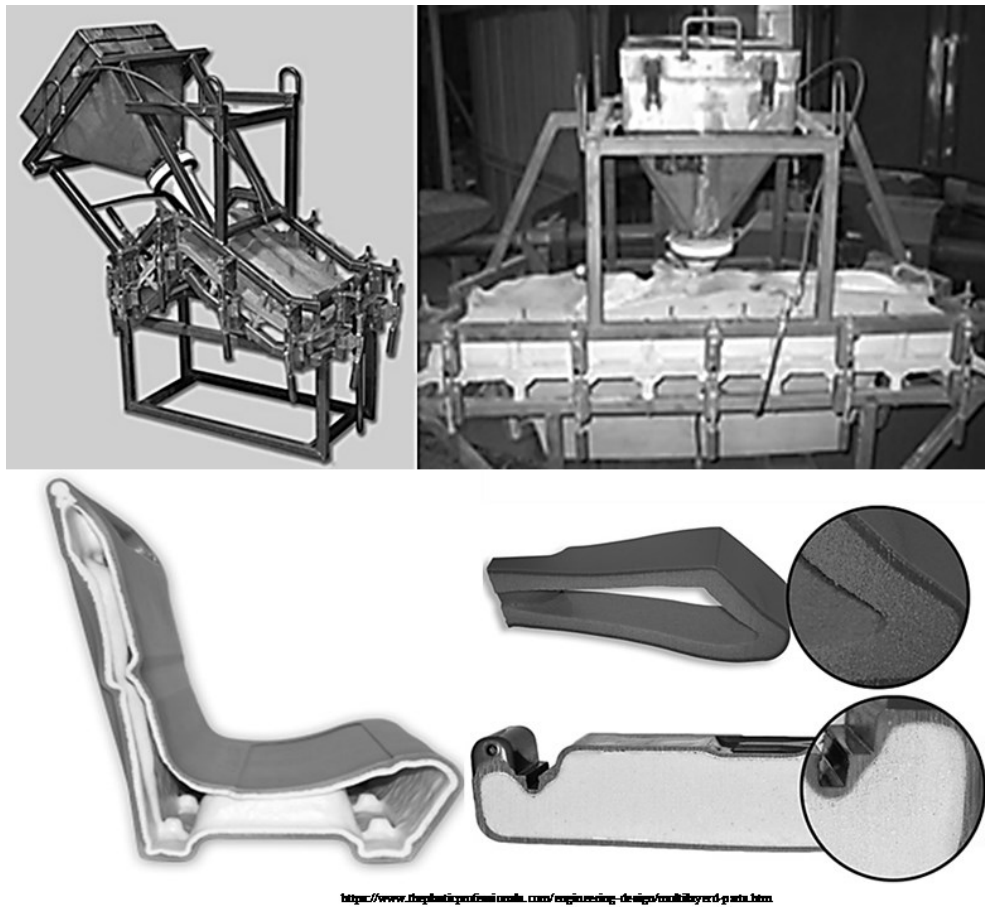
A drop-box is an insulated container that installations on the mold in a suitable position, which polymer or additives are packed within. Therefore, the polymer is separated into two parts in the mold and the drop box. The process starting when mold gets the heat, the first polymer starts to melt until completely. A drop-box will open and release the second polymer into the mold, the second polymer will be melted and coated with the first polymer that melted before. Finally of processing the last product obtaining is the multi-layer products. However, it should be noted that although this equipment is not complicated function, the cycle times are longer than typical process. Moreover, this equipment quite expensive and require the location for installing.

There are many researchers interested in the multi-layer process in rotational molding, especially the multiple-layer foam structures. According to Hoppe et al. [13] fabricated a rotational foam molding process, which takes knowledge of different material densities together with the centrifugal that occur during rotation of the mold. The polymer resin with the greatest density will be driven to the outer mold surface at high rotation speed cause creating the distinct skin layer. For the inner layer foam, should be the foamable material with a lesser density, to prevent affected from the centrifugal [14]. Rielly et al. [15] presented a rotational molding process of multi-layered thermoplastic products by using different melting points of materials to achieve distinct layers. It is

revealed that differences in melting temperature of at least 10 °F for each material are required to achieve to these layers. Therefore, the order of melting in each material will determine the sequence that happens the layer of the multi-layer products. For example, the foamable resin with the lowest melting point will adhere to the mold first creating the outer skin layer, while the foamable resin with a higher melting point will form a core layer. Hosoda et al. [16] and Lammers [17] they are of the opinion that in the same way, the powdered plastic should be melt first and adhere to the inner mold surface became to skin layer due to it has a larger contact surface area and the ability to move throughout the voids amongst the large particles and spread over a larger surface area, while the foamable pellets with a bigger size are still in the process of melting to form the core layer. In addition, they also describe that the range of difference in particle size required for this process should be from 3-10 times.

Similarly, Mori et al. [18] reported about possible to made distinct layers with rotational foam molding using various thermoplastic materials featuring different heat capacities, the result has shown that the material with a lower heat capacity (smaller particles) will melt and stick to the mold surface before another one with a higher heat capacity (larger particles) will be melted and creating a nearby layer. Slapnik [19] reveals the process for producing non-foamed thermoplastic skin foam core moldings. The foamed material is contained within the air-tight bag and made from thermoplastic, these are loaded into the mold. When the CBA within the foamable material is activated, the foam is expanding, causes the heat-softened thermoplastic bag to become the outer skin layer successfully encapsulating the foam.

In the rotational molding process, there are many factors that affecting to molded, the basic properties of materials such as the melting point, flow behaviors while the solid and liquid, particle size and shape etc. The importance of these variables will be examined in the following sections.



<https://www.theplasticprofessional.com/engineering-design/multilayered-parts.htm>

Figure 2.12 Drop-box equipment and multi-layer products.

2.4 Powder Properties

As well known, in the rotational molding process have to use a material with powder particles in order to obtain a complete product. The characteristics and properties of the powder particles used for molding were extremely important. This generally involves physical characteristics such as shape, size, and density. These variables will affect the production process and quality control, such as the movement and mechanism of particles in the mold, heat transfer or heat rate between particles to particles, the particles segregation in the mold as molding, surface quality, thickness distribution and including mechanical properties. The various parameters related to the powder properties are revealed in the following section, which seeks to identify the basic requirements of the rotational molding process [20-22].

2.4.1 Particle size

In the rotational molding process, the particle size is an important factor to control the quality of products. A smaller particle can be accepted molding better than a bigger particle in case of similar shape. The small particles have a larger surface area to volume ratio than larger particles, in solid state smaller particles have a void less than bigger particles. When get heated, small particles can easily to heat transfer between particles to particle faster than bigger particles. Cause the completely melting faster than at the same time, while bigger particles there are a lot of voids and melting or fusion more slowly. As a result, the cycle times are long, larger bubbles, and possibly poor inter-particle adhesion. Which is consistent with research Bellehumeur and Tiang (2002) [23], they found that particle size and packing density are most significant in determining the densification. The particle size decreased can reduce bubbles. They also found that reductions in cycle time could come at the expense of the densification process. It should be noted that the particle size distribution should have good packing of the big and small particles sizes, to reduce the gap between particles, which will reduce the porosity of the surface and the chance to trap air bubbles in the melt.

2.4.2 Particle shape

After grinding process, the shape of the plastic powder that received has a variety of forms ranging from spherical to acicular or fiber-like. There are many research reports on the effect of particle shape in the rotational molding process. According to [24], particle shape is acceptable and appropriate in the rotational molding, this shape has an ovoid side projection and a rectangular or square end projection called "squared egg". It has appropriate packing density and particle-particle contact, As a result, easier to start melting and sintering. However, should avoid spherical particles, because these are low packing density and connections between particles to particles. Acicular particles, fiber-like or have a tail. The particles shape have a tail should be avoided due to interrupt the connection between particle to particle, making the free volume of powders more, these will result in a melting process is slow, causing porosity and bridging in the products. The classification of particle shape can be achieved in several ways. The shape factor is one of the easiest ways, the ratio of the surface area of a sphere equal in volume to the particle to the surface area of the particle. The other ways are provided in the following Figure 2.13

Average Thickness	The average diameter between the upper and lower surfaces of a particle at its most stable position of rest.
Average Length	The average diameter of the longest chords measured along the upper surface of a particle in the position of rest.
Average Breadth	The average diameter at right angles to the diameter of average length along the upper surface of a particle in its position of rest.
Chunkiness	Reciprocal of elongational ratio.
Circularity	Ratio of circumference of a circle with the same projected area to the actual circumference of the projected area.
Elongational Ratio	The largest particle length to its largest breadth when the particle is in a position of rest.
External Compactness	The square of the diameter of equal area to that of the profile, divided by the square of the diameter of an embracing circle.
Feret's Diameter	The diameter between the tangents at right angles to the direction of scan, which touch the two extremities of the particle in its position of rest.
Martin's Diameter	The diameter which divides the particle profile into two equal areas measured in the direction of scan when the particle is in a position of rest.
Projected Area Diameter	The diameter of a sphere having the same projected area as the particle profile in the position of rest.
Roundness Factor	Ratio of the radius of the sharpest corner to the most round corner with the particle in a position of rest.
Specific Surface Diameter	The diameter of a sphere having the same ratio of external surface area to volume as the particle.
Surface Diameter	The diameter of a sphere having the same surface area as the particle.
Stokes Diameter	The diameter of a sphere having the same terminal velocity as the particle.
Volume Diameter	The diameter of a sphere having the same volume as the particle.

Figure 2.13 Classification of particle shape [2].

2.4.3 Bulk density

Bulk density was used to measure the effectiveness of the connection between particle to particle (packing fraction). It is important because it is a measure of a number of voids or size of the gap between the particles. Particles good quality (no tail) will have high bulk density. Bulk density is dependent upon particle shape, size, and size distribution. Typically, the bulk density is relating to powder flow or flowability, when an increase in bulk density, the flow rate increased, shown in Figure 2.14 [2].

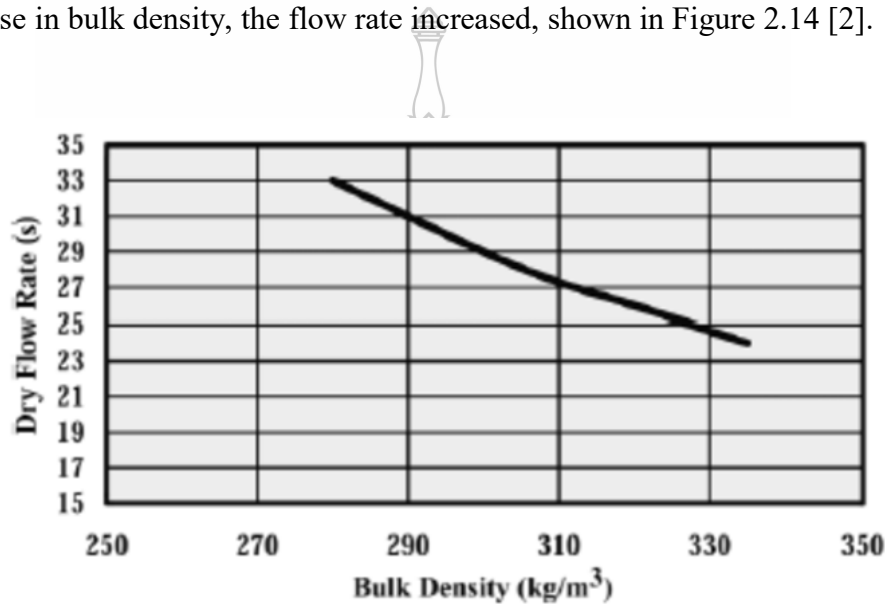


Figure 2.14 Relation of dry flow rate with bulk density flow.

The particle size distribution could influence the bulk density. When mixing very fine particles and coarse particles all together, the results will show in two opposing ways. The bulk density will decrease, if the weight ratio of fine particles beyond three times that of the coarse particles, due to fine particle separate the coarser particles apart. On the other hand, the bulk density will increase, if the fine particle filled in the interstices between the coarser particles.

2.4.4 Powder flow

In the rotational molding process, the dry flow properties are very important, because it is the simple way to determine the characteristic of the powder during molding and capabilities of powder to enter the molds with complex shapes. A particle with spherical shape is recognized for the best possible flow properties. Whereas the presence of tails in particles will reduce dry flow properties, leading to problems such as the bridging across narrow recesses

in the mold and high voids or bubbles content within the part wall. While a very fine particle and particle with large aspect ratio have a chance to be agglomerate and distribution poorly.

A characteristic of powder flow has been described by R.J. Crawford [2]. The flow behaviors of powders in the rotational molding process are classified into two form, Coulomb flow powders or viscous flow powders. For Coulomb flow powders, the particles remain in continuous contact with their neighbors in any situation. For viscous flow powder, contact forces are resisted by momentum transfer between particles that move relative to one another. Three types of bed motion have been observed (Figure 2.15). Steady-state circulation is observed when the mold surface is quite rough, the particle sizes are quite large, and powder volume is moderate when compared with the mold volume.

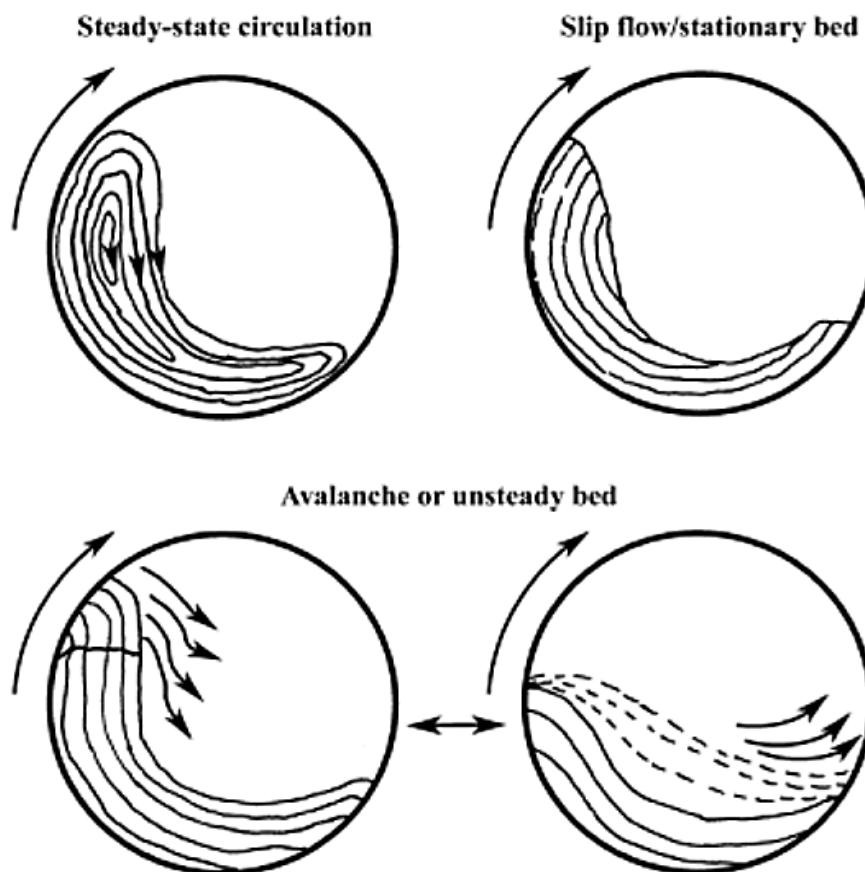


Figure 2.15 Three types of powder bed [2].

The powder is slightly tacky or is not free-flowing, and when the powder is acicular or two-dimensional, this characteristic caused the avalanche flow occurs. Since avalanche flow is not similar to a steady-state flow, it cannot be determined as either viscous flow or coulomb flow. Usually, the avalanche flow is mostly observed as the powder bed is depleted during the heating phase of the process.

Slip flow mostly occurs when the mold surface is very smooth and also another factor that causes slip flow such as powder particles very fine, big sphere particles and even too exceeds rotation speed.

There are many studies have been explained about behavior and characteristic of powder flow in the rotational molding process. Mellmann [25] and Henein [26, 27] they clearly explained about the different flow regimes while rotating speed increased. The influence of rotating speed, the level of filling, the coefficients of friction between particles and the mold surface. These parameters will affect directly to the behaviors of particles flow in the mold. The characterization of powder flow consists of slipping, slumping, rolling, cascading, cataracting and centrifuging will changing when the factors mentioned above are changes.

Huu Thuan Nguyen & Benoit Cosson [28], they studied on flow behavior during rotational molding by the experimental apparatus, which consists of a transparent thermoplastic cylinder filled, the cylinder has dimensions of 50 mm in length and 250 mm the inner diameter, the cylinder is rotating in a range of rotating speeds start from 2 to 105 rpm. This apparatus was used to observed the segregation of powder, bi-disperse (different in grain size) systems were used to analyze the behavior of segregation mechanisms of polymer powder. The Particles in bi-disperse systems are started by laying down them in layers in the mold. Which the particle sizes small 1,000 μm and large 2,500 μm . The initial bed is layered with a filling degree of 25 % at ratio 1:1 and rotating speed 20 rpm. The ratio of segregation is measured by calculating the ratio of the smaller particles over the total particle. The results have shown that when the time of rotating increased, the core layer is a small particle and large particles appear in the skin layer.

According to J. Olinek, C. Anand, C.T. Bellehumeur [12], they studied the flow and deposition of granular polymer particles in the rotational molding process. In this research, they selected three different materials form; LLDPE powder, LLDPE pellet and

olive stone. Three formed of particles were considered 1) powder size 100-mesh and powder size 40-mesh powder were mixed at 50% weight of each size fraction, 2) micropellets size 50-mesh and powder were mixed at 50% weight of each size fraction, and 3) olive stone particles size 60-mesh and powder size 60-mesh powder were mixed at 20% weight olive stone. These systems are selected to examine the effect of 1) particle size, 2) size and shape, and 3) density and shape differences in the segregation phenomena. The variables considered in this work were the load composition, heating rate, and mold rotational speed. The results showed that polymer powders are cohesive enough to prevent size segregation when mixed at room temperature. However, during molding, a new phenomenon of reverse cohesive segregation was observed. The final deposition patterns are controlled primarily by the initial segregation patterns, as well as by the heating rate and rotation speed, which affect the evolution of adhesive forces between particles during heating and melt deposition process.

2.4.5 Sintering

Polymer sintering has a major role in the rotational molding process. It affects the process and final products properties. The sintering incompletely will make high porosity and low mechanical properties of a specimen. The interface between the adhering surfaces, polymer-polymer or polymer-mold, the contact angle between two particles. These are called the sintering behavior. During sintering have a thermodynamic driving force for the particles to lower their surface energy by reducing their surface area. Surface tension is driving force the viscosity of the resin is the opposing factor. This can be explained through the relationship between the length of the neck growth between the two particles “ y ” divided by the radius of the particles “ a ” as shown in Figure 2.16. Thus, the sintering process is complete when the result of y/a approaches 1. The time for the completion coalescence can determine or controls a majority of the heating time in the molding cycle.

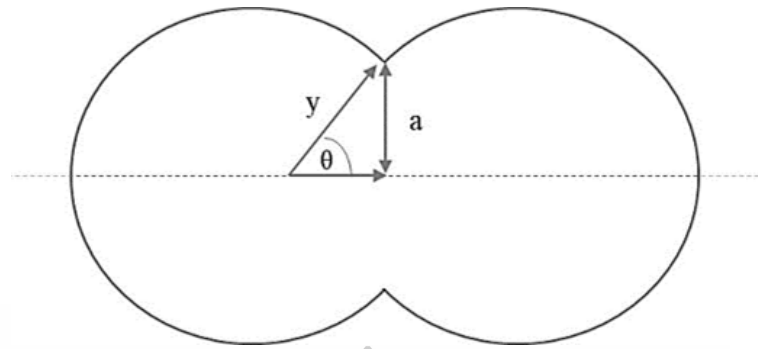


Figure 2.16 Schematic of particle sintering.

Another important factor in affecting the sintering is viscosity. The viscosity is one of the factors that play a role in the rheological properties. Because it means the resistance to polymer flow as melting. From many experiments confirmed that viscous flow is a major factor in sintering, the viscosity increasing made difficult to mobility in the molecules, causing of sinter rate decreased. But this effect is reduced by the size of the resin. However, it should be noted that the both of sintering process and rotational molding are non-isothermal, it is important to know the viscosity at zero-shear of the materials used in rotational molding dependence of the temperature. In addition, the melt elasticity has a role in sintering as well. The polymer with high melt elasticity will show slower sintering rate resulting difficult to processing, poor thickness distribution and a lot of bubbles appear in a specimen [29-31].

2.5 Polyethylene and Polypropylene

2.5.1 Polyethylene

Polyethylene (PE) is the most used in daily life. PE is the most popular plastic in the world. They have a variety thermoplastic processing such as bags, shampoo bottles, children's toys, septic tank, small boat etc. Generally, PE has a melting temperature about 115–135 °C and the density is between 0.91–0.96 g/cm³. The Chemical formula for PE is (C₂H₄)_n (as shown in Figure 2.17) and classified in polyolefin group. The classification of PE depends on the degree of branching level of branching within the polymer chains, the level of branches to increase PE limits of crystallinity in the material. While the degree of crystallinity increases the density of the material will increases. Therefore the more branching in a polymer causes a lower density material, which is the first kind of PE known as low-

density PE (LDPE). LDPE is a highly branched structure comprising a combination of ethyl and butyl groups with long chain branches in an orientation as shown in Figure 2.18. LDPE has many advantages such as not expensive, good chemical resistance, high impact strength at low temperatures, excellent electrical properties can be processed by all conventional methods, can be transparent in thin film form. The products made from LDPE have a variety for example lids, gaskets, toys, containers, packaging film, film liners, heat-seal films for metal laminates, pipe, cable covering, core in UHF cables.

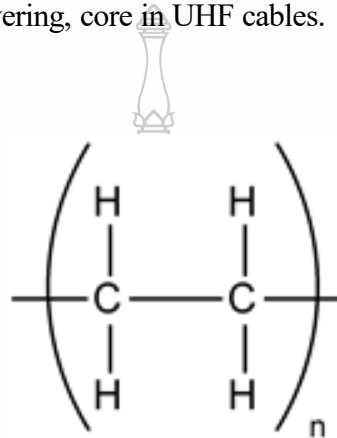


Figure 2.17 PE chemical formulas.

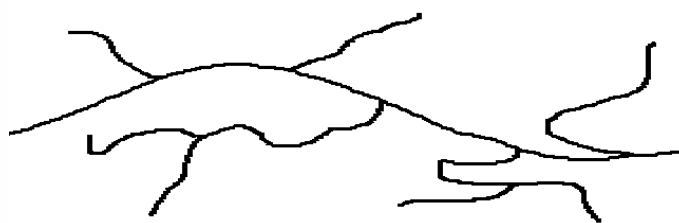


Figure 2.18 LDPE branch structure.

Linear low-density PE (LLDPE) have a fundamental structure similar to LDPE apart from having short alkyl groups attached at random intervals to the base polymer chains. Figure 2.19 is a representation of the LLDPE branches structure. LLDPE has many advantages such as semi-rigid, translucent, very tough, weatherproof, good chemical resistance, low water absorption, easily processed by most methods, low cost. There are many products made from LLDPE for example, toys, carrier bags, high-frequency insulation, chemical tank linings, septic tank, big gallon, general packaging, gas and water pipes.

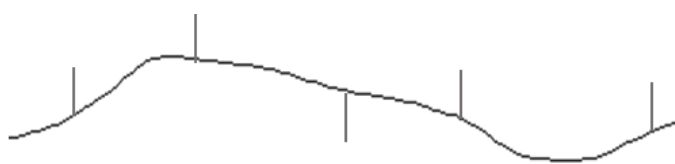


Figure 2.19 LLDPE branch structure.

Another common type is high-density polyethylene (HDPE), typically, the high-density material is more linear (fewer branches) cause more crystalline. HDPE branch structure shown in Figure 2.20, HDPE has many advantages such as flexible, translucent/waxy, weatherproof, good low-temperature toughness (to -60°C), easy to process by most methods, low cost, good chemical resistance. There are many products made from HDPE for example bottles for fruit juice, milk, water, kitchen cleaning products and even furniture [32].

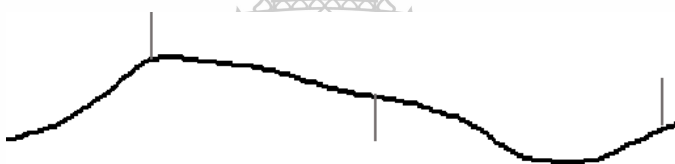


Figure 2.20 HDPE branch structure.

2.5.2 Polypropylene

Polypropylene (PP) is a linear hydrocarbon polymer, the chemical formula for PP is (C_nH_{2n}) (Figure 2.21) and classified in polyolefin group. Generally, the melting temperature of PP in the range 115–135 °C and the density is between 0.895 and 0.92 g/cm³. PP has many advantages when compared with polyethylene. The two most important are the higher melting temperature and the higher tensile modulus or stiffness while the density is kept low. However, the characteristics of PP with different structures differ from each other dramatically. it has the following advantages over conventional materials previously used for example high chemical and corrosion resistance, lightweight and rigid, high tensile strength, excellent thermal insulating properties, excellent abrasion resistance, excellent dielectric properties, low moisture absorption, long lifespan etc. And also it has widely used many applications such as automotive components, sailing, carpets, bailing twine, clothing, film (OPP), foam (structural foam, and low-density packaging).

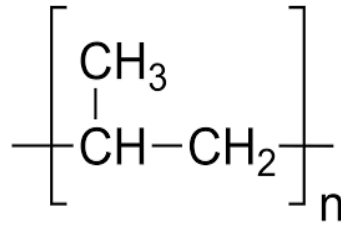
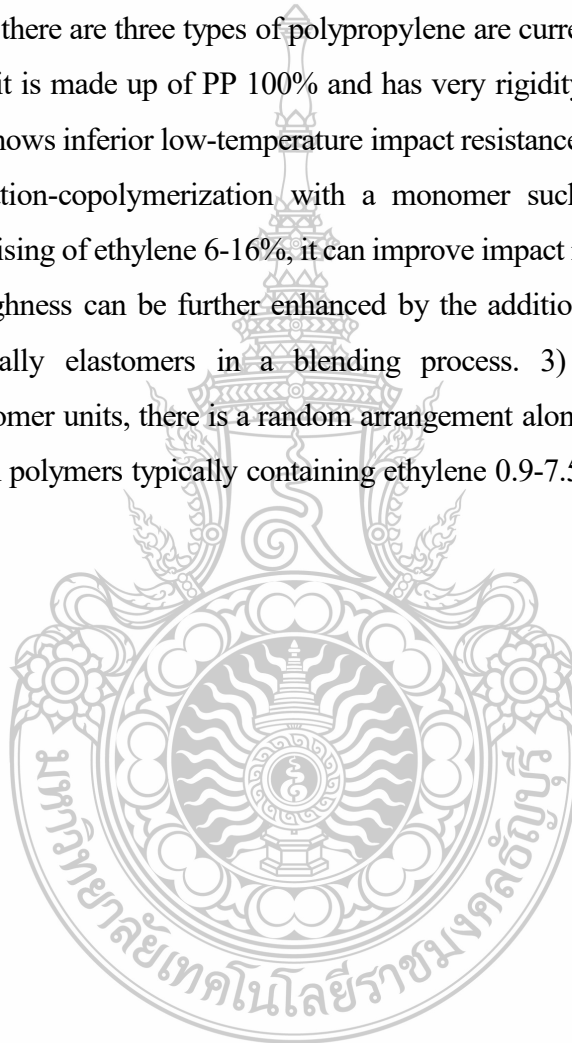


Figure 2.21 PP Chemical formulas.

Presently, there are three types of polypropylene are currently available consists of 1) Homopolymers, it is made up of PP 100% and has very rigidity and heat resistance. On the other hand, PP shows inferior low-temperature impact resistance (brittle) but can improve through polymerization-copolymerization with a monomer such as ethylene. 2) Block copolymers - comprising of ethylene 6-16%, it can improve impact resistance at temperatures below -20 °C. Toughness can be further enhanced by the addition of additive like impact modifiers, traditionally elastomers in a blending process. 3) Random copolymers - comprising co-monomer units, there is a random arrangement along the polypropylene long chain molecule such polymers typically containing ethylene 0.9-7.5% [33].



CHAPTER 3

RESEARCH METHODOLOGY

This chapter consists of description the selection of materials, the experimental apparatus and procedures, the materials used throughout this research are an assignment in section 3.1. The powder generation technique and powder characterization methods are described in 3.2. The rheological test methods used to characterize each of materials is presented in section 3.3. The information related to the axial powder flow apparatus studies are described in 3.4 the methods used to measure the quality of specimens and the mechanical properties are described in section 3.5.

3.1 Materials

Polypropylene (PP) and Polyethylene (PE) resins are used in this study. In experiments on PE, LLDPE commercial for rotational molding grade M3204RU with the MFI 4 (190°C/2.16kg) supplied by SCG chemical (Thailand) is chosen as the base materials. For PP resins, PP homogeneous polymer (PPH) grade 1100NK with a MFI 11 (230°C/2.16kg) supplied by IRPC Public Co., Ltd. and PP ethylene copolymer (PPC) grade EP549H with a MFI 11 (230°C/2.16kg) supplied by HMC Polymers Co., Ltd are selected for to study possibility PP/PE two-layered.

3.2 Generation and Characterization of PP and PE Powders

Firstly, a twin screw is used to mix resins with color for easy observation, LLDPE compound with yellow, PPH compound with red color and PPC compound with green color. After that, those resins are prepared in powder form. Generally, the pulverizing is the most used for generating powders because of high production capacity about 50 kg per hour (Figure 3.1). And achieve very fine particles about 300 microns. It was recognized that the suitable to use with PE. For PP as known that difficult to make in a powder form, it requires grinding at low temperature or called cryogenic technique, which makes the process more complicated. Therefore, in this study a blade grinder is used for grinding PP (Figure 3.2), the particles size

of PP is classified by sieve, the particles size distribution depends on the time of grinding, which is set at 15 minutes per batch (300g).



Figure 3.1 Pulverize (hammer mill) machine.



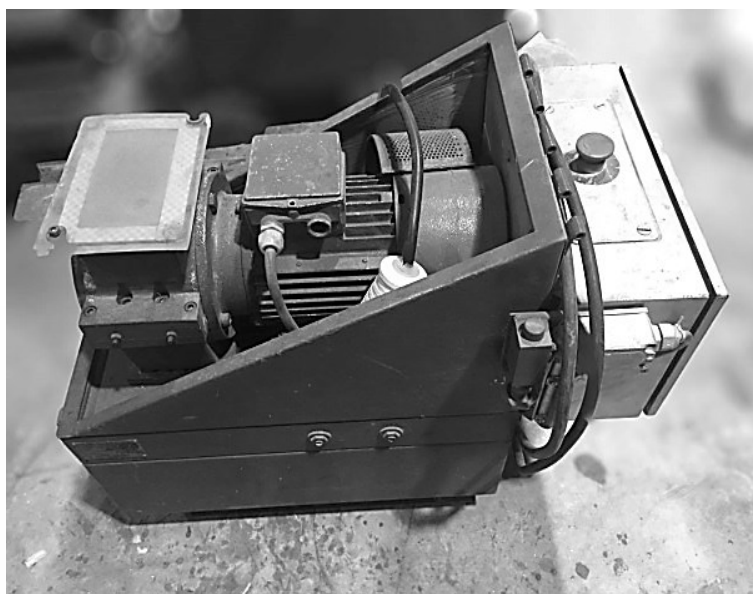


Figure 3.2 Grinder (blade mill) machine.

3.2.1 Powder characterization

Digital microscope with the maximum magnification 600x is used for investigates qualitative data such as particle size, shape and particle size distribution. After that these data are analyzed with computer software that called Image J (v.1.24) to achieve the quantitative data.

3.2.2 Thermal analysis

To obtain the processing temperature window of plastic, the differential scanning calorimetry (DSC) is used (Figure 3.3), to investigate a melting temperature transition (T_m), glass temperature transition (T_g) and crystallization temperature (T_c). In addition, the DSC can identify the immiscibility and miscibility in materials as well. The thermal analysis was carried out with a NETZSCH model DSC 200 F3 with a heating rate of 10 °C / min from temperature 30°C to 200 °C, when temperature reaches to 200 °C, hold 5 minutes to get rid of thermal history, then reduce the heat to 10 °C / min from 200°C down to 30°C.



Figure 3.3 The differential scanning calorimetry (DSC).

3.3 Rheological Characterization

To investigate the flow characteristics can be divided into two states solid and liquid.

3.3.1 Dry flow properties and Hausner ratio

The dry flow rate or flowability or pourability will be used to monitor the flow as a solid. According to ASTM D-1895 used for measuring the dry flow rate of a powder, which is described the time that powder has taken flow through a standard funnel. The dry flow rate is reported as seconds. The equipment used is shown in Figure 3.4.

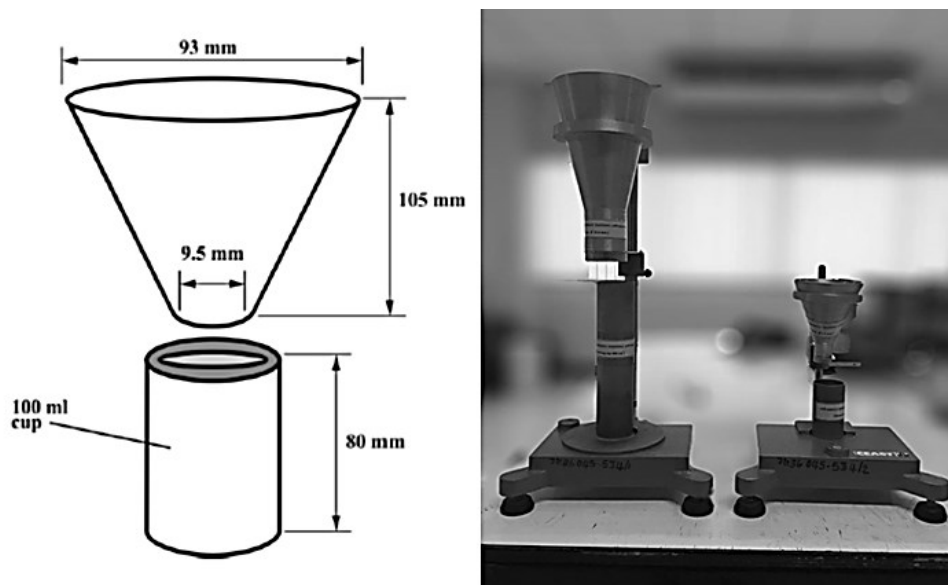


Figure 3.4 Bulk density apparatus.

The Hausner ratio is a value directly related to the ability of a solid particle to flow, which can explain the ability of small particles to move through large particle spaces, or called inter-particulate interactions. It can be calculated from the equation 3.1 and the values generally accepted are shown in Table.3.1 describes flow characteristic.

Table 3.1 Flow characteristic.

Flow character	Hausner ratio
Excellent	1.00-1.11
Good	1.12-1.18
Fair	1.19-1.25
Passable	1.26-1.34
Poor	1.35-1.45
Very poor	1.46-1.59
Very, very poor	>1.60

$$H = \frac{\rho T}{\rho B} \quad (3.1)$$

; Where ρB is a bulk density of the powder (in the condition of freely settled) and ρT is the tapped bulk density of the powder, which can be estimated from the density volume changes caused by constant and continuous force.

3.3.2 Melt flow properties

The melt flow rate (MFR) or melt flow index (MFI) according to ASTM D1238 standard (Figure 3.5), is a measured value relating to the viscosity of the polymer. This value represents the rate, which a molten polymer or mass of polymer in grams flowing in ten minutes through a capillary of a specific diameter and length by a pressure applied via load weights.



Figure 3.5 Melt flow indexers.

3.3.3 Powders sintering

Sintering experiments were performed on the sinter-rate testing machine as shown in Figure 3.7, which consists of a hot plate that can control and adjust heating level, and digital camera for recording in each the change. The result of this experiment is showing in the dimensionless quantity y/a is used to quantify the degree of completion of the sintering process (Figure 3.6). This variable is showing the ratio between the radius of the neck formed between the particles and the radius of the particles. Thus, a value of y/a nearly one indicates that a single particle has been formed and that the sintering process is complete.

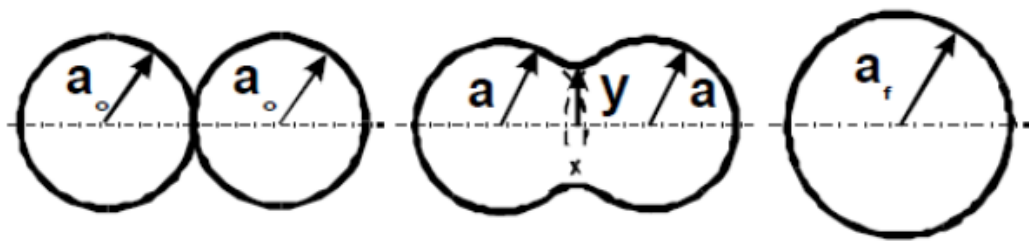


Figure 3.6 Schematic sintering sequence for two particles, where a , a_0 , a_f and y are the particle radius, initial particle radius, final particle radius, and neck radius.

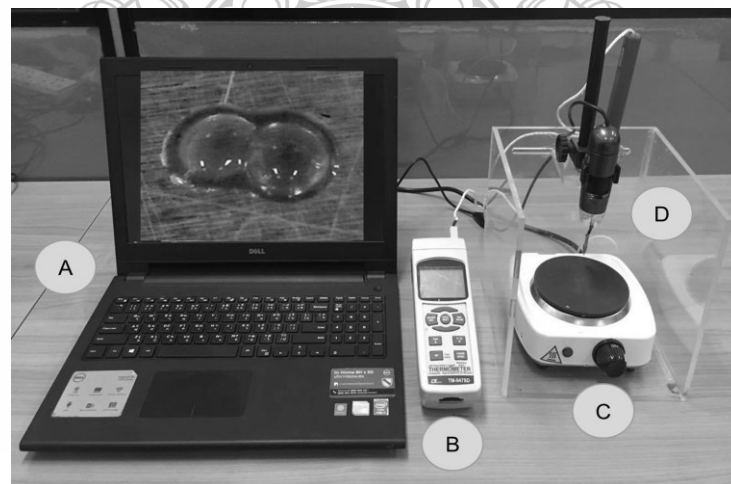


Figure 3.7 The sintering tester; where A is the processing system consists of a computer and image analysis program. B is temperature measurement and recording instrument. C is a heater plate, adjusts six level of heating. D is digital microscope, maximum zooms in 600X.

3.4 The Axial Powder Flow Apparatus

The axial powder flow apparatus was designed and built in our laboratory as seen in Figure 3.8, and the technical data was shown in Table 3.2.

The axial powder flow apparatus consists of the following system.

- a rotational system.
- a heating system.
- a cooling system.
- a VDO captured system.
- a record data system.

A rotational system of the machine consists a shaft with length 50 cm. diameter 25 mm, Spur gears, chain transmission and drive motor that can be adjusted within the range from 7 - 300 rpm and the mold is made of seamless steel pipe standard ASTM A53. The high-temperature tempered glass is installed in the mold as shown in Figure 3.9, to observe the various phenomena occurring within the mold during molding.

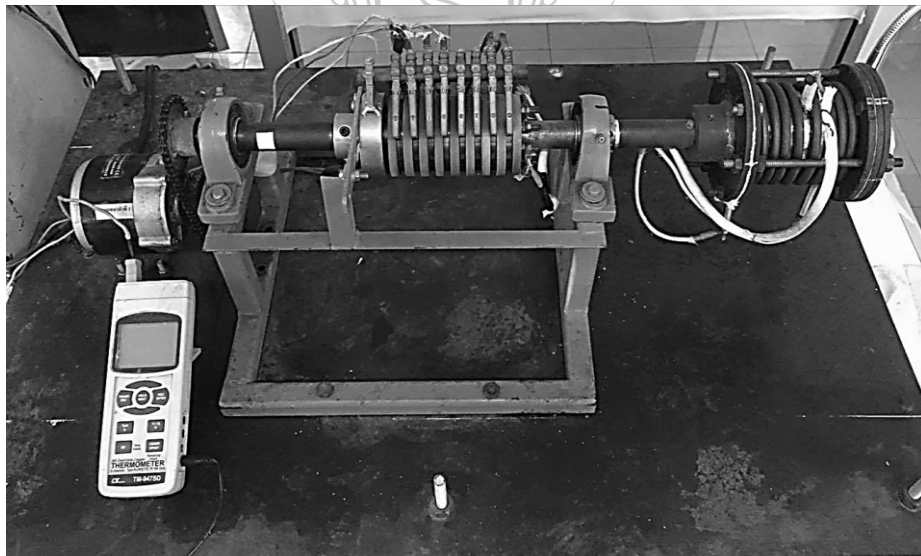


Figure 3.8 The axial powder flow apparatus.

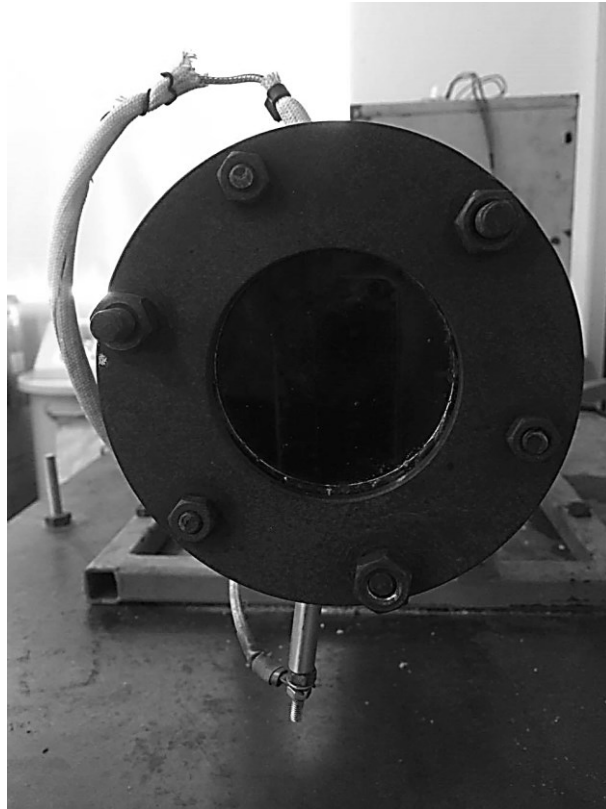


Figure 3.9 The high-temperature resistant glass.

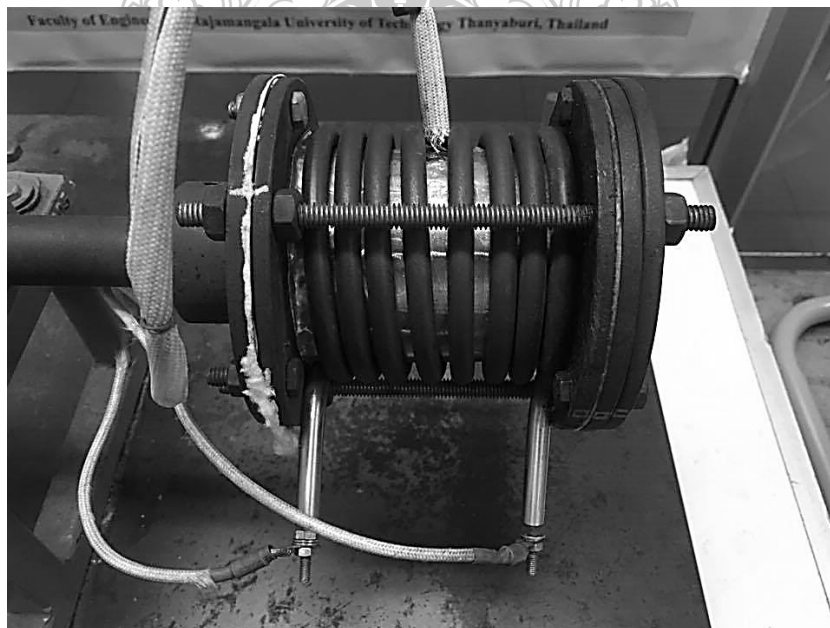


Figure 3.10 The mold and heating system.

A heating system consists of a tubular heater that can be adjusted the maximum temperature to 400 °C, which is installed at outside surface of the mold as shown in Figure 3.10. The temperature measuring is detected by the thermocouple transmission signal cables both inside and outside the mold. It can be seen that this machine uses a cable wire as the transmitter and receiver, thus it is necessary to use special devices to help prevent tangling of the wires while rotating the mold. That is a slip ring as an electrical device that acts as a bridge between moving and stationary point of the machine as shown in Figure 3.11. The components are as follows; 1. The input connector for cables, 2. The bakelite is electrical insulation in the middle between two copper plates to prevent short-circuit. 3. Carbon brushes will receive/transmit an electrical current that coming from the copper plate and forward to the output connector.

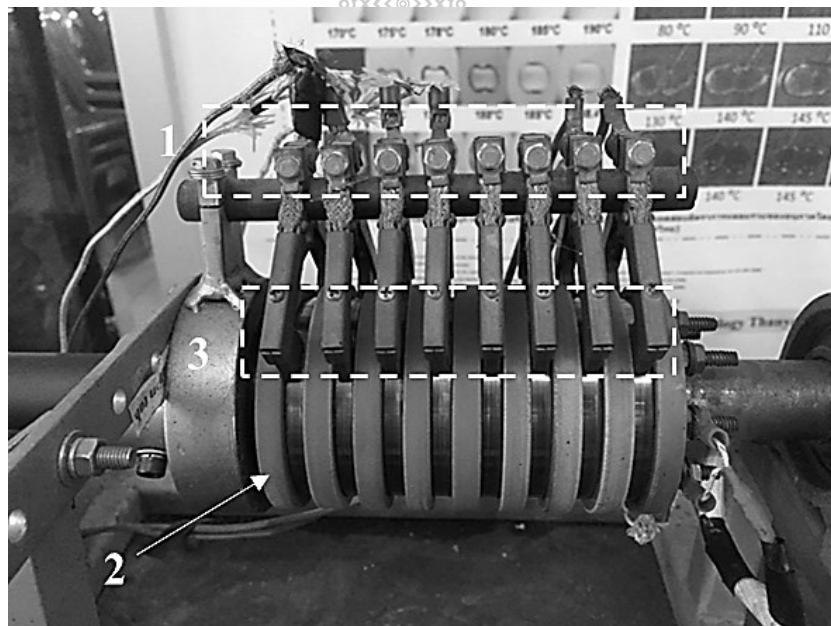


Figure 3.11 A slip ring component.

A fan is installed on the base machine for cooling and can be adjusted the cooling rate.

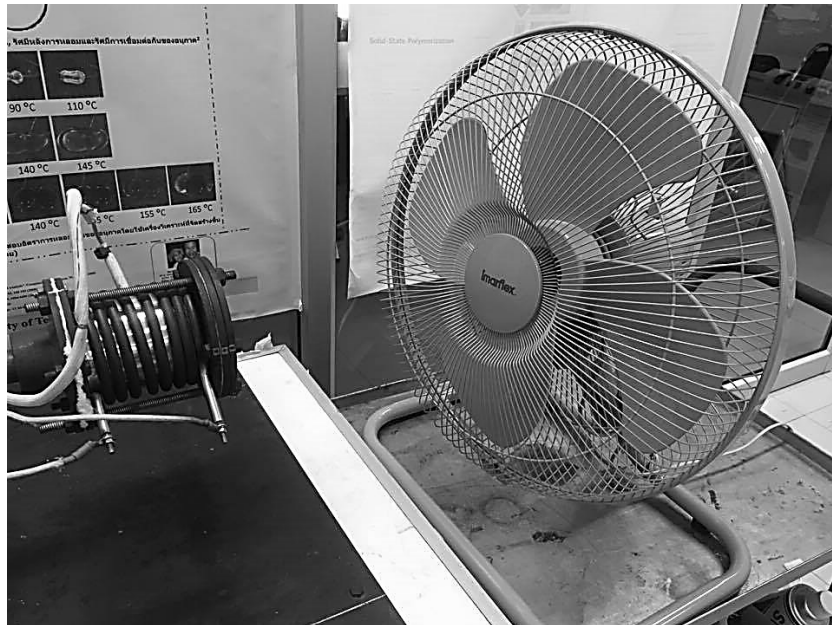


Figure 3.12 Cooling system.

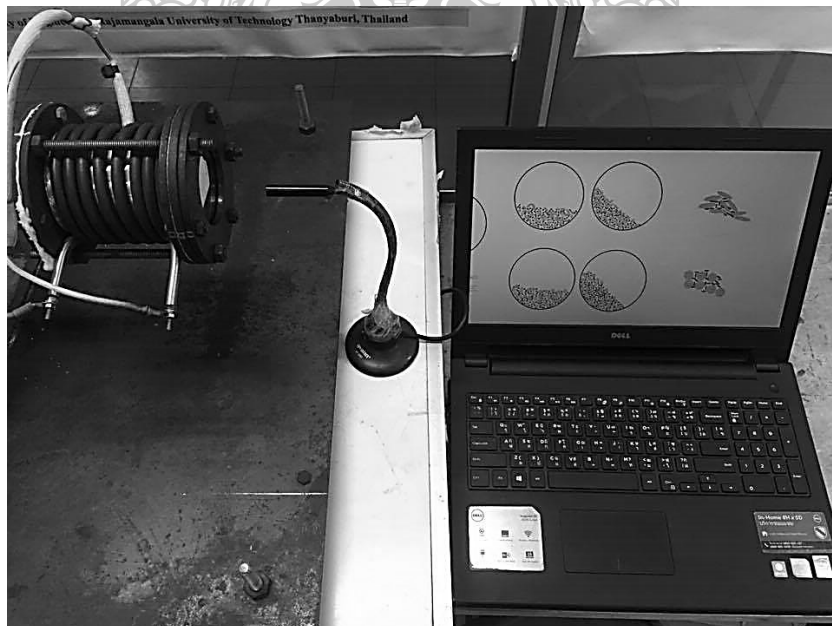


Figure 3.13 A VDO captured system.

A VDO captured system can be captured in processing since polymer in the solid state to molten state and also the behavior of polymer powder flow is observed using a digital camera to connect with computer to observe at real time.

A 4 channels data logger recorder is used in a record data system. It can be recorded the different temperature simultaneously 4 points. Which those values can be compared the temperature each point of the mold while processing.

The procedure of molding, in every time of the molding, the plastic powder 48 gram was used for producing a specimen with an approximate thickness 3 mm. The dry blend method was used at mixing ratio of 50: 50 (%wt.), the mold rotation speed at 7 rpm. The processing temperature was set at 190 °C when the air temperature inside the mold up to 190 °C, the heating process stopped works and the mold was cooled by air. Note that in every time before molding, the axial powder flow apparatus will be calibrated. The first step in testing and calibration measuring have to connect signal cable to the data logger recorder and after that immerse the thermocouples in the boiling (~100 °C) and cooling (~0 °C) water and record the data. The second step connects signal cables on slip ring and after that setting the temperature as same as above and record the data. The result of calibrations showed in Figure 3.14.

Table 3.2 The Axial powder flow apparatus technical data.

Component data	value
Mold dimensions (mm), wall thickness = 4 mm	$D_{outer}=64$,h=90
Rotation speed, rpm	7-300
Resolution borescope, (pixel)	640 x 480
Max. temperature (°C)	400
Heating power 220 volts, (Watt)	2,000
Motor 24 volt, (Watt)	10

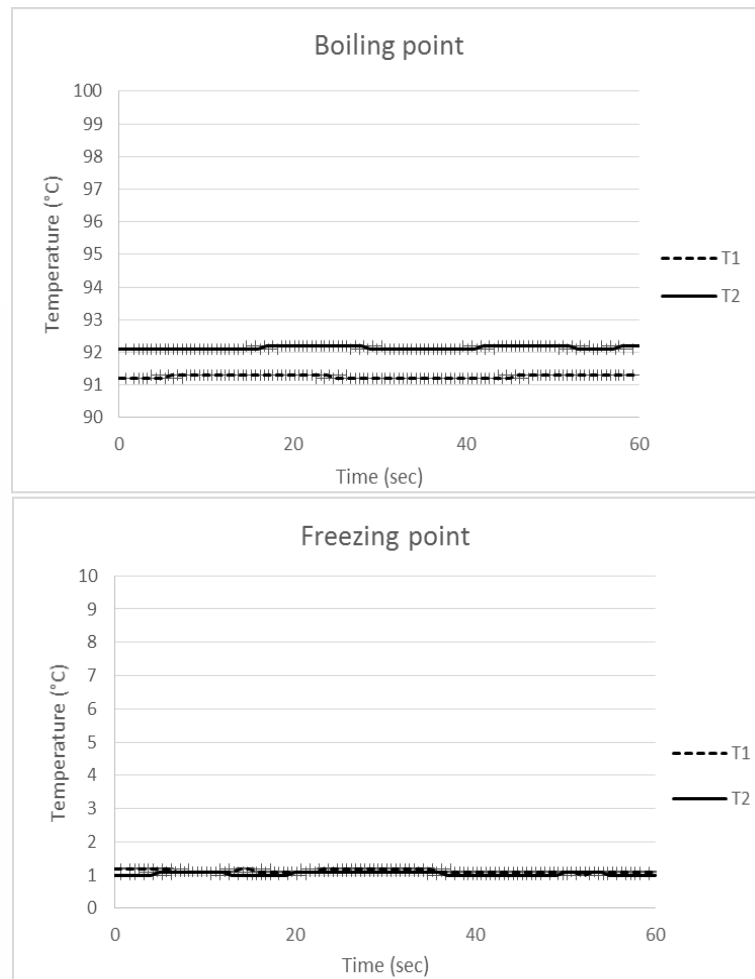


Figure 3.14 Temperature profile at freezing and boiling point;
 T1 = connecting cable signal passes to slip ring,
 T2 = connecting cable signal not passes slip ring.

3.5 Mechanical and Morphology Properties

3.5.1 Compressive strength

The mechanical strength of a rotationally molded part must always be considered in part design and applications. In this research, the specimens are obtained hollow cylinder with a length of 90 cm, outer diameter 60 cm, and a thickness 3 cm. Therefore, the appropriate test is a compressive strength test using universal tensile tester in mode compressive test. Which mostly test results are reported as the compressive modulus.

3.5.2 Morphology

The morphology investigations relate to the quality of specimens, they are investigated by the digital microscope with maximum magnification 600X (as shown in 3.15). The specimens will be cut to a size 1 x 1 cm. then images from the digital microscope will be analyzing by computer software that called Image J. In the same time, the miscibility or the separate layer of these two polymers will be investigating via the cross-section of specimens. After that, the specimens will be cut along the length for measuring to average thickness distribution.



Figure 3.15 The digital microscope.

3.5.3 Image analysis by ImageJ software

Image particle analysis has been used extensively in research because it is a simple and reliable method.

ImageJ is an image analysis and visualization program, which is a publicly available downloadable program and is available for a variety of operating systems such as Windows system, Mac OS X system and Linux system. It can be used with a variety of image files such as Tagged Image File Format (TIFF), Graphics

Interchange Format (GIF), Joint Photographic Experts Group (JPEG), Bitmap (BMP) or Raster, Digital Imaging and Communications in Medicine (DICOM), Flexible Image Transport System (FITS) and raw file format ('raw'). It has many functions such as calculating the area or pixel value, measure distances, angles and generating histograms and line graphs from obtaining previous data, and also has basic image processing such as sharpness, brightness, cropping, resizes, rotation, flips, zoom out, zoom in and color adjustment etc. these functions are always developed by the programmer. For this research, it will be used to measure the particle size, shape and roughness of the surface. The procedures of analysis are as follows.

3.5.3.1 The particle size and shape measuring

- Start the program and open the image that wants to measure as shown in Figure 3.16

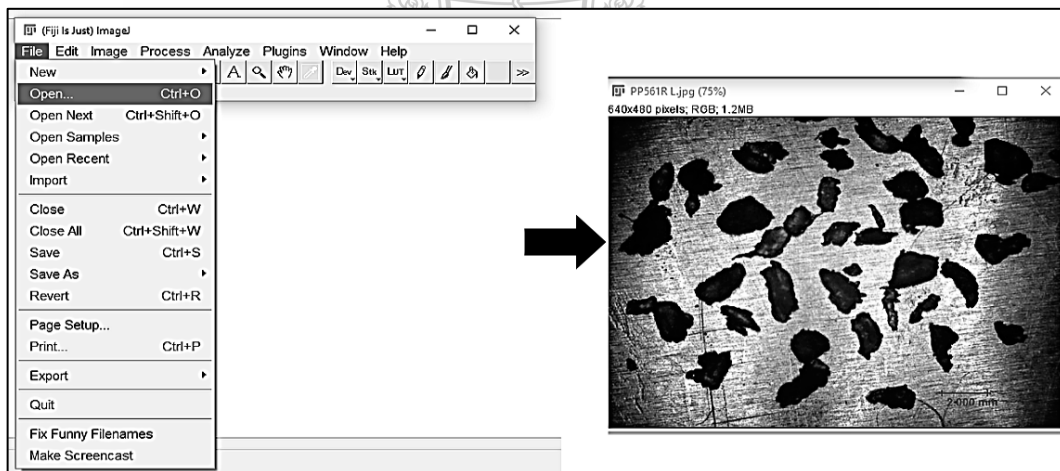


Figure 3.16 Image analysis step 1.

- Each time before analysis, the measurement distance is determined by reference to the area of the active image. Start with a 'straight-line' in the toolbar and drag a line as long as that known distance (recommend compared to the scale bar), As shown in Figure 3.17, then go to the menu bar and select Analyze, then select Set Scale and enter the distance in mm, cm, μm , and \AA etc. And if the user wants to use this value for

every image, select 'global' and choose 'OK', The distance in pixels format will be automatically replaced by the length of the selected line, as shown in Figure 3.18.

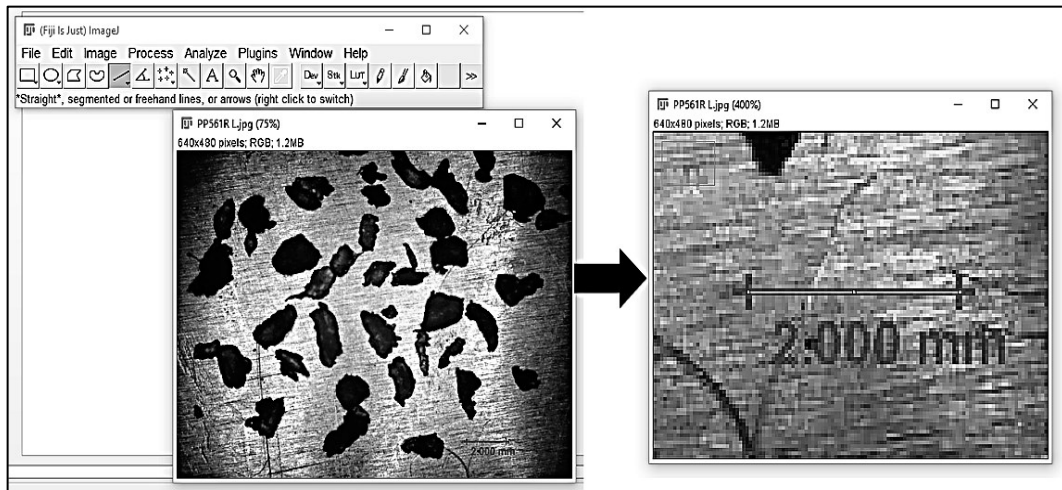


Figure 3.17 Image analysis step 2

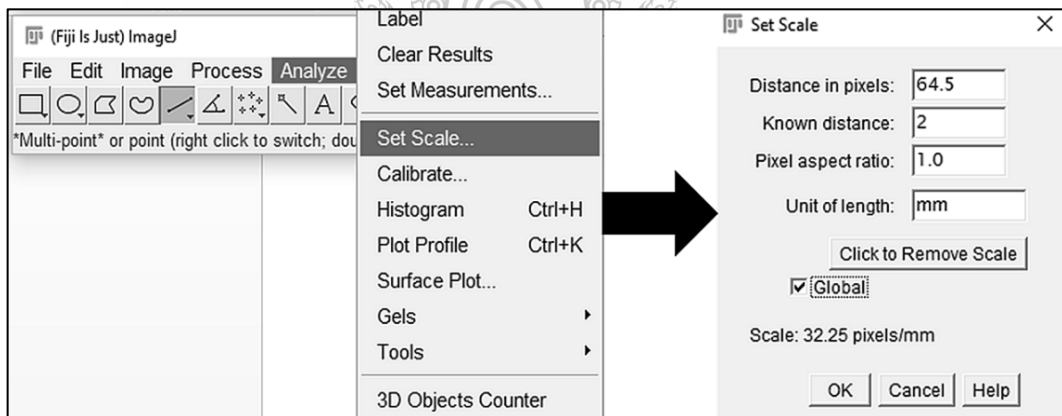


Figure 3.18 Image analysis step 3.

- Select the type of calculation and display that will be displayed on the results table, either the length, the angle of the line or the coordinates, which can be measured from the menu bar, select 'Analyze', then 'Set Measurements' and choose 'OK' as shown in Figure 3.19.

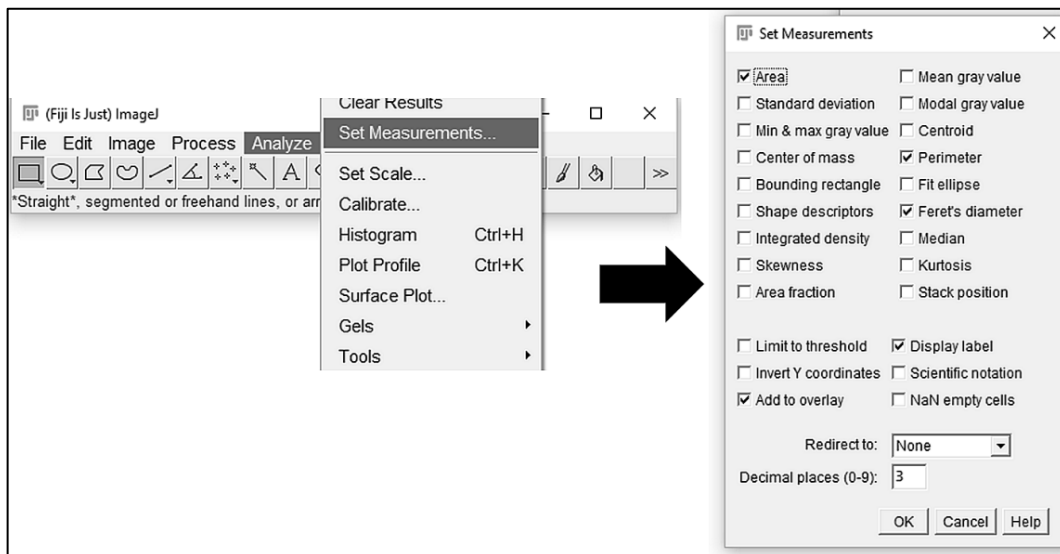


Figure 3.19 Image analysis step 4.

- In a counting and measuring the objects need to use as a binary or thresholded images. Therefore, must make the image in binary mode by selecting 'image' in the menu bar and then going to 'type' then choose '8-bit' as shown in Figure 3.20, Then adjust the image to threshold mode by selecting 'image' on the menu bar, then go to 'adjust' and 'threshold', respectively, as shown in Figure 3.21, in the dialog box, adjust the contrast or sharpness. As desired, and select 'apply'.

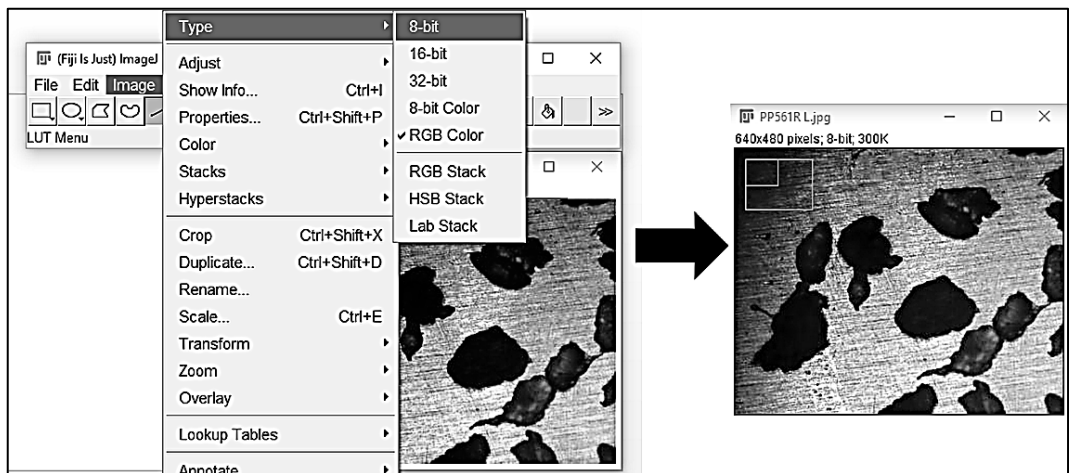


Figure 3.20 Image analysis step 5.

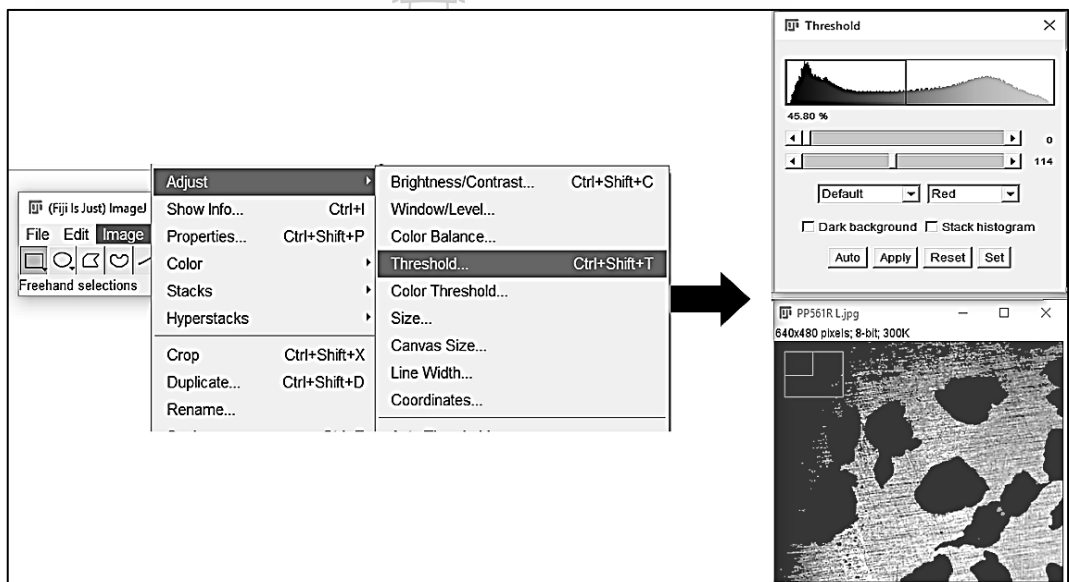


Figure 3.21 Image analysis step 6.

- The analysis can be done using the 'analyze particles' command, In the menu bar select 'analyze' then selecting 'analyze particles' as shown in Figure 3.22. The analysis is rendered on the existing area selection, if no selection is present, it will choose all image. Its principle is to scan the image or selection until it reaches the boundary of the object. In the dialog box, it can select the size, area or scope of measurement from 0 - infinity for particles that are not in the measuring range are skipped.

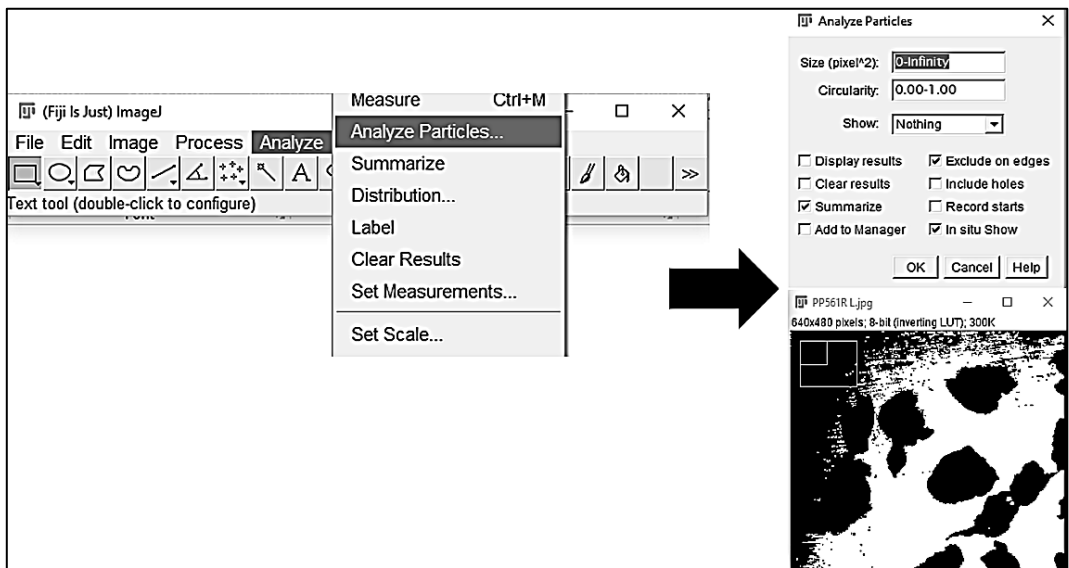


Figure 3.22 Image analysis step 7.

- Another command that can be analyzed as same is the use of the 'Measure' command, which is different from clause 2.5. This method defines the boundary by drawing a line around the object with the 'freehand selection' tool in the toolbar shown in Figure 3.23-3.25, After that go to the menu bar and select 'analyze' and 'Measure' (Ctrl + M) respectively. The results are shown in the table summary.

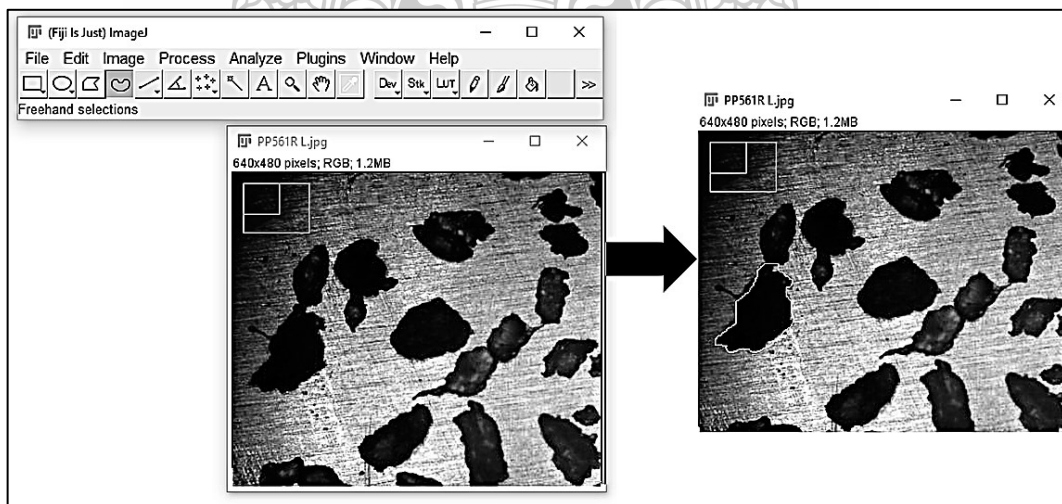


Figure 3.23 Image analysis step 8.

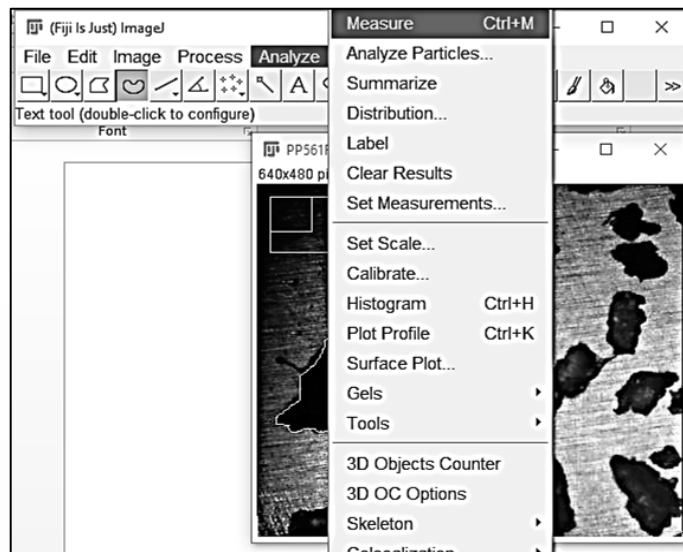


Figure 3.24 Image analysis step 9.

Label	Area	Perim.	Circ.	Feret	FeretX	FeretY	FeretAngle	MinFeret	AR	Round	Solidity
1 PP561R L.jpg	2.504	6.578	0.727	2.522	3.844	8.594	33.887	1.346	1.965	0.509	0.941

Figure 3.25 Image analysis step 10.

The result of the analysis is shown in the table summary as shown in Figure 3.25, Shape Descriptions are calculated and displayed from a mathematical relationship as follows.

- Circularity is calculated from the formula $4\pi \times [\text{Perimeter} / \text{Area}]^2$. A perfect circle will indicate the value approaching 1, while if it indicates an increasingly elongated shape will show the value approaching 0. However, the Values may not be accurate for the particles with a very small size. It is shown in the table of a column named 'Ciru'
- Aspect ratio is a function of the largest and smallest diameter of the particle (or Width / Height). The square or roundness of the object is indicated by this ratio. The aspect ratio is a 1

means a circle or a square, while the aspect ratio approach to 0 means as the line. It is shown in the table of a column named 'AR'

- Roundness is calculated from the formula $4 \times [\text{Area}] \pi \times [\text{Major axis}]^2$ or the inverse of Aspect Ratio, the value approaches 1 mean that the object is quite round. It is shown in the table of a column named 'Round'
- Solidity is a value demonstrates that the object has a smooth surface with no indentations or distortion, which is calculated from the area of the object divided by its convex area. $[[\text{Area}]/\text{Convex area}]$. It is shown in the table of a column named 'Solidity'. Feret's diameter is a value of the longest distance between any two points along the selection boundary. It is shown in the table of a column named 'Feret'. And The 'FeretAngle' on a column is an angle (0–180 degrees) of the Feret's diameter, then the minimum or the narrowest diameter of the object is shown in 'MinFeret' column. For columns of 'FeretX' and 'FeretY' are the starting coordinates of Feret's diameter.

In this work, the min-feret is used to determine particle size, since this value is commonly used and accepted for sieving particle by the sieve. While the average of circularity is used to indicate the shape of particles, which each particle will be measured two dimensions in the top and side views.

3.5.3.2 Surface roughness analysis

'SurfCharJ' is a function to investigate characteristic surfaces. It can be used with high or low alternate images of a particular area or the topographic image derived from laser measurement system, a white light interferometer, AFM etc. The input is a 32-bit image or stack in which the pixel values displays distance, z, to a surface. The user also needs to provide the transverse spacing between the pixels, expressed in the same units as the range data. The features of ImageJ have been improved to estimate level surface roughness data along with skewness, root

mean square deviation and kurtosis. The Gaussian filtering has been used to partition the waviness from the roughness, and to estimate the different wavelengths in the structure.

The surface roughness analysis is measured by R-values on the whole surface, which indicated roughness values according to the standard ISO 4287/2000.

Where; R_a , R_q , R_{ku} , R_{sk} , R_v , R_p , and R_t are the Arithmetical mean deviation, Root mean square deviation, Kurtosis of the assessed profile, Skewness of the assessed profile, Lowest valley, Highest peak and The total height of the profile respectively. The procedures of analysis are as follows.

- Change the image to binary, selecting 'image' in the menu bar, and then select '32 bit' type as shown in Figure 3.26

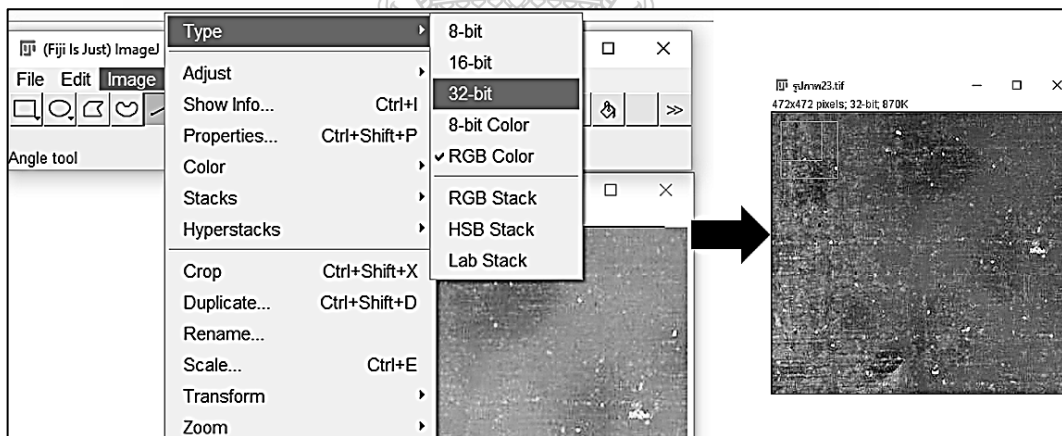


Figure 3.26 Surface roughness analysis step 1.

- The Analysis with the 'SurfCharJ 1q' command is accessed by a list of plugins on the menu bar, which inside the dialog box can be customized to a wide range of measurements depending on the user's needs, as shown in Figure 3.27.

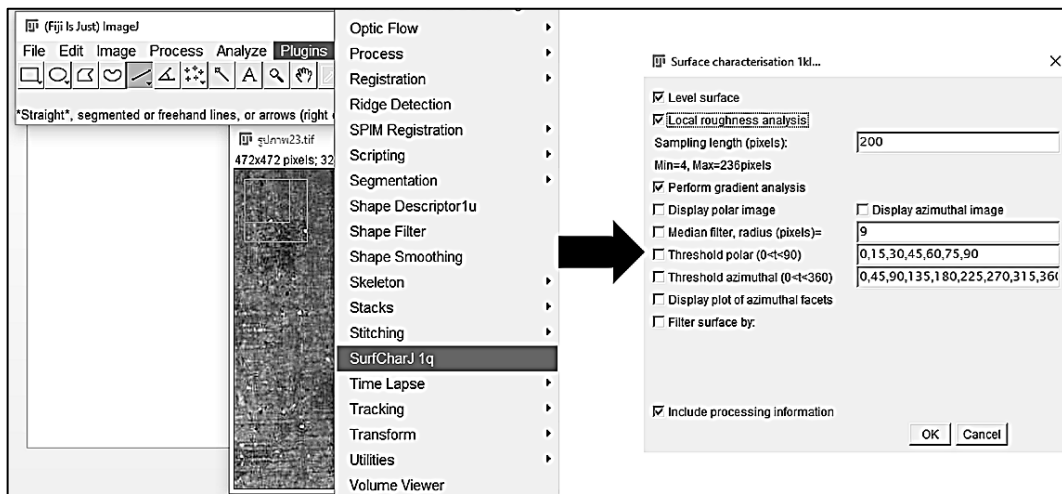


Figure 3.27 Surface roughness analysis step 2.

- The results of the analysis are shown in the Figure 3.28, the displayed roughness value will vary depending on the user selected, from the image appearing after the analysis shows different shades, which represent different degrees of coarseness, which they displayed based on the previous user setting. For this research, Ra is used in comparison because it is being commonly used value.

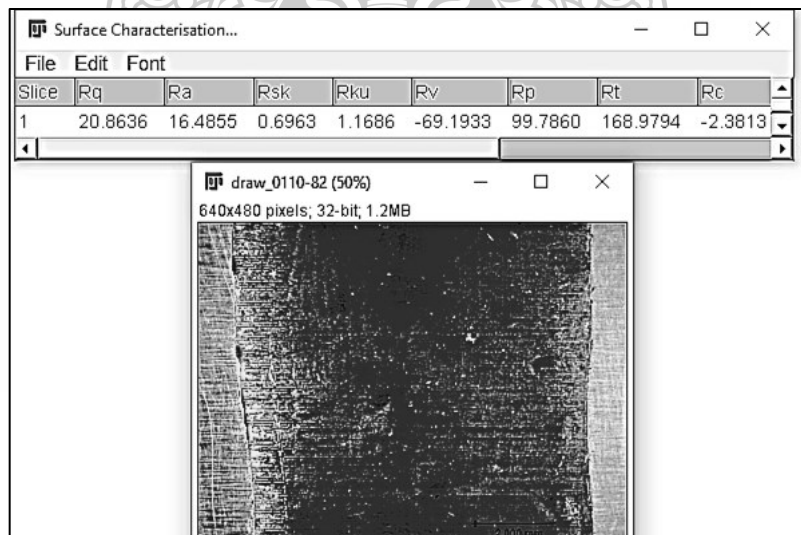


Figure 3.28 Surface roughness analysis step 3.

CHAPTER 4

RESULTS AND DISCUSSION

4.1 The Effect of Particles Size of Polypropylene on Two-Layered Process

The aim of this experiment is examined the possibility to molding PP/LLDPE two-layered in the rotational molding process by using techniques uncomplicated, where using PP with the different particle size of PP, and mixed in 50-50 ratio by dry blend method. After molding, the specimens will be investigating the layer separation, thermal properties, surface roughness, thickness distribution and mechanical properties.

4.1.1 Experimental

4.1.1.1 Materials

In this experiment, PP copolymer was exempt because one of the purposes of this research not only to produce the two-layered products but also required to improve LLDPE stiffness, which is well known that PP homopolymer has a higher strength than PP copolymer. Thus, it was chosen for this experiment.

Two types of materials were used: linear low-density polyethylene grade M3204RU (powder form) with MFI 4 (190 °C/2.16 kg), a density of 0.932 (g/cm³), and thermal conductivity of 0.34 ((W·m⁻¹·K⁻¹, (20 °C)), as supplied by SCG Chemical (Thailand) and polypropylene homopolymer, or PPH grade 1100NK (pellet form), with MFI 11 (230 °C/2.16 kg) and 4.89 (190 °C/2.16 kg), a density of 0.914 (g/cm³) and thermal conductivity of 0.22 ((W·m⁻¹·K⁻¹, (20 °C)), as supplied by IRPC Public Co., Ltd. Before processing, to clearly observe the behavior and phenomena of the molding materials, a twin screw extruder was used for compounding resins with a color pigment of 1% by weight; in addition, LLDPE resin was compounded with a yellow color, and to control the quality of the particles similarly to a commercial grade, it was reduced in size by hammer mill pulverizer. In the case of PP, it is well known that it is difficult to reduce the size to powder, so it will be reduced in size by blade mill machine, the qualities of particles such as shape, size, and size distribution are controlled by weights of particles per grinding time in each batch, which was determined at 300 g/5min per batch, then the sieve is

used to classified the size, the different three size such bigger than and equal LLDPE are selected. The average particle size was selected as shown in Table 4.1. Where PP-L represents a large particle, PP-M represents a medium particle and PP-S represents a small particle.

4.1.1.2 Experimental procedure

An axial powder flow apparatus was used in the experiment, which was designed and built in our laboratory to investigate the behavior of a powder flow while molding, as shown in Figure 4.1. During each molding, 48 g of plastic powder was used for producing a specimen with an approximate thickness of 3 mm. A dry blending method was used at a mixing ratio of 50:50 (%wt.) and a mold rotation speed of 7 rpm. The processing temperature was set to 190 °C when the air temperature inside the mold reached up to 190 °C, at which point the heating process was stopped and the mold was cooled in air. The specimen obtained after molding as a shape of the cylindrical with an inner diameter of 60 mm, length of 90 mm.

4.1.1.3 Characterization

The properties of the powder particles in terms of their bulk density and dry flow rate were investigated according to ASTM D1895-96. The Hausner ratio was used to describe the inter-particulate interactions. The melt flow properties were investigated using a CEAST® Modular Melt Flow Indexer (Model 8331) according to ASTM D1238. A heater plate and digital microscope were used together along with ImageJ computer software to investigate the sintering rate. The thermal properties were determined through differential scanning calorimetry (NETZSCH, DSC 200 F3) using a temperature range of 303.15 to 473.15 Kelvin(K), and heating and cooling rates of 283.15 K/min and 278.15 K/min respectively. A digital microscope (600X) was applied along with the roughness analyzer software (ImageJ) to investigate the phase-separated layer and surface roughness of the specimens. The standard deviation of wall thickness was investigated by cutting along the length of specimens. Finally, the compressive test was selected for investigation the mechanical properties because it is a method with the most appropriate with the shape of the specimen.

4.1.2 Results and discussion

4.1.2.1 Powder properties

The bulk density and dry flow rates shows the efficiency of particles packing and particle mobility. In case of pure polymer PP-L with the large size has the highest values, followed by PP-M and LLDPE of similar size. While the PP-S with a small shape similar to the fiber shown the lowest values, which is consistent with previous research, the particle has looked like fiber or needles and including the presence of particles with tail, which obstructs the movement of the surrounding particles causes low flow performance, and probably result in lower packing coefficients as well. In case of the mixed polymer, PP-L/LLDPE has higher and faster bulk density and dry flow rates than PP-M/LLDPE and PP-S/LLDPE respectively, these show clearly that LLDPE improves the bulk density and dry flow rates of PP especially in case of PP-S/LLDPE. These results directly related to the particle size distribution, which has been described from previously reported that the increasing or decreasing of the bulk density of polymer often depends on the particles size and the appropriate particle size distribution. For the dry flow rate, it shows clearly as a result of the particles shape, which the decreasing of an irregular particle shape shows the increasing rates of the particles flow [2, 11, 34].

The Hausner ratio is a test method that demonstrates the efficiency of particle motion passes gap. The test results ranged from 1.12 to 1.18 indicated the particle high flowability, while the particle with moderate flowability is indicated in the range from 1.19 to 1.25 [35]. The results of the tests in Table 4.1 show that in the case of a pure polymer, PP-L, PP-M, and PP-S shows a higher flowability, whereas LLDPE shows a moderate flowability. In the cases of mixed polymer, PP-L/LLDPE shows a high flowability, whereas both PP-M/LLDPE and PP-S/LLDPE shows a moderate flowability. These results are shown that LLDPE with small particle moves through the gap of PP-L better than both PP-M and PP-S.

4.1.2.2 Melt flow index (MFI)

It is well-known that polymers that undergo heat one or more times may change their flow properties, which may affect the molding or quality of the specimen. Thus, testing of melt flow properties in this work aims to investigate the melt flow properties of the material after color compounding. All materials are tested at the same temperature by referring to the ASTM D638 test for PE test. The results are shown in Table 4.1, LLDPE after passes

through the color compounding unchanged the MFI, while PP after color compounding has slightly increased the MFI around 4.29 % as compared to PP without the color compounding. In the case of a mixed polymer found that they have slightly increased the MFI around 10 % as compared to pure PP after color compounding, which indicates that PP improves the melt flow of LLDPE. The change in melt flow properties of the polymer that passes more than 1 heating time, maybe depends on thermo-mechanical and thermo-oxidative degradation while processing makes the reaction with the molecular chain in a various manner such as chain scission, branching, or crosslinking [36–39].

Table 4.1 Powder properties of a pure and mixed polymer (different the size of PP).

Materials	Mean particle size (μm)	Mean circularity		Bulk density (g/cm^3)	Dry flow (sec)	Hausner Ratio	MFI ($\text{g}/10\text{min}$) ¹
		Top view	Side view				
LLDPE	368	0.67	0.53	0.34	9.40	1.19	4
PP-L	1,421	0.77	0.72	0.38	10.10	1.14	5.10
PP-M	758	0.66	0.66	0.36	11.87	1.16	5.17
PP-S	356	0.57	0.37	0.28 ²	128 ²	1.16	5.11
PP-L/LLDPE	-	-	-	0.39	10.10	1.17	5.61
PP-M/LLDPE	-	-	-	0.38	10.97	1.19	5.52
PP-S/LLDPE	-	-	-	0.28	11.57	1.19	5.47

¹ Measured at 190°C after color compounding.

² Cannot measure in standard conditions, required to apply the force to flow of powder.

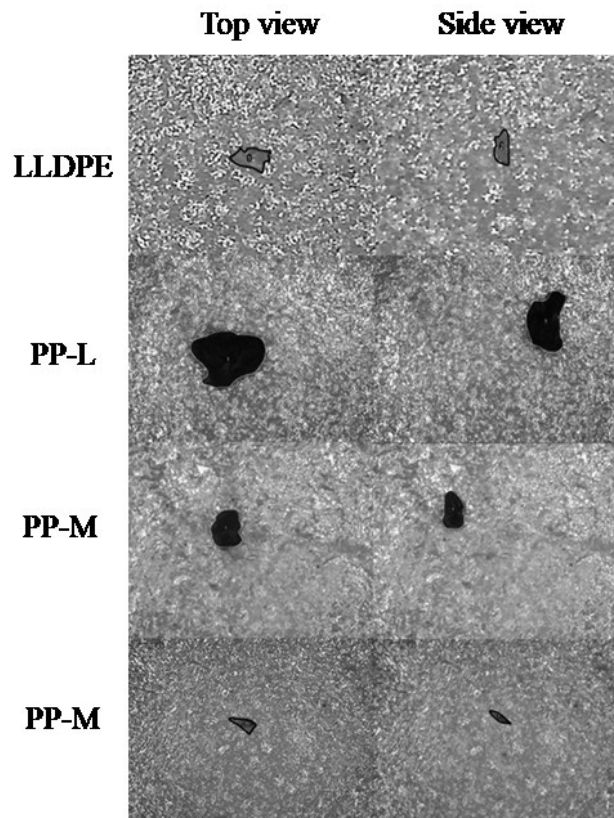


Figure 4.1 The particle shape and size of LLDPE, PP-L, PP-M, and PP-S.

4.1.2.3 Sintering rate

This experiment plays a very important role in predicting the heating duration and quality control of the specimen. The test machine consisting of a digital camera with a maximum magnification of 600X with heating plate and data loggers. The experiments were carried out by two equal sized particles are placed on the heating plate with the surface contact of the particles close together. The heating is kept constant, and immediately the heating plate operates, the digital microscope and data recorder operate at the same time. The phenomena occurring during the test will be recorded video and all data will be analyzed the neck growth ratio, “ y/a ”; where “ y ” is the length of the neck between the two particles and “ a ” is the mean radius of the particles [33,40] (as shown in Figure 4.2). As expected, the results showed in Figure 4.3. In the case of PP, smaller particles can fuse faster than large particles. A comparison between LLDPE and PP-M with similar size and flow rate showed that the materials with low melting points had a faster sintering rate. However, the previous report describes that the rate of sintering will have occurred from the effect of the melt flow rate or viscosity more than the elastic

melting. The experiments often found that the experimental results were inaccurate because the initial contact of the two particles was not in a good position [3,41].

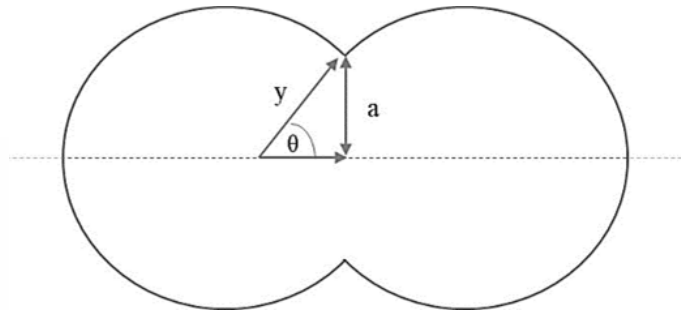


Figure 4.2 Schematic of the neck growth ratio (particles sintering).

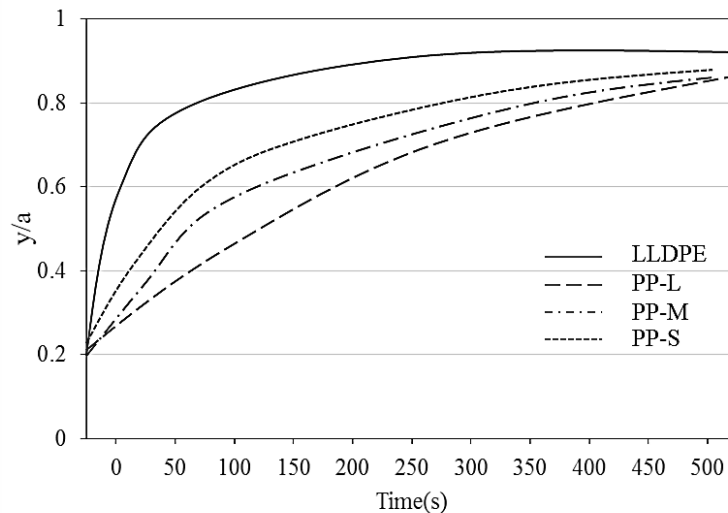


Figure 4.3 The sintering rate of LLDPE, PP-L, PP-M, and PP-S.

4.1.2.4 Temperature profile of air inside the mold

The behavior of air temperature variations inside the mold was investigated and recorded using the data logger during the molding process. The internal air temperatures of a pure and mixed polymer are as shown in Figure 4.4. For the internal air temperature of a pure polymer, shown in Figure 4.4(A), at the first stage point A, the heat passes into the mold and the internal air temperature begins to steadily increase. The first particles then stick and are coated on the mold surface. LLDPE particles easily melt and stick to the mold surface at around 50 °C, followed by PPC and PPH at around 70 and 80 °C respectively, when compared with the different shapes of the PP. It can be seen

that particles with a large contact surface have better heat conduction between the particle and mold surface than those with a small contact surface [42]. The heat rates slowly increase until point B. At point B, all of the particles inside the mold stick together completely, and the particles have no movement. In LLDPE, this was observed at around 70 °C, followed by at around 120 and 130 °C for PPC and PPH, respectively. The processing period took a long time between points B and C because of the effects of the sintering and coalescence processes, the heat transfer to the thermocouples inside the mold was quite difficult to achieve because of the wall thickness layer of the polymer increases. As expected, LLDPE showed a faster rate of heating than PPC and PPH, and the results were consistent with the rate of the particle sintering shown in the previous experiments. At point C, the heater was stopped at 190 °C. The rate of heating was decreased owing to the starting of the cooling system, and the molten polymer gradually formed a solid. From points C to D, LLDPE cooled faster than PPC and PPH, and it should be recalled that the thermal conductivity of the material is also important in terms of the process time because, while the mold is cooling, the polymer adjacent to the mold surface becomes a solid state, trapping the heat inside the mold [43, 44]. In the case of a polymer with a high thermal conductivity, it was found that the heat is easy to transfer out of the layer of a solid [45, 46].

In the case of mixed polymer shown in Figure 4.4(B), indicates that the mold was heated to an internal temperature of about 50 °C, some particles begin to stick to the mold surface, referred to as tack temperatures point, which all three cases are showed similarly. Then the heat gradually enters into the mold, with the heat rate is decreasing slightly as the amount of particle in the mold surface gradually increases until the point is called the kink temperature point. All particles stick together perfectly, no moving particles. The effect of the difference in PP particle size on the kink temperature point clearly shows that PP-L/LLDPE has a lower kink temperature point of about 80 °C, followed by PP-M / LLDPE and PP-S/LLDPE at about 90 and 100 °C respectively. This seems to be a result of the heat transfer between mold to particle and particle to particle, which directly related to the particles flow characteristic in the mold while rotating, it has been described that a good flow characteristic exhibits a better the heat transfer than a poor flow characteristic. In addition, this also relates to the amount of powder charged to

the mold; as followed Figure 4.4 (C) showed that PP-S/LLDPE has higher the amount of powder charged to the mold than PP-L/LLDPE approximately 18% (at the same of weight). After passing the kink temperature point, it will be the proceeding of sintering and coalescence, which observed that the heating rate gradually increases until to the set temperature at 190 °C.

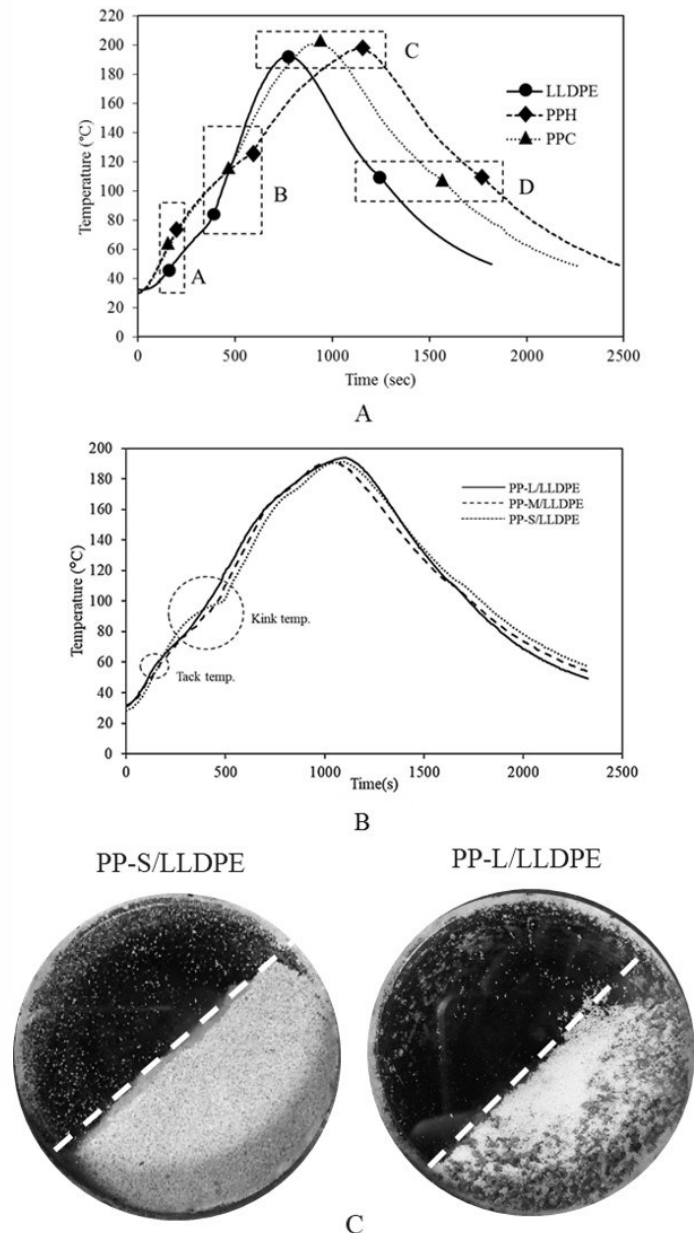


Figure 4.4 Internal air temperature of (A) pure polymer, (B) mixed polymer and (C) amount of powder charged to the mold.

4.1.2.5 The particles segregation and melt deposition of the PP/LLDPE with the different particles size of PP.

In general, the particle movement behavior is unique which depending on the size, shape, and type of material. For this research, the variables considered were: The particle size and the different types of materials, while the shape of the material will be considered later, since it is well known that it is difficult to control the shape of the particle after the reduction, and even though it can control its shape but probably increase the complexity of the work, so it may not be suitable for use in the real industry. The analysis is performed using a photo analysis program which works by distinguishing contrast of color appearance. The results are shown in Figure 4.5, the appearance of PP/LLDPE particles with different PP sizes, it showed that the different particle sizes affect the radial segregation pattern of the particles. In general, small particles travel through the gap of large particles to a position lower than the flow surface or core of the cylinder [2, 47], which in turn demonstrates consistency with the case of PP-L/LLDPE. In addition, it also was found that there are some of the LLDPE particles roll up to the surface of the flow as the mold rotated. In the case of PP-M/LLDPE with the same particle size, the LLDPE particles spread over the area of motion which shows the poor particle mobility. The results indicated that a little different material density does not affect the radial separation pattern of the particle. While the case of PP-S/LLDPE is similar to PP-M/LLDPE, although PP is smaller, it cannot pass through the gap of LLDPE particles, it may result from either the particle size distribution narrow or the particle low mobility. In addition, the existence of very small particles or abnormal particles will be reduced the particles ability to move. The particle separation makes the appearance of the melting deposition different as shown in Figure 4.6. In the case of PP-L/LLDPE, small LLDPE particles and low melting points easily move through the gap to the mold surface, causing it to melt and form the outer surface slowly. At the same time, the PP with larger particles and higher melting points will continue to roll, some of which will be pinned to the molten LLDPE by a stickiness, when these particles get the heat enough, will stop the roll and lay down on the layer of molten LLDPE, and become the inner layer. This phenomenon occurs within a case of PP-M/LLDPE as well, but different in the amount of LLDPE that form as the outer layer, LLDPE particles move to the mold surface less than the previous

case, causing the low thickness outer layer, become just only the thin film layer. Moreover, most of the LLDPE particles that cannot move to the mold surface, they were trapped at the inner layer, and when the heat increased, these particles were melted and mixed with PP particles. In the case of PP-S/LLDPE, LLDPE particles cannot move through the gap of PP due to its similar size, allowing it to move to the molded surface simultaneously. LLDPE with a lower melting point cannot form the outer layer when the heat increased all the particles both PP and LLDPE are fused together and turned into polymer blends.

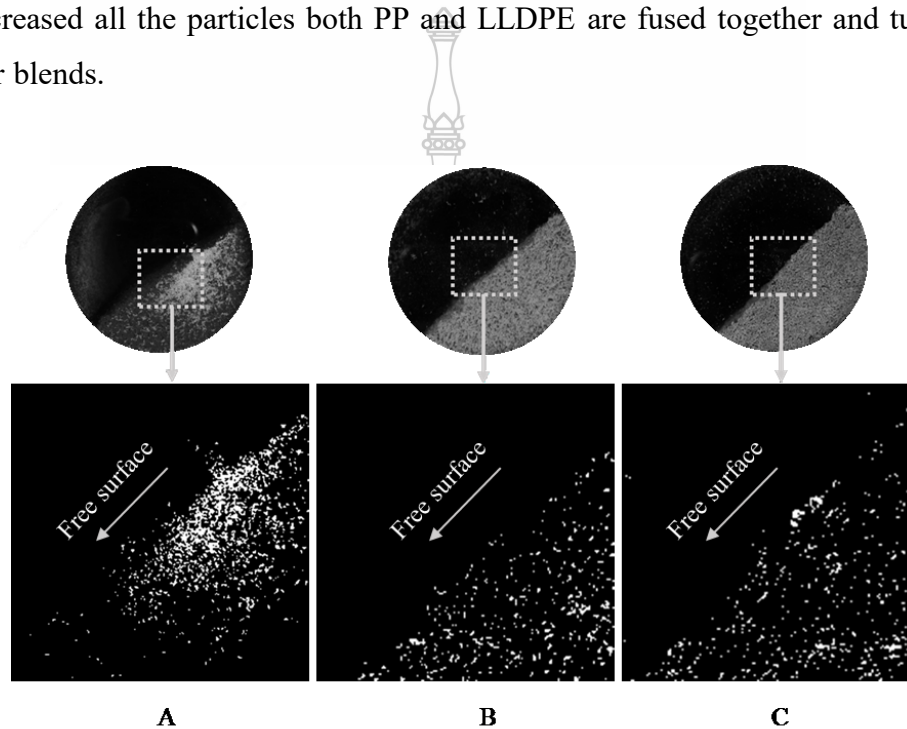


Figure 4.5 The distribution of PP particles at free surface area; A is PP-L/LLDPE, B is PP-M/LLDPE and C is PP-S/LLDPE; where white colors are LLDPE particles.

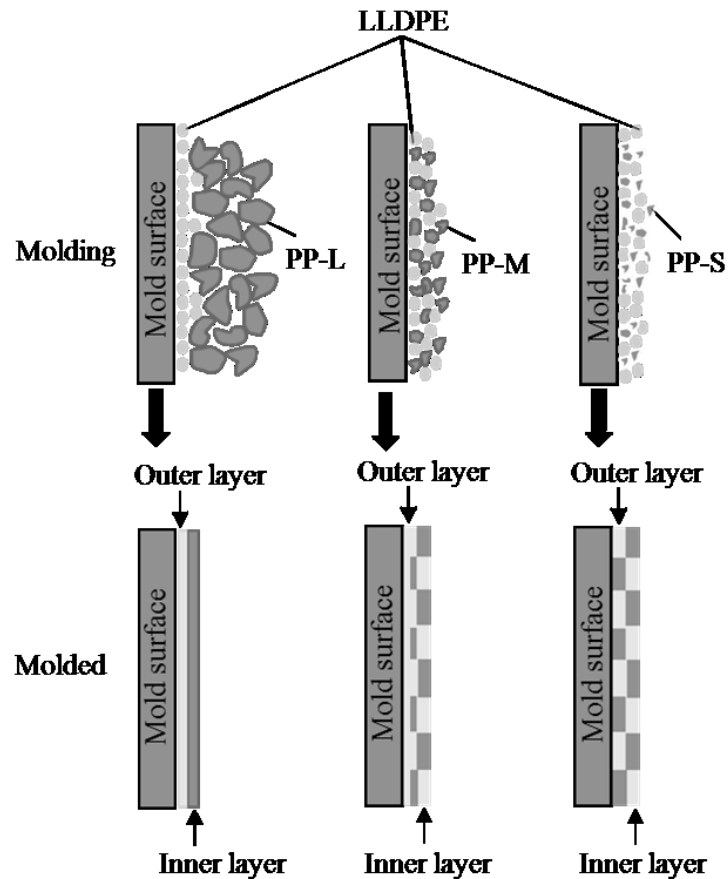


Figure 4.6 Schematic of the melting deposition of PP/LLDPE at the different PP particle size.

4.1.2.6 Morphology

The cylindrical specimen was cut along the length in the same position to investigate the layer separation by the digital microscope. The test results are shown in Figure 4.7 A is PP-L/LLDPE, B is PP-M/LLDPE and C is PP-S/LLDPE, it can be seen that the size of the smaller PP affects the separation of the PP/LLDPE clearly, the smaller PP particles make the specimen more likely to mix well. On the other hand, larger PP particles tend to separate layers.

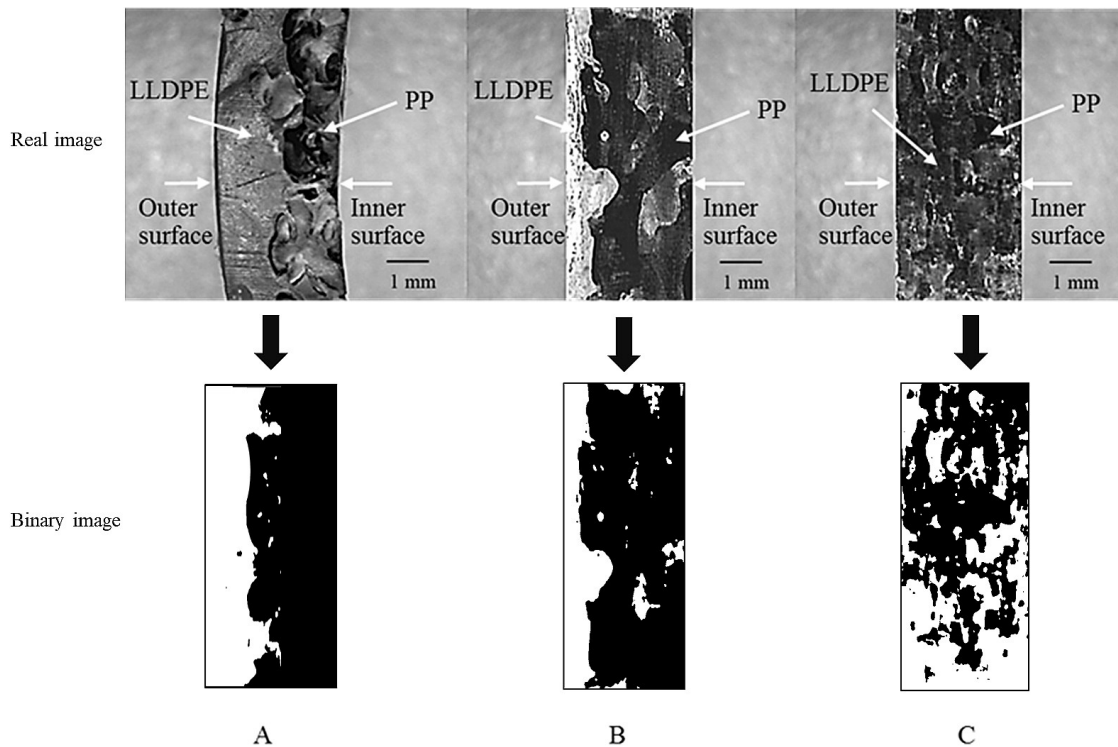


Figure 4.7 Separation phase in specimens; A= PP-L/LLDPE, B = PP-M/LLDPE and PP-S/LLDPE.

4.1.2.7 Thermal properties

This test is intended to verify polymer compatibility, the melt temperature transition (T_m) and polymer distribution on the specimen surfaces. The specimen of the DSC test cut from the cylindrical parts and separated as the inner, middle and outer surfaces as shown in Figure 4.8(A). The middle surface used for investigation the compatibility of polymers. The result showed in Figure 4.8(B), in the case of a pure polymer shows single-peak, where T_m was found at 129.4 and 169.7 °C of LLDPE and PP, respectively, in the case of the mixed polymer shows little changes, but it is noteworthy that the temperature peaks have double-peak, which means PP incompatible with LLDPE, where the first peak at a lower temperature is LLDPE, and the second peak at a higher temperature is PP. The inner and outer surfaces specimen previous preparations were used to investigate the distribution of the polymers on surfaces. The specimen with the separation as two-layered must exhibit the change of temperatures similar to pure polymer, with has single-peak of T_m both the inner and outer surfaces. Conversely, the specimen non-separation as two-layered has to exhibit the change of

temperatures similar to the polymer blend, with has double-peak of T_m both the inner and outer surfaces. The T_m thermograms of the inner and outer surfaces of the specimens were shown in Figure 4.8(B). In the case of both PP-M/LLDPE and PP-S/LLDPE, T_m has double-peak both the inner and outer surfaces, means that PP and LLDPE distribute cover both the inner and outer surfaces similar to the polymer blend, the separation as two-layered not happens. In the case of PP-L/LLDPE, T_m has single-peak both the inner and outer surfaces. It indicates that the specimen has separation as two-layered, PP distributes to the inner surface and LLDPE distributes to the outer surface, which observing from the temperatures peak appearance on the inner and outer surfaces have similar to pure PP and pure LLDPE respectively.

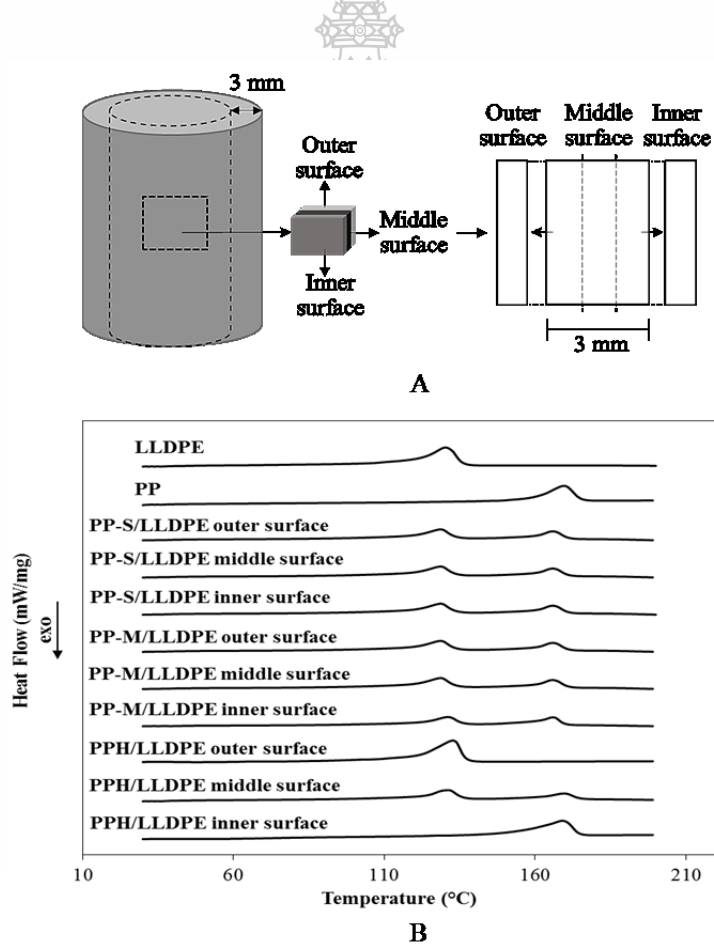


Figure 4.8 DSC specimen preparation in (A) and (B) melt transition temperature (T_m) thermograms.

4.1.2.8 Surface roughness

In this inspection, the specimen is cut from the midpoint of the cylindrical specimen and captured by the digital microscope both the inner and outer surfaces as shown in Figure 4.9, After that, the images of each specimen will be analyzed to show the value of the surface roughness in term of the arithmetic mean of the surface roughness by image analysis program as called ImageJ in function the 'surfJ', the results are shown in Table 4.2. The analysis showed that the inner surface of the specimen was tended more smooth when the size of the PP was smaller, but when considering the roughness of the outer surface, it was found that in the case of PP-L/LLDPE has a smoother surface than PP-S/LLDPE and PP-M/LLDPE respectively, it seems to be the result of the separation as two-layered of the specimen. In the case of PP-L/LLDPE, small LLDPE particles percolate to the gap and undergo to get the heat on the mold surface easily, resulting in sufficient time to sintering and coalescence, causing the surface is smoother. At the same time, large PP particles and higher melting points will still continue to roll until sufficient heat is obtained, it will soften and attach to the molten LLDPE. As the process progresses to this stage, the heat rates generated within the mold are slowed down by the thickness of molten polymer, thereby causing the large PP particles obtained to under-heat and no more sufficient time for complete fusion, which causes the inner surface of the specimen is higher rough. Although that behavior has occurred as same as in the case of PP-M/LLDPE, the results of a lower mobility or poor flow characteristics, causing LLDPE particle separate and move to the mold surface less, which makes it just a thin layer that coated on the outer surface only. In the case of PP-S/LLDPE, the roughness of the inner and outer surfaces is similar, indicating that the PP and LLDPE particles are well mixing and without the separation as two-layered.

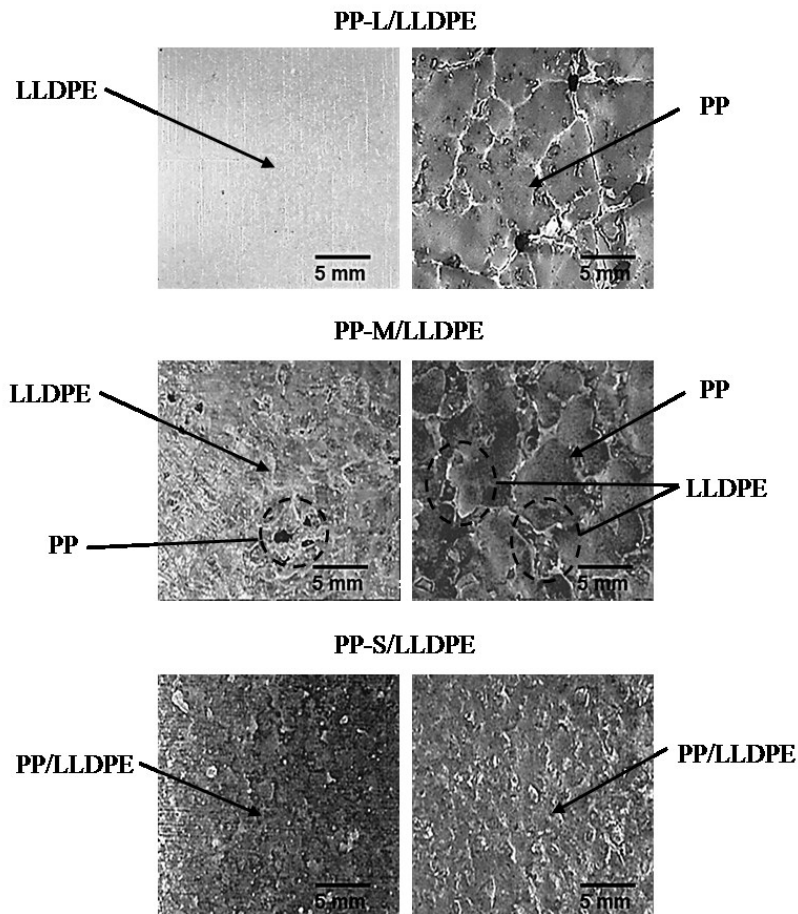


Figure 4.9 Surface roughness; the left hand is an inner surface and the right hand is an outer surface.

Table 4.2 The arithmetic mean of surface roughness of a mixed polymer (different size of PP).

Materials	Arithmetic mean of surface roughness, Ra(micron)	
	Inner surface	Outer surface
PP-L/LLDPE	23.78	11.90
PP-M/LLDPE	20.67	14.89
PP-S/LLDPE	14.37	14.22

4.1.2.9 The wall thickness distribution

The wall thickness distribution was performed by longitudinal cutting and was evaluated by a digital micrometer at a spacing of 5 mm as shown in

Figure 4.10, the standard deviation of wall thickness distribution. As expected, PP particle size decreasing shows greater the uniformity of PP/LLDPE wall thickness distribution, as result of smaller particles have a faster sintering rate than larger particles make it flow faster and thoroughly distribute the mold. In addition, it will be noted that the results are related to the surface roughness. The specimen with a smooth both the inner and outer surfaces is more uniformly the wall thickness distribution than the specimen with a smooth one-side surface.

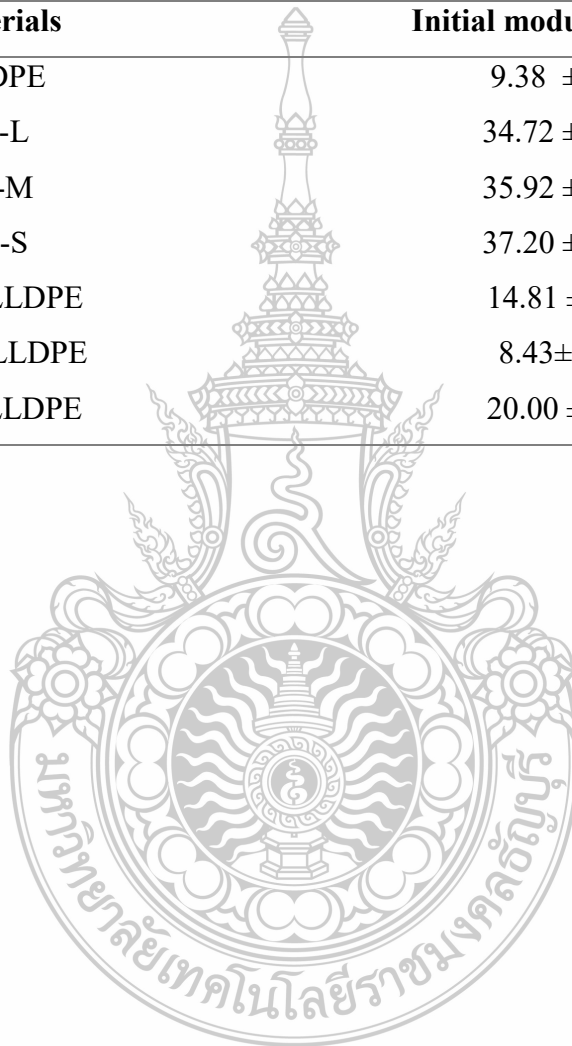
4.1.2.10 Mechanical properties

The mechanical properties were tested for a cylindrical specimen with an inner diameter of 60 mm, length of 50 mm, and thickness of 3 mm. The tensile test machine was used for the compressive test, at a load of 1 kN and speed of 10 mm/min. This test is reported in terms of the initial modulus [48]. The relation of a stress-strain curve as shown in the Figure 4.11. As expected, PP pure exhibits high compressive strength and low elongation. In contrast, LLDPE pure has low compressive strength but high elongation. As mixing PP and LLDPE together, it was found that LLDPE improved the elongation properties of PP. For considering the effect of particle size of PP on the initial modulus of PP/LLDPE, as shown in Table 4.3, it was found that PP-S/LLDPE has a higher modulus than PP-L/LLDPE and PP-M/LLDPE at about 20.00, 14.81 and 8.43 MPa respectively. It is well known that smaller particles are mixing and fusion better and faster than larger particles, making it less the defects and have higher strength. However, even if the large particles are poorly mixing and fusion, the separation as two-layered of the specimen is one factor that may make a higher strength because of each of polymers that forming as the outer and inner more likely to complete fusion, which clearly to see in case of PP-L/LLDPE. In addition, from observing during testing and considering the deformation characteristics of the specimen from the graph in Figure 4.11, it was found that PP-M/LLDPE and PP-S/LLDPE showed the deformation characteristics in ductile materials, whereas PP-L/LLDPE showed the deformation characteristics both the brittle and ductile deformation characteristics, which seem to be a result of separation as two-layered of the specimen, the first period of test the PP inner layer with higher strength gradually deformed by appearance a micro-crack, which cause

a graph of strength is dropped. Although the cracks reduce the strength of the specimen, LLDPE is the outer layer and highly flexible, help to maintain the shape, prevents the specimen from fracture, and also helping the specimen withstand continuously load.

Table 4.3 The initial modulus of pure and mixed polymer (different the size of PP).

Materials	Initial modulus (MPa)
LLDPE	9.38 ±2.25
PP-L	34.72 ± 3.01
PP-M	35.92 ± 2.51
PP-S	37.20 ± 3.21
PP-L/LLDPE	14.81 ±1.72
PP-M/LLDPE	8.43±1.75
PP-S/LLDPE	20.00 ±1.85



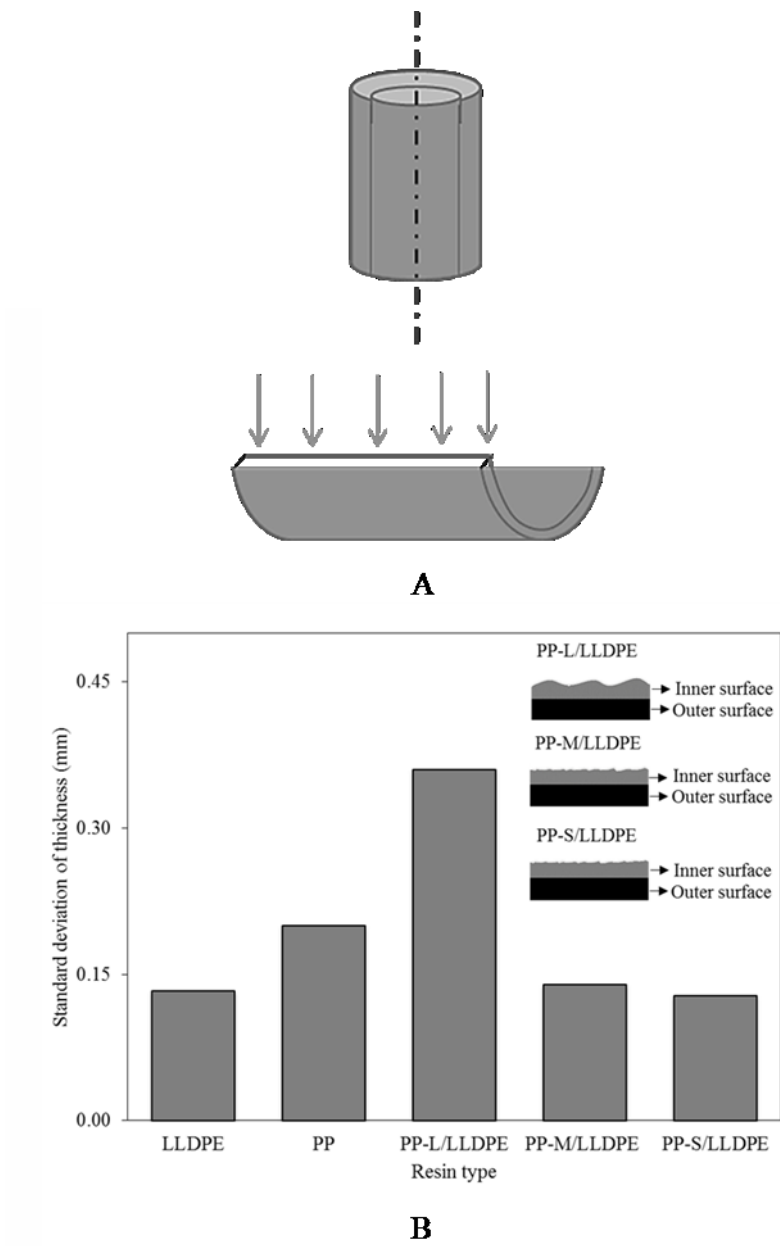


Figure 4.10 The specimen preparation is A and the standard deviations of thickness is B.

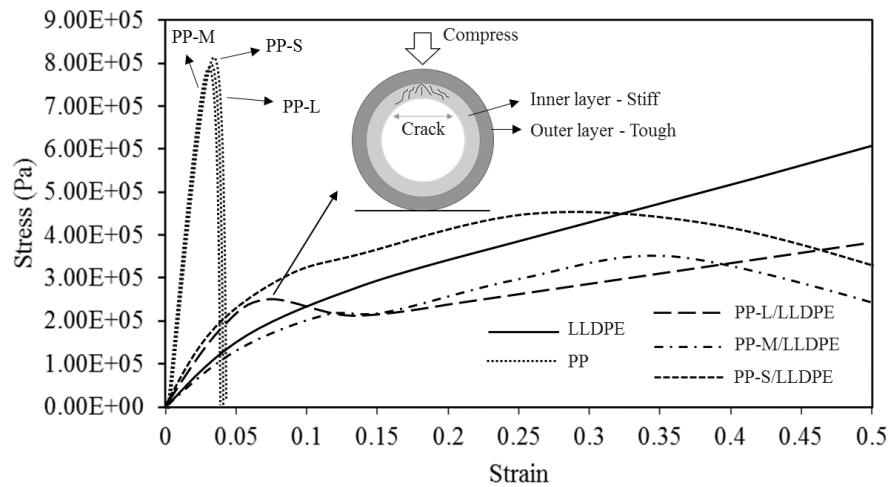


Figure 4.11 The stress-strain curve of pure and mixed polymer (different the size of PP).

4.2 The Effect of Particles Shape of Polypropylene on Two-Layered Process

The aim of this experiment is examined the possibility of molding PP/LLDPE two-layered in the rotational molding process by using techniques uncomplicated, where using PP with the different particle size of PP. Thus, the equipment, experiment procedure, and the characterization were performed as same as in a topic 4.1.1.2 and 4.1.1.3.

4.2.1 Experimental

4.2.1.1 Materials

From the previous research about the particle shape of materials after grinding indicated that the different of polymer structure affects the characteristics of the particles after grinding. Thus, this experiment used different of PP.

Three types of materials were used: linear low-density polyethylene grade M3204RU (powder form) with MFI 4 (190 °C/2.16 kg), a density of 0.932 (g/cm³), and thermal conductivity of 0.34 ((W·m⁻¹·K⁻¹, (20 °C)), as supplied by SCG Chemical (Thailand); polypropylene copolymer, or PPC grade EP549H (pellet form), with MFI 11 (230°C/2.16 kg), stabilizers (trade secret) < 5 wt.%, and a density of 0.90 (g/cm³), as supplied by HMC Polymers Co., Ltd.; and

polypropylene homopolymer, or PPH grade 1100NK (pellet form), with MFI 11 (230 °C/2.16 kg), and a density of 0.914 (g/cm³), as supplied by IRPC Public Co., Ltd. Both PPs have an equal thermal conductivity of 0.22 ((W·m⁻¹·K⁻¹, (20 °C)). Before processing, to clearly observe the behavior and phenomena of the molding materials, a twin screw extruder was used for compounding resins with a color pigment of 1% by weight; in addition, LLDPE resin was compounded with a yellow color, and to control the quality of the particles similarly to a commercial grade, it was reduced in size by a pulverizer. The PPH and PPC resins were compounded with red and green color, respectively. In addition, because it is difficult to reduce the size of the PP using a pulverizer, in this research the size of the PP was reduced using a rotary knife cutter machine, and the particle size was controlled after determining the rate and amount of materials used as 15 min/batch (300 g).

The powder morphology was examined under a digital microscope, and the powder characteristics such as the mean circularity and mean particle size were determined using an image analysis (ImageJ 1.46r). This program has been widely used and accepted in various researches [49–51] and has many features depending on the demands of the operator. The particle shape and results of the particle analysis of LLDPE, PPC, and PPH are shown in Table 4.4, and the results after the size reduction indicate differently shaped particles; the LLDPE and PPC particles have a rather flat shape because they were elongated from the shearing, which is a characteristic typically found in the deformation of ductile materials. In the case of PPH, a rounder shape was found than in the previous cases because it is a brittle material and does not elongate much [52].

4.2.2 Results and discussion

4.2.2.1 Powder properties

The results of the bulk density, dry flow rate, and the particle characteristics are shown in Table 4.4 and Figure 4.12 respectively. As expected, the particles showed a fast flow rate, which causes the bulk density to increase. LLDPE, with the smallest particle size, showed a bulk density and dry flow rate of 0.34 g/cm³ and 9.4 seconds respectively. PPH and PPC were also compared, and showed a similar particle size distribution and mean particle size, but a difference in particle shape. The results

indicate that the first case has a higher bulk density and faster dry flow rate than the latter case. However, with regard to the different particle shapes, relatively little analytical data exist on the correlation between particle shape and bulk density. Most analyses have similarly indicated that particles with a regular shape (rather spherical) have a higher bulk density because they have either a higher packing fraction or a lower fraction of voids than irregularly shaped particles. Irregular shapes have been described as coming in various types, such as a tail-like appearance, or a flat and fiber-like needle shape. When LLDPE and PP were mixed at a ratio of 50:50, the bulk density and dry flow rate were increased for both cases owing to LLDPE with a small size appropriately improving the particle size distribution in the system; in addition, the particle size distribution directly affects the bulk density when small particles are mixed with large particles at an appropriate proportion (over 3 times), and the bulk density increases because small particles fill in the gaps between large particles, resulting in a narrower distance between particles [53]. This also affects the separation or degree of mixing of the particles, and if the particle distribution is wide, the particle separation will be strong, indicating that the degree of mixing is low [54]. With the case of PPC/LLDPE, the dry flow rate was increased noticeably as compared to pure PPC, because the number of particles with a flat shape and large size decreased while mixing with the LLDPE at a ratio of 50:50.

Table 4.4 Powder properties of a pure and mixed polymer (different the shape of PP).

Materials	Mean particle size (μm)	Mean circularity		Bulk density (g/cm^3)	Dry flow (sec)	Hausner ratio	MFI ($\text{g}/10 \text{ min}$) ¹
		Top view	Side view				
LLDPE	365	0.67	0.53	0.34	9.40	1.19	4.00
PPC	1,471	0.73	0.56	0.34	21.00	1.16	6.81
PPH	1,403	0.76	0.71	0.38	10.70	1.14	5.10
PPC/ LLDPE	-	-	-	0.37	10.90	1.22	5.71
PPH/ LLDPE	-	-	-	0.39	13.33	1.17	5.61

For the Hausner ratio (shown in Table 4.4), it was shown the mobility of the particles that moving passes through the gap of the neighboring particles. The Hausner ratio lower is better flow characteristics. The results are reported on the scale of the flowability. The particles with good the flow characteristics exhibited values in the range 1.12-1.18, whereas the particles with moderate of flow characteristics exhibited values in the range 1.19–1.25 [35]. The results showed that the case of pure PPH and PPC exhibit the values in the range of a good the flow characteristics at 1.14, 1.16 respectively, whereas LLDPE exhibit a moderate the flow characteristics at 1.19. The case of mixed polymer PPC/LLDPE and PPH/LLDPE show that the first case exhibit the values in the range of a good the flow characteristics at 1.17, and the latter case exhibit a moderate the flow characteristics at 1.22. These results indicate that the characteristics of particles such as size, shape, and size distribution affected to the Hausner ratio. The particles with the irregular shape or both a smaller size and an irregular shape have the inter-particulate interactions higher than the regular particles shape. Moreover, the increasing content of the particle with an irregular shape is decreased the particles mobility, thereby causing a higher the Hausner ratio.

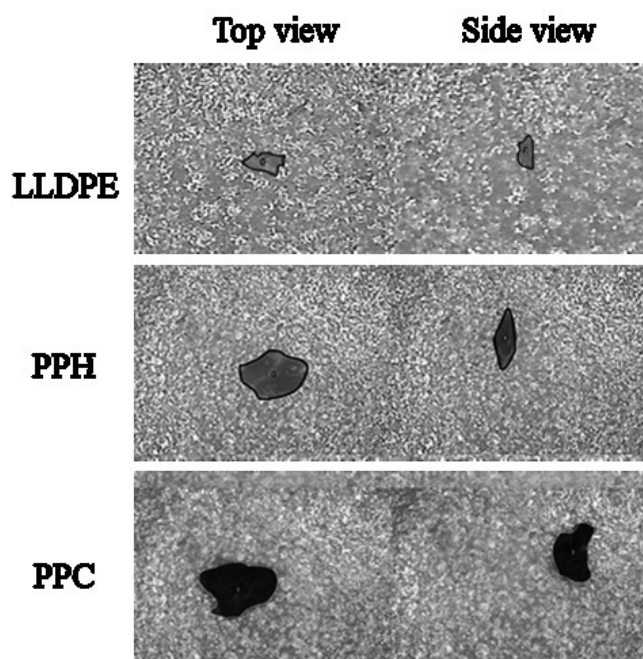


Figure 4.12 The particle characteristics of LLDPE, PPC, and PPH.

4.2.2.2 Melt flow index (MFI)

Melt flow index tests were used to investigate the flow properties of all materials after compounding. As the results shown in Table 4.4, the LLDPE compound was not different from pure LLDPE, from which previous reports have described that molding often encounters thermo-mechanical and thermo-oxidative degradation during the reactions of molecular chain scission, branching, and crosslinking. These affect the polymer molecular weight and molecular weight distribution (MWD). It has also been found that when a polymer is recycled or heated several times, it will result in unchanging flow properties, which may be due to the branching and cross-linking that occur in the molecular structures. On the other hand, if the chain of molecules is destroyed, it will affect the flow properties of the polymer because the molecular weights are reduced [36–39]. Because the molding conditions in this experiment were determined at a temperature of 190 °C, both PPs required testing under the same conditions as LLDPE. The results show that the MFI of PPC and PPH decreased to 6.81 and 5.10 (g/10 min), respectively, which indicate that the melt flow properties of both PP tend to approach those of LLDPE. In the case of the mixed polymer, both PPC/LLDPE and PPH/LLDPE show similar MFI of 5.71 and 5.61 respectively.

4.2.2.3 Sintering rate

The results are as shown in Figure 4.13, LLDPE changed to a rubbery state at around 70 °C, and sintering was complete at 110.4 °C, whereas PPC and PPH changed to a rubbery state at 110 °C, although PPC sintered faster at 148.4 °C than PPH at 157.7 °C. In general, the effect of the sintering rate usually depends on the viscosity of the polymer and the incipient contact angle of the particles. In this experiment uses PPC and PPH with the similar viscosities but different the particle shape. Thus, the reason why PPC faster sintering than PPH seems to be the incipient contact angle between the particles. PPC with the large contact surface shows well heat induction, causing the rate of the integrity of the melting increases, and also directly affects the melting deposition and the rate of melt formation of the two-layered proceeding.

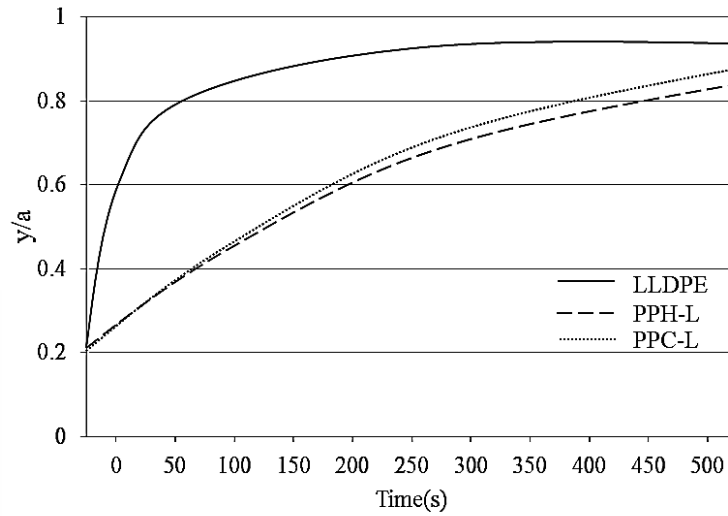


Figure 4.13 Sintering rate of LLDPE, PPC, and PPH.

4.2.2.4 Temperature profile of air inside the mold

In the case of a mixed polymer (shown in Figure 4.14), based on observations, it was found that at point A, where the temperature is around 50 °C, LLDPE with a lower melting point and smaller particle size than PP gradually softened and started to be coated on the mold surface. At the same time, some of the PP particles became sticky and were pinned to the LLDPE. However, most of the PP particles were still rolling until the temperature inside the mold reached point B. At this point, all of the particles stopped moving and were ready to enter the particle sintering and coalescence processes. When comparing the difference between PPH/LLDPE and PPC/LLDPE, it was found that the internal air temperature profile of the first case showed a slightly lower heat rate within the range of point A to point B. This was probably the result of the melting deposition pattern; in addition, point B to point C, and point C to point D, for both cases also showed a slight difference.

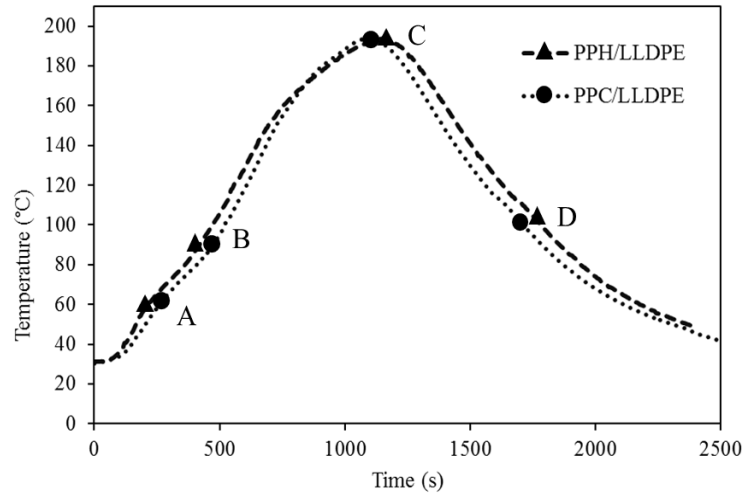


Figure 4.14 Internal air temperature of (A) pure polymer and (B) mixed polymer (different the shape of PP).

4.2.2.5 The particles segregation and melt deposition of the PP/LLDPE with the different particles shape of PP.

In general, the mixing and segregation patterns of particles with a similar melting point or the same kind of polymer, but with different sizes at a ratio of 50:50 in a horizontal rotation, have been described for two cases: at room temperature and at the processing temperature.

At room temperature, the particle segregation pattern form takes place in a similar manner while the mold is rotated. Large particles appear at the top of the flow layer (free surface), and the solid body rotation area is full of large particles. At the same time, small particles are gradually percolated through the gaps between large particles into the core, as shown in Figure 4.15(A). The mechanism of this occurrence is evident when the particles have a high flowability and proper particle size distribution. However, the presence of irregularly shaped particles will decrease the ability to percolate [47], which may affect the pattern of particle segregation. At the processing temperature, the melting deposition patterns depend on the rate of the melt formations. At a low rate, the heat transfer between the mold surface and the particles will occur slowly and thus the particles will gradually become a liquid. An adhesion force between the particles and the mold surface will occur. When the particles stick to the mold surface, it indicates that the adhesion force is sufficient to defeat the pull of gravity. Thus, small particles with a high surface area are able to receive heat and

melt faster than larger particles; in addition, they have sufficient adhesion force to defeat gravity, making them stick to the mold surface faster than large particles. At the same time, large particles with less adhesion force than gravity will continue rolling and stop when the adhesion force between them and the liquid (previously melted particles) is sufficient to defeat gravity [12]. Thus, at the mold surface, the fraction of small molten particles is higher than that of large particles. On the other hand, at a high rate, differences in the melt deposition pattern are shown, and the heat transfer between particles and the mold surface occurs rapidly. The small and large particles become liquid and are coated on the mold surface at nearly the same time, which makes the fractions of molten particles equivalent at the mold surface. In spite of different materials used in this experiment, the results are the same as described above. At room temperature, the small LLDPE particles appear at the core and tend to roll up to the free surface, as shown in Figures 4.15(B) and (C). Although this pattern occurs in both PPC/LLDPE and PPH/LLDPE, it should be noted that their patterns of occurrence are slightly different. In the first case, there are fewer LLDPE particles in the core than in the latter case, which may be due to the influence of the particle shape, resulting in the inability to move because PPC particles with a flat shape block the movement or percolation of LLDPE particles, as shown in Figure 4.15(D) and the percolation of particles in the case of PPH/LLDPE shows in Figure 4.15(E).

At the processing temperature, PPH/LLDPE represents a melting deposition pattern similar to the case of a low rate of melt formation. The small particles with low melting points melt and stick to the mold surface faster than large particles with high melting points. The difference in melting point of small and large particles shows a clear melting deposition pattern. The amount of fluid that is coated on the mold surface in the initial stage depends on the ability of the small particles to percolate and pass through the voids to the mold surface. Increasing the layer thickness slows the heat rate within the mold. In the case of PPC/LLDPE, although the melting deposition pattern demonstrates that the first period of heating is similar to the first case, the small particles are coated on the mold surface first, but from the visual observation during molding, it was found that, while the mold is rotating, the small particles have difficulty percolating to the mold surface to receive heat because they are blocked by large particles with a flat shape, which lowers the fraction of small particles appearing at the mold surface. When these particles are melted, they become

a thin film layer coating the mold surface, resulting in a slightly higher initial heat rate than the first case. The heat transfer occurs quickly from the film layer toward the inside of the mold, causing the inner particles to receive heat faster, resulting in a higher rate of melt formation between the PPC and LLDPE particles. The PPC particles rapidly become stuck to the film layer (molten LLDPE). Thus, the specimens have an unclear layer separation and seem to resemble a polymer blend.

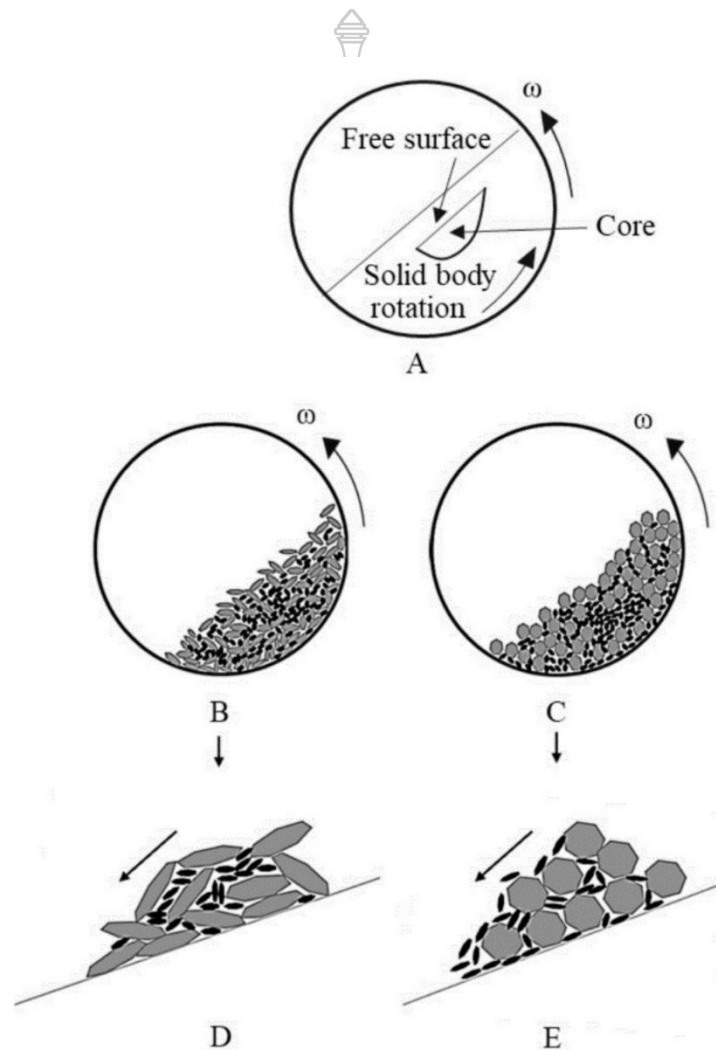


Figure 4.15 Characteristics of powder formation in radial segregation: (A) particle segregation diagram; particles segregation patterns of (B) PPC /LLDPE and (C) PPH /LLDPE; (D) and (E) are the percolation of particles during avalanche of PPC/LLDPE and PPH/LLDPE respectively; where gray color indicates PPC and PPH, and black color indicates LLDPE.

4.2.2.6 Morphology

After molding, the cylindrical specimens were longitudinal cutting to investigate the phase separations using a digital microscope. The results show in Figure 4.16, where (A) indicates PPC/LLDPE and (B) is PPH/LLDPE. It was clear that the PPH/LLDPE specimens tend to separate in a two-layered mold. The boundaries between the outer and inner surfaces are quite clear, and LLDPE with a small size and low melting point reaches the outer surface, and PPH reaches the inner surface. In the case of PPC/LLDPE, an unclear separation is shown, with PPC particles distributed all throughout both the inner and outer surfaces. This phenomenon is described in the following section on a two-layered mold.



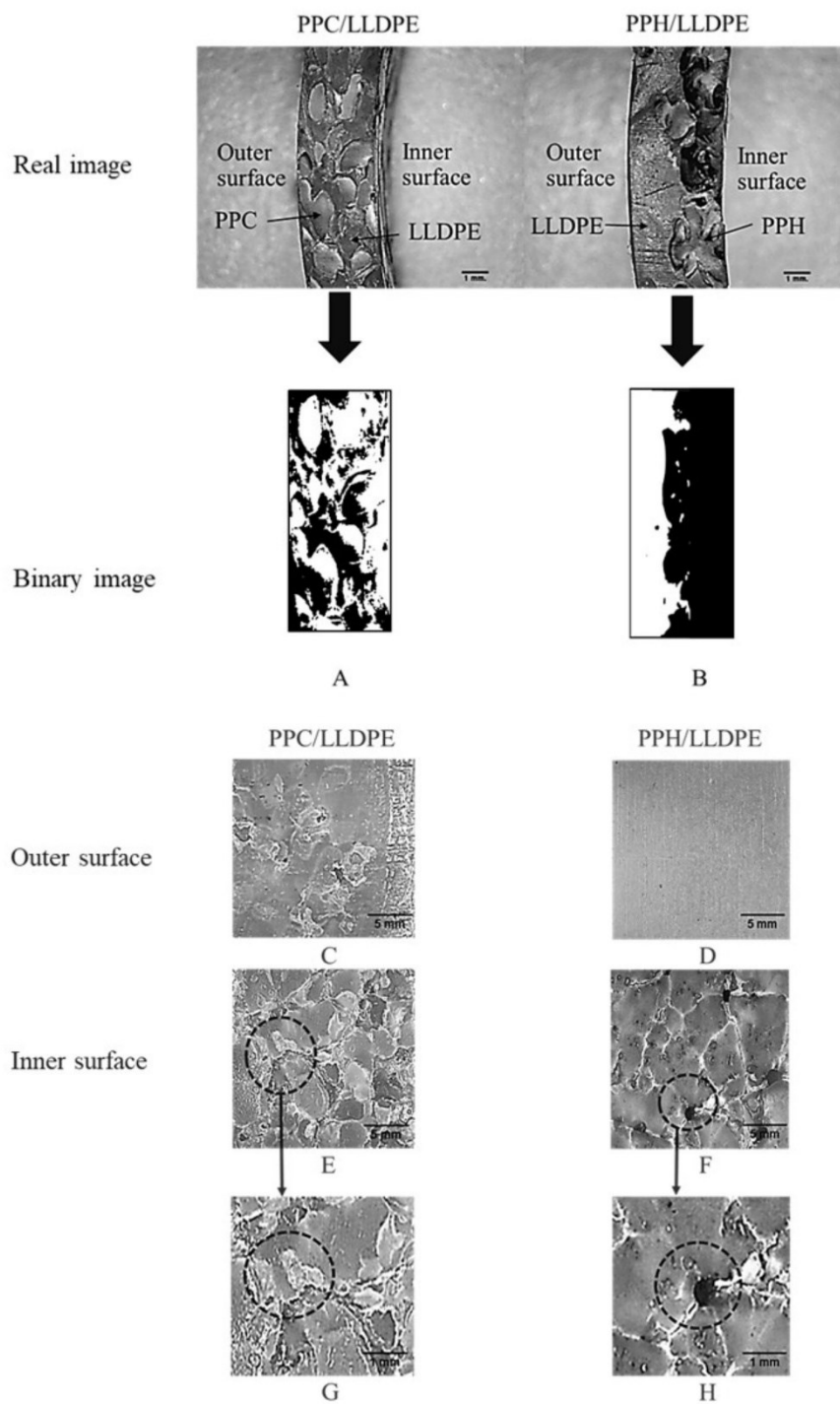


Figure 4.16 Separation phase in (A) PPC /LLDPE and (B) PPH /LLDPE specimens; the surface of specimens: (C, D) outer surface, (E, F) inner surface, and (G, H) appearance of defects on the inner surface of PPC/LLDPE and PPH/LLDPE, respectively.

4.2.2.7 Thermal properties

This test is intended to verify polymer compatibility, the melt temperature transition (T_m) and polymer distribution on the specimen surfaces. The specimen of the DSC test preparation as same in Figure 4.8(A). The middle surface was used for investigation the compatibility of polymers. The result was shown in Figure 4.17, in the case of a pure polymer shows single-peak, where T_m was found at 129.4 °C, 169.0 °C, and 169.7 °C of LLDPE, PPC, and PPH, respectively, in the case of PPC/LLDPE and PPH/LLDPE shows little changes, but it is noteworthy that the temperature peaks have double-peak, which means the both of PPH and PPC are incompatible with LLDPE, where the first peak at a lower temperature is LLDPE, and the second peak at a higher temperature is PP. The inner and outer surfaces specimen previous preparations were used to investigate the distribution of the polymers on surfaces. The specimen with the separation as two-layered must exhibit the change of temperatures similar to pure polymer, with has single-peak of T_m both the inner and outer surfaces. Conversely, the specimen non-separation as two-layered has to exhibit the change of temperatures similar to the polymer blend, with has double-peak of T_m both the inner and outer surfaces. The T_m thermograms of the inner and outer surfaces of the specimens were shown in Figure 4.17. In the case of PPC / LLDPE, T_m has double-peak both the inner and outer surfaces, means that PPC and LLDPE distribute cover both the inner and outer surfaces similar to the polymer blend, the separation as two-layered not happens. In the case of PPH / LLDPE, T_m has single-peak both the inner and outer surfaces. It indicates that the specimen has separation as two-layered, PPH distributes to the inner surface and LLDPE distributes to the outer surface, which observing from the temperatures peak appearance on the inner and outer surfaces have similar to pure PPH and pure LLDPE respectively.

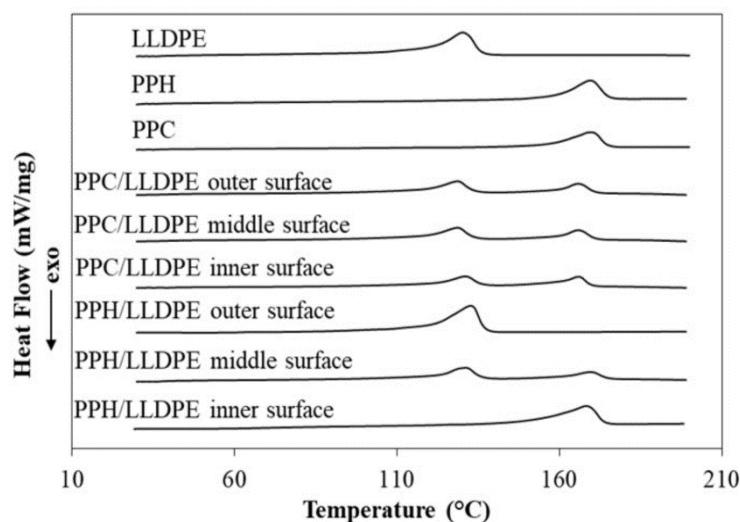


Figure 4.17 DSC thermograms of a pure and mixed polymer (different the shape of PP).

4.2.2.8 Surface roughness

The outer and inner surfaces of the specimens were monitored using a digital microscope combined with a photo analysis program (ImageJ). This program is widely accepted and can be used to analyze the surface roughness [55, 56]. The surface appearances of the specimens based on the arithmetic mean of the surface roughness shown in Table 4.5. In the case of a pure polymer, as expected, the outer surface (adjacent the mold wall) showed an arithmetic mean surface roughness lower than that of the inner surface owing to the outer surface being directly heated, which causes complete sintering and coalescence. Thus, it is normal for a commercial grade LLDPE to show a smoother surface than both PPs. For the mixed polymer, it was shown that the outer and inner surfaces of PPH/LLDPE have less surface roughness than those of PPC/LLDPE as shown in Figures 4.16(C, D) and (E, F). In addition, it was observed the defects as a result of poor particle segregation appeared on the inner surfaces of PPC/LLDPE and PPH/LLDPE, as indicated in Figures 4.16(G) and (H) respectively, and in the case of PPC/LLDPE, the sintering of the PPC was disturbed by some of the LLDPE particles, whereas in PPH/LLDPE, it was shown that PPH formed as an inner layer and tended to melt more homogeneously. However, it is noteworthy that even though it formed a complete inner layer, holes still remained on the surface. This event is related to the sintering and densification, which have been found to be less complete than they should be [57]; in addition, the large sizes of the

PP particles disrupt the complete sintering because they do not receive sufficient heat, which seems to result from the thickness of the polymer layer, which is a good thermal insulator, and the heat has difficulty passing into the inside of the mold. An incomplete fusion of particles can be easily solved by increasing the temperature or the molding time [26], including increasing the rotational speed, but it should be recalled that a polymer with a low thermal degradation point or that is unstable due to heating, has a chance to lose its rheological properties, making it difficult to mold. In addition, the final products will show low mechanical properties or the appearance of burn markings.

Table 4.5 Arithmetic mean of surface roughness of a pure and mixed polymer (different the shape of PP).

Materials	Arithmetic mean of surface roughness, Ra (micron)	
	Inner surface	Outer surface
LLDPE	3.98	3.49
PPC	13.73	10.99
PPH	14.65	10.77
PPC/LLDPE	25.96	13.94
PPH/LLDPE	23.78	11.90

4.2.2.9 The wall thickness distribution

The wall thickness distribution was performed by longitudinal cutting and was evaluated by a digital micrometer at a spacing of 5 mm as shown in Fig. 4.10(A). The standard deviation of wall thickness distribution showed in Figure 4.18. As expected, PPC/LLDPE shows a slightly better wall thickness distribution, because PPC has a faster sintering rate than PPH make it flow faster and thoroughly distribute the mold. However, although in this experiment has described the wall thickness distribution based on the sintering rate that makes a polymer to flow faster, it should be noted that in the other cases that different from this experiment may have to consider the melt viscoelastic properties too.

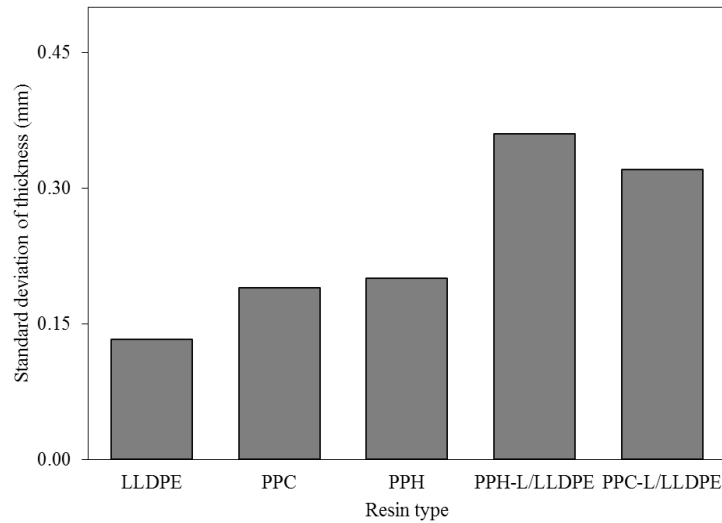


Figure 4.18 The standard deviation of the wall thickness of a pure and a mixed polymer.

4.2.2.10 Mechanical properties

The mechanical properties were tested for a cylindrical specimen with an inner diameter of 60 mm, length of 50 mm, and thickness of 3 mm. The tensile test machine was used for the compressive test, at a load of 1 kN and speed of 10 mm/min. This test is reported in terms of the initial modulus [48]. The results of initial modulus and stress-strain curves as shown in Table 4.6 and Figure 4.19 respectively. In the case of a pure polymer as PPH, PPC and LLDPE show initial modulus at 34.72, 18.51 and 9.38 MPa respectively. Because, PPH has CH_3 attached to main chain structure, which inhibits rotation of the chain making a stronger but less flexible material [58]. In contrast, LLDPE with linear structure has lower initial modulus but higher flexible than both PPs, whereas PPC with ethylene groups in main structure has higher flexible than PPH, and initial modulus is between PPH and LLDPE. In the case of the mixed polymer, the initial modulus was compared to pure LLDPE, because one of the objectives of this work is to improve the stiffness of LLDPE. The result showed that PPC/LLDPE decreased by 63.43% and PPH/LLDPE increased by 57.89% as compared to pure LLDPE, and from the stress-strain curves also showed that LLDPE improved flexible both PPs. A comparison between the initial modulus of PPC/LLDPE and PPH/LLDPE showed clearly that the latter case had higher initial modulus than the first case because pure PPH is stronger than pure PPC. Moreover, the defects in the specimen may be one of the

factors that decrease mechanical properties, in the case of PPC / LLDPE with non-separation as two-layered shows more the defects due to an incomplete melting of the particles as shown in Figures 4.16(E) and (G), while PPH / LLDPE with separation as two-layered shows fewer the defects as the particles tend to melt more homogeneously than the PPC / LLDPE as shown in Figures 5(F) and (H).

Table 4.6 The initial modulus of a mixed polymer (different the shape of PP).

Materials	Initial modulus (MPa)
LLDPE	9.38 ±2.25
PPC	18.51 ±2.31
PPH	34.72 ± 3.01
PPC/LLDPE	3.43 ±0.75
PPH/LLDPE	14.81 ±1.72

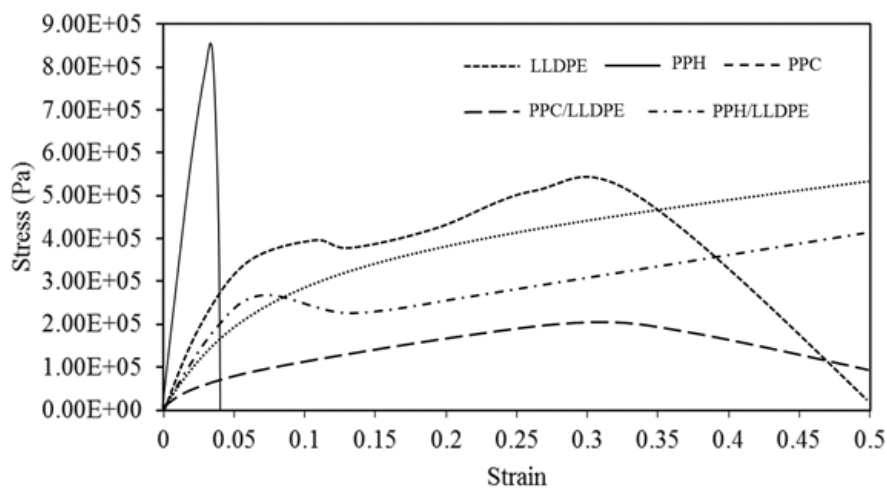


Figure 4.19 Stress-strain curves and initial modulus of a pure and mixed polymer (different the shape of PP).

4.3 The Effect of Rotational Speed on Two-Layered Process

Based on prior experimental results, it has been demonstrated that the particles flow characteristics contribute significantly to the separation layer of the specimens. The clarity of the segregation usually occurs when small particles easy to percolate gap between the particles and going to the mold surface. However, from the previous research, it was found that the increase in rotational speed would affect the flow pattern and separation of the particles while solid, the small particles go to the edge rather than the middle of the mold. This phenomenal mechanism is quite complex, depending on many factors such as the length of the mold, the acceleration, the gravity, and the nature of the materials used. The purpose of this experiment is simply to observe the phenomena occurring during the forming and to compare the properties after the molding. So, to see clearly the differences that occurred during the molding and in the specimen, the rotational speed is set at 60 rpm.

4.3.1 Experimental

From the results in topic 4.1 and 4.2 showed clearly that large PP particles are likely to separate into a two-layered, so PPH sizes L, M, and PPC size L are used in this experiment. The Experimental procedure different with topic 4.1.1.2 only the speed of rotation, this experiments determined at 60 rpm. The Characterization used in the experiments are the same with topic 4.1.1.3.

4.3.2 Results and discussion

4.3.2.1 Powder properties

The bulk density and dry flow rates shows the efficiency of particles packing and particle mobility. The particle characteristics are shown in Figure 4.20. The results are shown in Table 4.7, In case of the pure polymer, PPH-L has the highest values, followed by PPH-M, PPC-L, and LLDPE respectively. In case of the mixed polymer, PPH-L/LLDPE has higher and faster bulk density and dry flow rates than PPH-M/LLDPE and PPC-L/LLDPE respectively, these show clearly that LLDPE improves the bulk density and dry flow rates of PP. These results directly related to the particle size distribution, which has been described from previously reported that the increasing or decreasing of the bulk density of polymer often depends on the particles size and the appropriate particle size distribution. For

the dry flow rate, it shows clearly as a result of the particles shape, which the decreasing of an irregular particle shape shows the increasing rates of the particles flow.

Table 4.7 Powder properties of a pure and mixed polymer.

Materials	Mean particle size (μm)	Mean circularity		Bulk density (g/cm^3)	Dry flow (sec)	Hausner Ratio	MFI (g/10min) ¹
		Top view	Side view				
LLDPE	368	0.67	0.53	0.34	9.40	1.19	4
PPH-M	758	0.66	0.66	0.36	11.87	1.16	5.17
PPH-L	1,403	0.76	0.71	0.38	10.70	1.14	5.10
PPC-L	1,471	0.73	0.56	0.34	21.00	1.16	6.81
PPH-M/LLDPE	-	-	-	0.38	10.97	1.19	5.52
PPH-L/LLDPE	-	-	-	0.39	10.10	1.17	5.61
PPC-L/LLDPE	-	-	-	0.37	10.90	1.22	5.71

¹ Measured at 190°C after color compounding.

² Cannot measure in standard conditions, required to apply the force to flow of powder.

The Hausner ratio is a test method that demonstrates the efficiency of particle motion passes gap. The test results ranged from 1.12 to 1.18 indicated the particle high flowability, while the particle with moderate flowability is indicated in the range from 1.19 to 1.25 [21]. The results of the tests in Table 4.7 show that in the case of a pure polymer, PPH-L, PPH-M, and PPC-L shows a higher flowability, whereas LLDPE shows a moderate flowability. In the cases of mixed polymer, PPH-L/LLDPE shows a high flowability, PPH-M/LLDPE shows a moderate flowability, and PPC-L/LLDPE shows a poor flowability. These results are shown that LLDPE with small particle moves through the gap of PPH-L better than PPH-M and PPC-L respectively.

4.3.2.2 Melt flow index (MFI) and 4.3.2.3 sintering rate

The MFI test and the sintering rate are shown in Table 4.7 and Figure 4.21, the results were discussed in the previous experiments in a topic 4.1.2.2 and 4.2.2.2 for the melt flow properties and 4.2.1.3, 4.2.2.3 for the sintering rate respectively. The small particles affect melt flow properties slightly because air trapped in the molten polymer, whereas the sintering rate test shows that smaller particles result in a higher sintering rate.

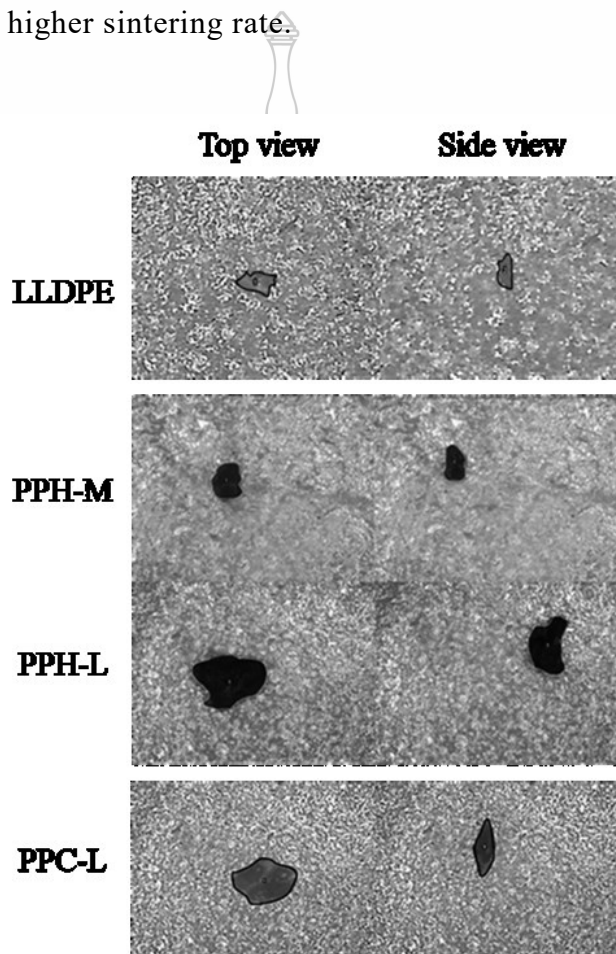


Figure 4.20 The particle characteristics of LLDPE, PPH-M, PPH-L, and PPC-L.

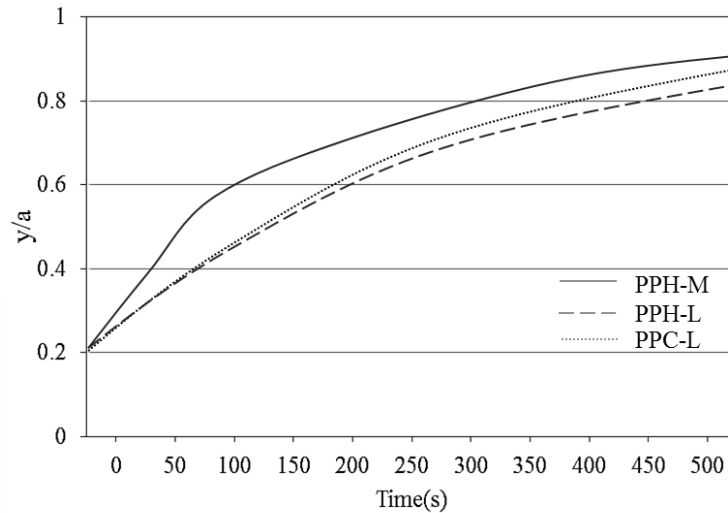


Figure 4.21 The sintering rate of PPH-M, PPH-L, and PPC-L.

4.3.2.4 Temperature profile of air inside the mold

The heat rate inside the mold is shown in Figure 4.22, In the case of PPH-L/LLDPE, PPH-M/LLDPE and PPC-L/LLDPE showed similar the tack temperature and the kink temperature of about 50 °C and 110 °C respectively. The increase in rotational speed causes the segregation pattern to be reversed, LLDPE particles overcome the friction, easy segregate or percolate to the mold surface, causing it easy and clear to the formation as the outer layer. The proceeding of the layer formation start as the mold is heated, LLDPE particles with a low melting point are melted and coated on the mold surface first, while PP particles with a higher melting point are not melted and most of it still rolling, but some of it is pinned by the molten LLDPE. The thickness of LLDPE that form as the outer layer gradually increases until PP particles which rolling inside take enough the heat, it will gradually melt and coat on the LLDPE molten as become to the inner layer. For considering the influence of the speed of rotation on the heat rate, PPH-L/LLDPE molded 7 and 60 rpm were used for compeering because they clearly show the separation as two-layered both 7 and 60 rpm of molding. The results are shown in Figure 4.23, At high-speed rotation, the internal heat rate increases rapidly during the first phase, as the particle contacts the mold surface in a short period of time, resulting in slower the heat transfer from the mold to particle and particle to particle,

and for this reason also make the high-speed rotation has higher the kink temperature point than the low-speed rotation.

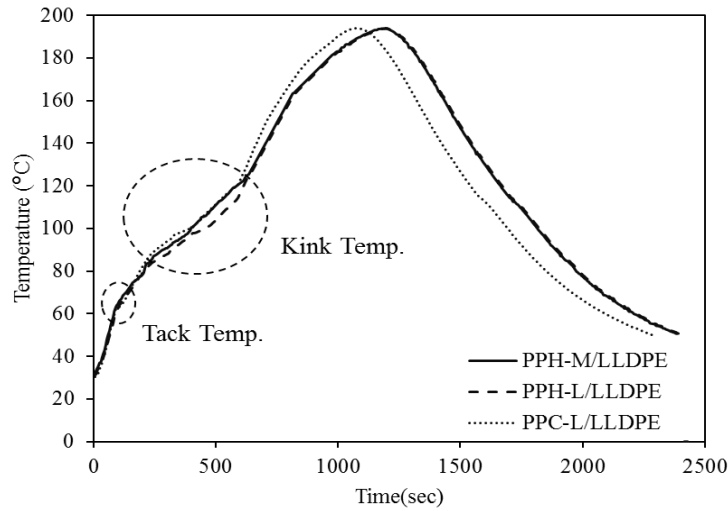


Figure 4.22 Internal air temperature of the mixed polymer at rotational speed 60 rpm.

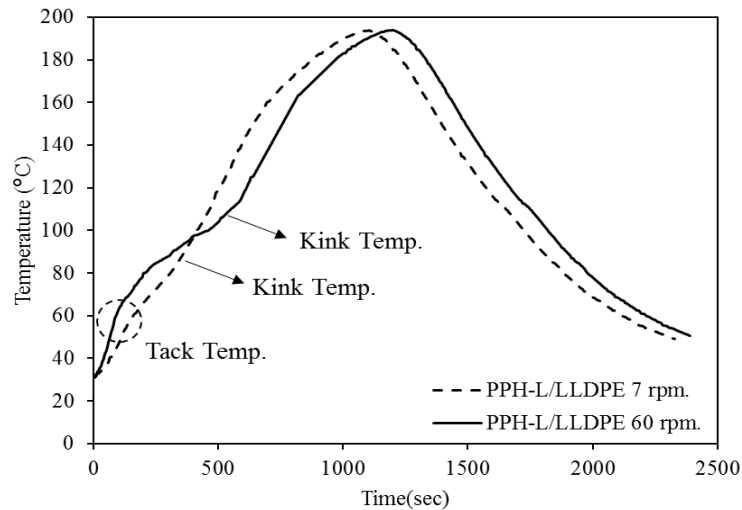


Figure 4.23 Internal air temperature of the mixed polymer at rotational speed 7 and 60 rpm.

4.3.2.5 The particles segregation and melt deposition of the PP/LLDPE with the different rotational speed.

As expected, when considering the influences of PP particle size for PPH-L/LLDPE and PPC-L/LLDPE found that in cases of PP size L had a proportion of LLDPE appeared at the edge and core area oversize M (as shown in Figure 4.24), as a result of the particle large size will have a larger gap and less

friction, making small particles move more easily. The high-speed rotation changes the pattern of the segregation or the radial segregation of the particle inside the mold, the small particles are floated in the air by centrifugal force (fluidized bed) and some will climb up on the top flow surface, instead of shrinking to the position of core (as shown in Figure 4.25). In addition, the increase in rotational speed often causes the granular materials to segregate into axial bands, which is sometimes found to be related to particle mobility. However, the phenomenon is quite complex and depends on many factors, making it difficult to understand deeply. At present, this topic is still of interest to many researchers.

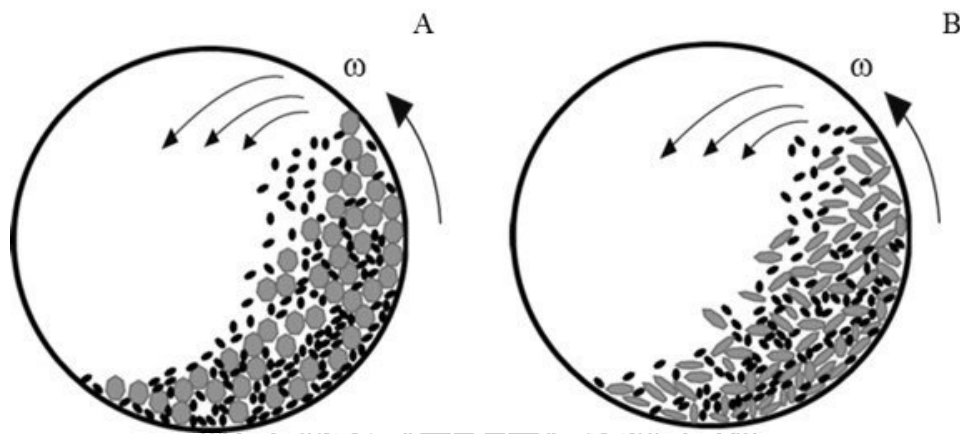


Figure 4.24 The flow characteristic; A is PP-L/LLDPE, B is PP-M /LLDPE and C is PP-S/LLDPE; where the white color is LLDPE particles.

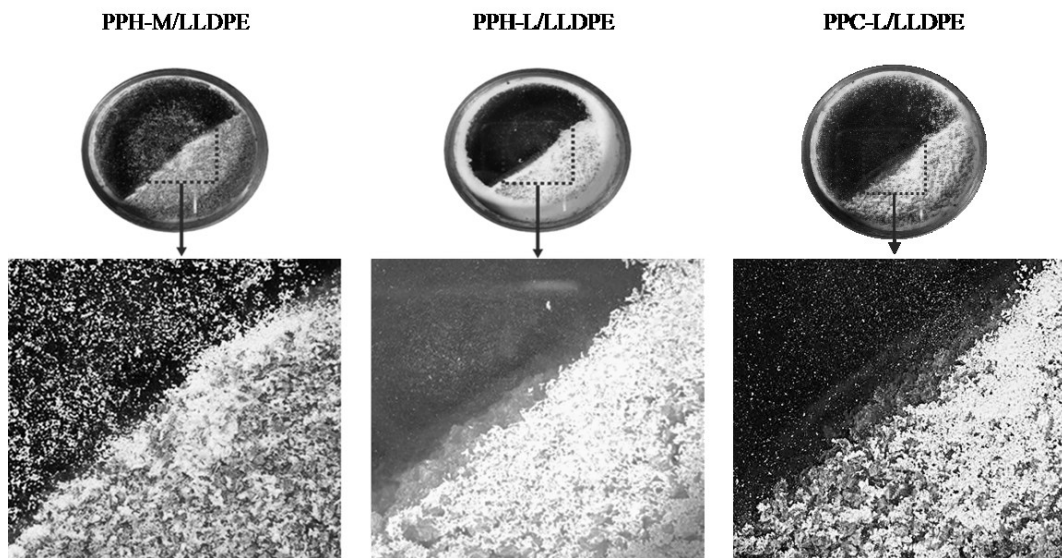
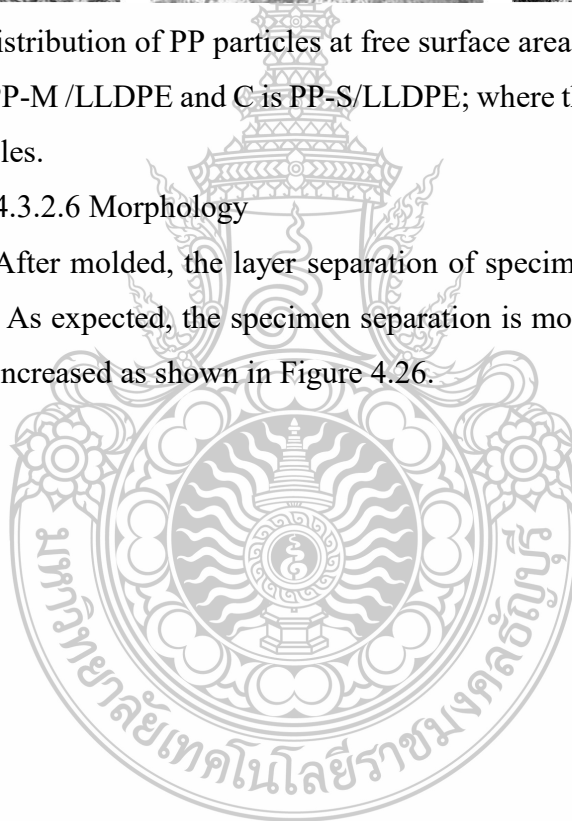


Figure 4.25 The distribution of PP particles at free surface area; A is PP-L/LLDPE, B is PP-M /LLDPE and C is PP-S/LLDPE; where the white color is LLDPE particles.

4.3.2.6 Morphology

After molded, the layer separation of specimens was investigated by digital microscope. As expected, the specimen separation is more pronounced when the rotational speed is increased as shown in Figure 4.26.



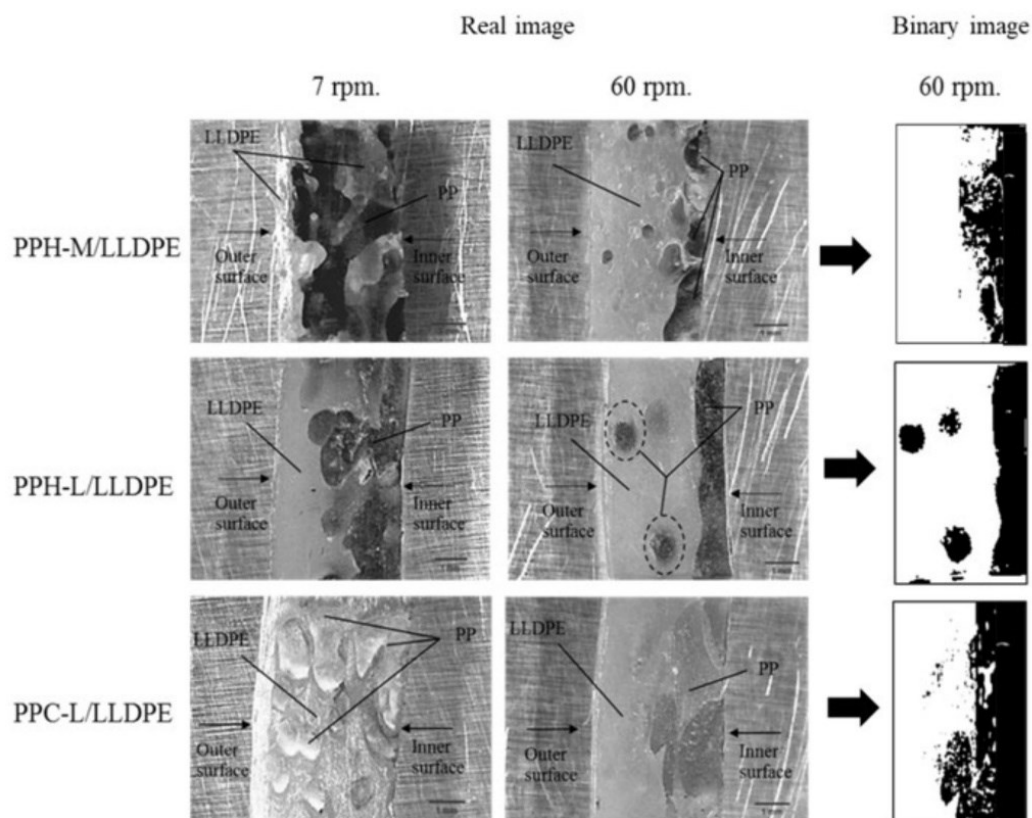


Figure 4.26 Separation phase in specimens of PPH-M/LLDPE, PPH-L/LLDPE, and PPC/LLDPE.

The LLDPE particles can overcome friction then percolation to the mold surface, resulting in quite clear layers separation. However, although it is possible to separate layers by increasing the rotational speed, the proportion of LLDPE and PP is not as the determination in 50-50 ratio. It seems to be the result of the granular materials segregate into axial bands especially evident in the case PPH-L/LLDPE and PPH-M/LLDPE. In addition, from the observation in the cases of PPH-L/LLDPE and PPH-M/LLDPE found that PP particles were not uniformly distributed in along with the axis, they have the high content at the head and the end of the specimens, while the case of PPC-L/LLDPE has a uniform proportion of PP along the axis which indicated that the particle distribute well.

4.3.2.7 Thermal properties

This test is intended to verify polymer compatibility and polymer distribution on the specimen surfaces. The specimen of the DSC test was cut from the cylindrical parts and separated as the inner, middle and outer surfaces as shown in Figure

4.8(A). The middle surface was used for investigation the compatibility of polymers. The result was shown in Figure 4.27, in the case of the mixed polymer shows double-peak, which means PP incompatible with LLDPE, where the first peak at a lower temperature is LLDPE, and the second peak at a higher temperature is PP. The polymers distribution on the specimen surfaces were shown in Figure 4.27 as well. All of the cases of PPH-L / LLDPE, PP-M/LLDPE, and PPC-L/LLDPE have double-peak of T_m both the inner and outer surfaces, means that PP and LLDPE the specimen has separation as two-layered, PP distributes to the inner surface and LLDPE distributes to the outer surface, which observing from the temperatures peak appearance on the inner and outer surfaces have similar to pure PP and pure LLDPE respectively.

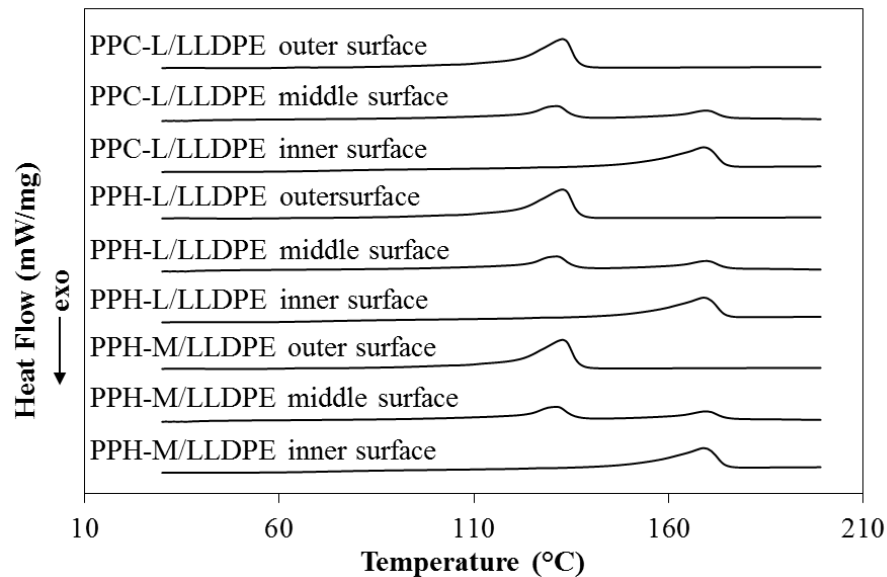


Figure 4.27 The DSC thermograms of a mixed polymer at rotational speed 60 rpm.

4.3.2.8 Surface roughness

The analysis method is based on the topic 4.1.2.8, the arithmetic mean surface roughness showed in Table 4.8. Considering the influence of the rotational speed found that the surface specimen was smoothed by increasing the rotational speed (as shown in Figure 4.28). As a result of the high rotational speed make shear increases resulting in the particles faster sintering and homogenization. However, the smoothness of the surface specimen depends on many variables such as elasticity, flow rate, heating time etc. Form this work in the case of different

materials, it has been shown that not only the above-described parameters but the particle separation characteristics also have affected the smoothness of the surface specimen.

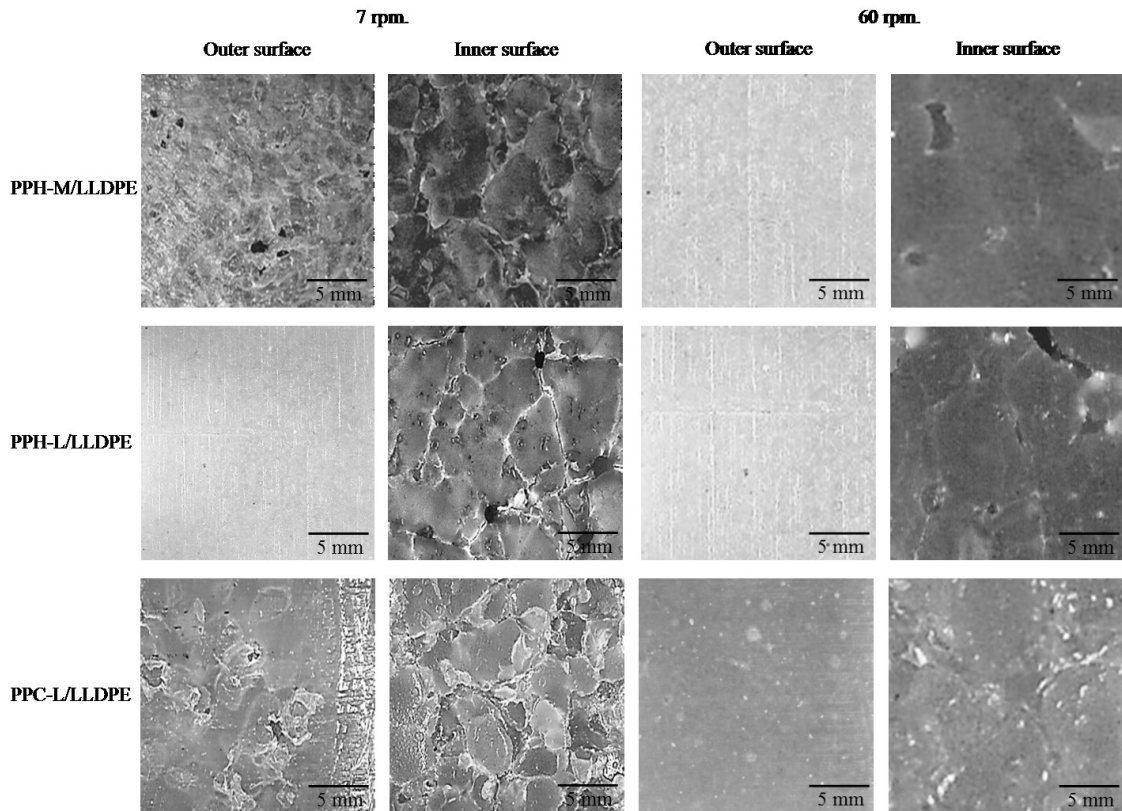


Figure 4.28 Surface roughness with different rotational speed.

Table 4.8 Arithmetic mean of surface roughness of specimen at rotational speed 60 rpm.

Materials	Arithmetic mean surface roughness, Ra (micron)			
	Rotational speed 7 rpm.		Rotational speed 60 rpm.	
	Inner surface	Outer surface	Inner surface	Outer surface
PPH-M/LLDPE	19.45	16.80	13.15	5.22
PPH-L/LLDPE	23.78	11.90	14.71	6.49
PPC-L/LLDPE	25.96	13.94	19.61	7.10

4.3.2.9 The wall thickness distribution

The results are shown in Figure 4.29, it is a graph comparing the standard deviation of wall thickness at different rotational speeds of 7 and 60 rpm. It was found that the standard deviation of wall thickness distribution increases with increasing the rotational speed, except the case of PPC-L/LLDPE with decreasing. These results demonstrate the behavior of the particle segregation along the axis with the specific characterized. Most of these behaviors often involve several factors, such as particle size, shape, size distribution, density, friction, including the appearance of the mold etc.

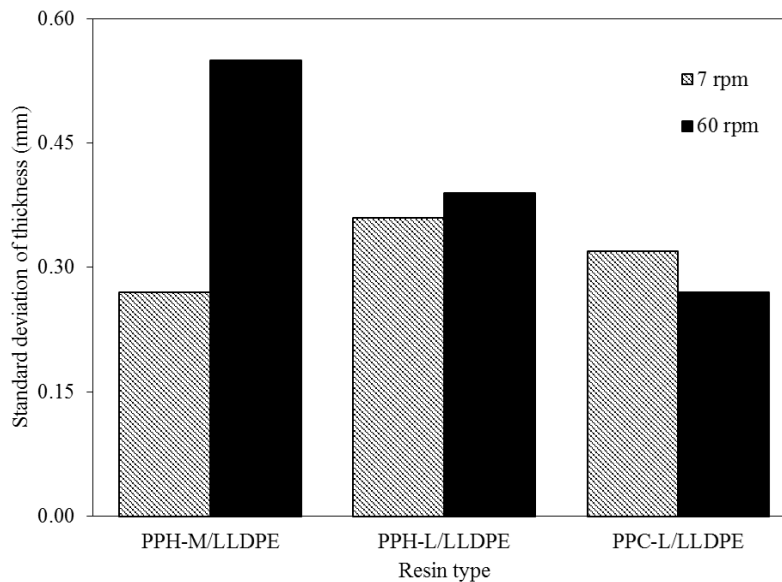


Figure 4.29 The standard deviation of wall thickness at rotational speed 7 and 60 rpm.

4.3.2.10 Mechanical properties

The results of compressive modulus showed in Table 4.9 and the stress-strain curve also showed in Figure 4.30. It was found that the compressive modulus of PPH-M/LLDPE has highest followed by PPH-L/LLDPE and PPC-L/LLDPE at about 13.77, 11.94 and 5.13 respectively. The stress-strain curve showed that the case of PPC-L/LLDPE shows the behavior deformation as a type of ductile materials and not fractured during testing, whereas both PPH-L/LLDPE and PPH-M/LLDPE shows combination of the behavior deformation between brittle and ductile materials, occurrence the micro-cracking during testing, the

specimen shows brittle behavior in the first period and shows the ductile behavior in the last period of testing. The variables that affect the compressive strength of the two-layered specimen include; the relationship of the wall thickness distribution of the specimens along the axis, the smoothness both inner and outer surfaces and the proportion of layer thickness in each polymer, the relationship of these phenomena often related the particle motion. At comparison the different of rotational speed found that the initial modulus both PPH-M/LLDPE and PPC-L/LLDPE increases with increasing rotational speed, this seem to be the result of the separation as two-layered of the specimen at the high-speed rotation, whereas in case of PPH-L/LLDPE decreases with increasing rotational speed, which seem to be the result of the proportion layer thickness of PPH as inner layer in case of high-speed rotation has less than the low-speed rotation. When considering the failure characteristics of the specimen from the stress-strain curve with different the rotational speed as shown in Figure 4.31 found that in the case of PPC-L / LLDPE shows the failure characteristics similar to the low-speed rotation. While in the case of both PPH-L/LLDPE and PPH-M/LLDPE shows the failure characteristics different from the low-speed rotation. At the high-speed rotation, PPH both size L and M as forming inner layer has a lower proportion than it should be, causing an immediately micro-cracking at the inner surface. In the other hand, the gradually micro-cracking happened in case of the low-speed rotation, which this propagation of the micro-cracking makes the compressive strength decrease. In addition, from the observation positions proceeding of the micro-cracking that appeared in both PPH-M/LLDPE and PPH-L/LLDPE specimen at the high-speed rotation, the first crack starting from the part that touch with lower plate followed by the part that touch with upper plate of the test machine, after that the part in the perpendicular with the direction of compressive force will be cracking respectively as shown in Figure 4.30, this reason showed that why the graph shows failure characteristics more than one times.

Table 4.9 The initial modulus at rotational speed 7 and 60 rpm.

Materials	Compressive Modulus (MPa)	
	Rotational speed 7 rpm	Rotational speed 60 rpm
PPH-M/LLDPE	8.43 ±1.75	13.77 ±1.36
PPH-L/LLDPE	14.81 ±1.72	11.94 ±1.22
PPC-L/LLDPE	3.43 ±0.75	5.13 ±1.42

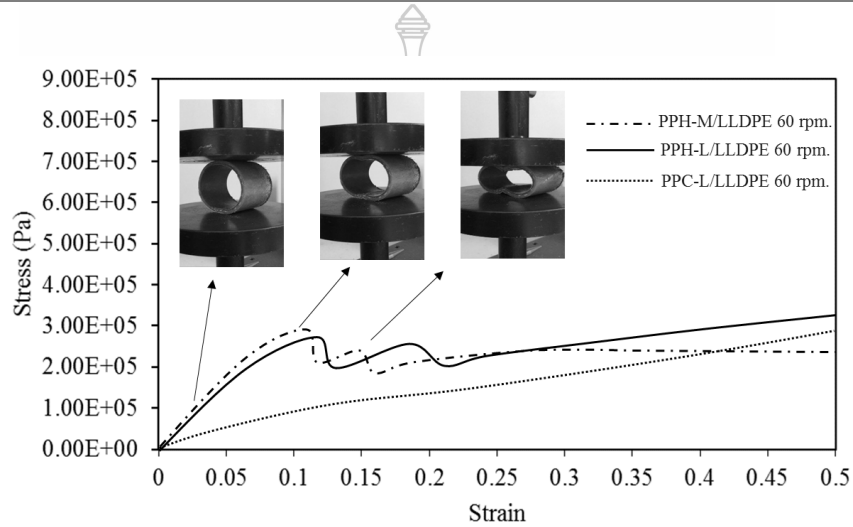


Figure 4.30 The stress-strain curve of the mixed polymer at rotational speed 60 rpm.

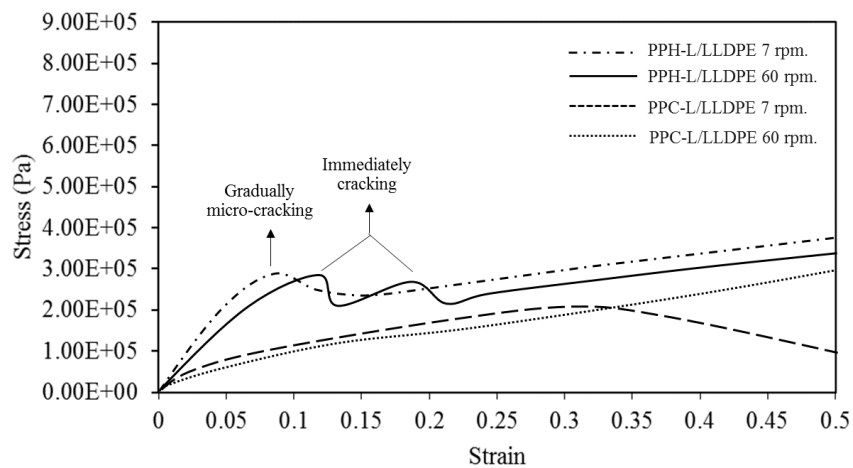


Figure 4.31 The stress-strain curve with different rotational speed.

CHAPTER 5

CONCLUSIONS AND RECOMMENDATION

5.1 The Effect of Particles Size of Polypropylene on PP/PE Two-Layered Process

In this study, to examine the effect of the particle size of PP on PP/LLDPE two-layered by one step rotation molding process. The results indicated that there is the separation as two-layered in the case of PP-L/LLDPE clearly. The different sizes of PP directly affect the particle segregation pattern, the larger PP makes LLDPE particles move to the mold surface easier than the smaller PP, which results in LLDPE more likely to form as the outer layer completely. For the effect of the sintering rate of the particles on the two-layered molds, although it does not clearly show the impact, it shows the different surface quality of the specimen, a smaller PP has higher the sintering rate than the larger PP, causing the surface specimen tend to smoother and better average of wall thickness distribution. The compressive testing shows that PP-L/LLDPE with clearly the separation as two-layered and PP-S/LLDPE with a good mixing have the initial modulus increased by 57.89% and 113.22% respectively, while PP-M/LLDPE with unclearly the separation as two-layered and a poor mixing has the initial modulus decreased by 10.13% when compared to a pure LLDPE.

5.2 The Effect of Particles Shape of Polypropylene on PP/PE Two-Layered Process

The results of these experiments clearly show that the completion of the separation as two-layered of PP/LLDPE is defined by a shape of PP particles. PPH with a more rounded shape has a slower sintering and a good of particle segregation, causing a low the rate of melt formation makes PPH/LLDPE specimen separation as two-layered. In contrast, PPC with a flat shape has a faster sintering and a poor the particle segregation, causing the rate of melt formation is high resulting in PPC/LLDPE specimen non-separation as two-layered, and it also shows more the defects due to an incomplete melting of the particles. As a result, the initial modulus of PPC/LLDPE decreased by 63.43%, whereas PPH/LLDPE increased by 57.89% as compared to pure LLDPE.

5.3 The Effect of Rotation Speed on PP/PE Two-Layered Process

The experimental results show that the increasing speed of rotation at 60 rpm can make the specimens separated as the two-layered. The increase in rotation speed directly affects the particle segregation pattern, the rate of formation of the molten polymer. The small particle size of LLDPE being thrown and/or percolate to the mold surface. It makes a possible to form the outer wall clearly and it also makes the PP particles that residence next to LLDPE layer melts homogeneous more, resulting in smooth both inner and outer surfaces of the specimen. However, the increased rotational speed results in an unstable particle separation, which results in the wall thickness distribution along the axis and the proportion of polymers that formation as the inner and outer layer has the variance. Finally, in a term of initial modulus, it has increased with increasing speed of rotation, except for the case of PPH-L/LLDPE.

All of the experiments show that the key factors that contribute to layer separations and clarity in the separations of PP and LLDPE are the melting point and particle mobility, in the latter case, it directly relates to the size and shape of the different particles between PP and LLDPE. These factors affect the operations in the process, such as the melt deposition pattern, particle fusion, thickness distribution, and mechanical properties of the specimens.

5.4 Recommendations

This work has answered some questions about PP/LLDPE two-layered molding in a single axial rotational mold, such as the effect of particle size and shape, particle percolation and deposition pattern. These variables have a great influence on the evaluation of the feasibility or efficiency of molding. The preliminary processing condition or the processing window has been shown in table 5.1. In addition, when uses the two axial rotational machine for molding accord to the processing window in the preliminary, it was found that the results of molding show consistent with a single axis rotational machine. All of the results show that it would be useful and a guide for factories that want to mold two or more layered products without having to rely on special equipment.

5.3 Future Work

Although this research has succeeded in two-layered molding between PP/LLDPE, in terms of mechanical properties, specimens uniformity, and extent of separation are not satisfactory. Therefore, the improvement and development of such properties are interesting. In addition, other factors that have not yet been considered for two-layered molding such as heating rates, flow rates and mixing ratios, are equally interesting as well.



Table 5.1 Processing window

Particles shape of PP (A circularity of top and side views)	Particles size of PP (μm)	Particles shape of LLDPE (A circularity of top and side views)	Particles size of LLDPE (μm)	Rotational speed /set-up temperature	Surface roughness (μm)		Wall thickness distribution (SD)	Initial modulus (MPa)	Results
					Inner surface	Outer surface			
0.77, 0.72	1,421	0.64, 0.55	368	7 rpm./ 190°C	23.78	11.90	0.36	14.81 \pm 1.72	Two-layered
0.73, 0.56	1,471	0.64, 0.55	368	7 rpm./ 190°C	13.73	10.99	0.32	14.81 \pm 1.72	Blend
0.66, 0.66	758	0.64, 0.55	368	7 rpm./ 190°C	20.67	14.89	0.14	8.43 \pm 1.75	Blend
0.57, 0.37	356	0.64, 0.55	368	7 rpm./ 190°C	14.37	14.22	0.13	20.00 \pm 1.85	Blend
0.77, 0.72	1,421	0.64, 0.55	368	60 rpm./ 190°C	14.71	6.49	0.39	13.77 \pm 1.36	Two-layered
0.73, 0.56	1,471	0.64, 0.55	368	60 rpm./ 190°C	19.61	7.10	0.27	5.13 \pm 1.42	Two-layered
0.66, 0.66	758	0.64, 0.55	368	60 rpm./ 190°C	13.15	5.22	0.55	13.77 \pm 1.36	Two-layered

List of Bibliography

- [1] Iwakura, K., Ohta, Y., Chen, C., White, J. (1989). Experimental Investigation of Rotational Molding and the Characterization of Rotationally Molded Polyethylene-Parts. **International Polymer Processing**, 4(3), 163-171.
- [2] Crawford, R. J., Crawford, R. J., Throne, J. L. (2001). **Rotational molding technology**: William Andrew.
- [3] Kulikov, O., Homung, K., Wagner, M. (2009). Novel processing additives for rotational molding of polyethylene. **International Polymer Processing**, 24(5), 452-462.
- [4] Ramkumar, P., Kulkarni, D., Chaudhari, V. (2014). Parametric and mechanical characterization of linear low density polyethylene (LLDPE) using rotational moulding technology. **Sadhana**, 39(3), 625-635.
- [5] Kontopoulou, M., Bisaria, M., Vlachopoulos, J. (1997). An experimental study of rotational molding of polypropylene/polyethylene copolymers. **International Polymer Processing**, 12(2), 165-173.
- [6] Wang, W., Kontopoulou, M. (2004). Rotational molding of polypropylene/ultra-low-density ethylene- α -olefin copolymer blends. **Polymer Engineering & Science**, 44(9), 1662-1669.
- [7] Liu, S. J., Ching, H.Y. (2001). Rotational molding of two-layered polyethylene foams. **Advances in Polymer Technology**, 20(2), 108-115.
- [8] Löhner, M., Drummer, D. (2017). Characterization of layer built-up and inter-layer boundaries in rotational molding of multi-material parts in dependency of the filling strategy. **Journal of Polymer Engineering**, 37(4), 411-420.
- [9] Barhoumi, N., Lamnawar, K., Maazouz, A., Jaziri, M., Abdelhedi, R. (2008). Reactive rotational molding process of PP/PA6 bilayer systems: experimental investigations. **International Journal of Material Forming**, 1, 671-674.
- [10] Pop-Iliev, R., Rizvi, G. M., Park, C. B. (2003). The importance of timely polymer sintering while processing polypropylene foams in rotational molding. **Polymer engineering and science**, 43(1), 40.

List of Bibliography (Continued)

- [11] Greco, A., Maffezzoli, A. (2004). Powder-shape analysis and sintering behavior of high-density polyethylene powders for rotational molding. **Journal of applied polymer science**, *92(1)*, 449-460.
- [12] Olinek, J., Anand, C., Bellehumeur, C. (2005). Experimental study on the flow and deposition of powder particles in rotational molding. **Polymer Engineering & Science**, *45(1)*, 62-73.
- [13] Peter, H., Erwin, W., Karl, B. (1962). "A method of centrifugally molding cellular plastics": Google Patents.
- [14] Throne, J. L. (1996). "Thermoplastic Foams. Sherwood Technologies", Inc., Hinckley, Ohio: Sherwood Publishers.
- [15] Rielly, F. J., Nungesser, H. (1970). "Rotational molding method for forming multilayered articles": Google Patents.
- [16] Hosoda, K., Sugita, T., Hashimoto, M., Suzuki, N., Shiina, N., Kadowaki, Y. (1974). "Method for producing a composite foamed article": Google Patents.
- [17] Lammers, S. G. (1976). "Method of rotational molding": Google Patents.
- [18] Mori, H., Adachi, E., Noguchi, Y. (1976). "Method of producing composite foamed shaped articles from thermoplastic resins": Google Patents.
- [19] Joseph, S. (1961). "Plastic process": Google Patents.
- [20] Smit, T., de Bruin, W., (1996). **The Production of High Quality Powders for Rotational Molding by Professional Grinders**; Rotation, pp. 10-13, Spring.
- [21] Spence, A., Crawford, R. (1996). The effect of processing variables on the formation and removal of bubbles in rotationally molded products. **Polymer Engineering & Science**, *36(7)*, 993-1009.
- [22] Throne, J., Sohn, M. S. (1989). Structure-property considerations for rotationally molded polyethylenes. **Advances in Polymer Technology**, *9(3)*, 193-209.
- [23] Bellehumeur, C., Tiang, J. (2002). Simulation of non-isothermal melt densification of polyethylene in rotational molding. **Polymer Engineering & Science**, *42(1)*, 215-229.
- [24] Rao, M. A., Throne, J. L. (1972). Principles of rotational molding. **Polymer Engineering & Science**, *12(4)*, 237-264.

List of Bibliography (Continued)

- [25] Mellmann, J. (2001). The transverse motion of solids in rotating cylinders—forms of motion and transition behavior. **Powder Technology**, *118(3)*, 251-270.
- [26] Henein, H., Brimacombe, J., Watkinson, A. (1983). The modeling of transverse solids motion in rotary kilns. **Metallurgical transactions B**, *14(2)*, 207-220.
- [27] Henein, H., Brimacombe, J., Watkinson, A. (1983). Experimental study of transverse bed motion in rotary kilns. **Metallurgical transactions B**, *14(2)*, 191-205.
- [28] Nguyen, H. T., Cosson, B., Lacrampe, M. F., Krawczak, P. (2015). Numerical simulation on the flow and heat transfer of polymer powder in rotational molding. **International Journal of Material Forming**, *8(3)*, 423-438.
- [29] Asgarpour, M., Bakir, F., Khelladi, S., Khavandi, A., Tcharkhtchi, A. (2012). 3D model for powder compact densification in rotational molding. **Polymer Engineering & Science**, *52(9)*, 2033-2040.
- [30] Guillén-Castellanos, S., Lin, W., Bellehumeur, C., Weber, M. (2003). Effect of processing history on the sintering of ethylene copolymers. **International Polymer Processing**, *18(1)*, 87-90.
- [31] Liu, F. (2001). "Processing of Polyethylene and Polypropylene Foams in Rotational Molding". University of Toronto.
- [32] Peacock, A. (2000). Handbook of polyethylene: "structures: properties, and applications": CRC Press.
- [33] Karger-Kocsis, J. (1994). "Polypropylene Structure, blends and composites: Volume 1 Structure and Morphology": Springer Netherlands.
- [34] Command USAM (1975). Engineering Design Handbook: "Rotational Molding of Plastic Powders", AMC; Virginia.
- [35] Bhandari, B. R., Bansal, N., Zhang, M., Schuck, P. (Eds.). (2013). "Handbook of food powders: Processes and properties". Elsevier.
- [36] Choudhury, A., Mukherjee, M., Adhikari, B. (2005). Thermal stability and degradation of the post-use reclaim milk pouches during multiple extrusion cycles. **Thermochimica acta**, *430(1)*, 87-94.

List of Bibliography (Continued)

- [37] Da Costa, H. M., Ramos, V. D., Rocha, M. C. (2005). Rheological properties of polypropylene during multiple extrusion. **Polymer Testing**, 24(1), 86-93.
- [38] Da Costa, H. M., Ramos, V. D., de Oliveira, M. G. (2007). Degradation of polypropylene (PP) during multiple extrusions: Thermal analysis, mechanical properties and analysis of variance. **Polymer Testing**, 26(5), 676-684.
- [39] Jin, H., Gonzalez-Gutierrez, J., Oblak, P., Zupančič, B., Emri, I. (2012) The effect of extensive mechanical recycling on the properties of low density polyethylene. **Polymer degradation and stability**, 97(11), 2262-2272.
- [40] Chaudhary, B. I., Takacs, E., Vlachopoulos, J. (2001). Processing enhancers for rotational molding of polyethylene. **Polymer Engineering & Science**, 41(10), 1731-1742.
- [41] Sharma, T., Mahanwar, P., Bambole, V. (2009). Study of modified polypropylene for rotational moulding applications. **International Journal of Plastics Technology**, 13(1), 83-94.
- [42] Sun, D. W., Crawford, R. J. (1993). Analysis of the effects of internal heating and cooling during the rotational molding of plastics. **Polymer Engineering & Science**, 33(3), 132-139.
- [43] Tcharkhtchi, A., Perrot, E., Chinesta, F. (2004). Simulation of thermal phenomena on the interface molten polymer/powder polymer during rotational molding. **International Polymer Processing**, 19(3), 296-302.
- [44] Qin, L., Ding, Y.-M., Zhu, G.-C., Yu, H.-C., Yang, W.-M. (2015). Heat Flow Analysis and Efficiency Optimization of Rotational Molding Equipment for Large Plastic Products. **International Polymer Processing**, 30(2), 194-201.
- [45] Banerjee, S., Yan, W., Bhattacharyya, D. (2008). Modeling of heat transfer in rotational molding. **Polymer Engineering & Science**, 48(11), 2188-2197.
- [46] Lim, K., Ianakiev, A. (2006). Modeling of rotational molding process: Multi-layer slip-flow model, phase-change, and warpage. **Polymer Engineering & Science**, 46(7), 960-969.

List of Bibliography (Continued)

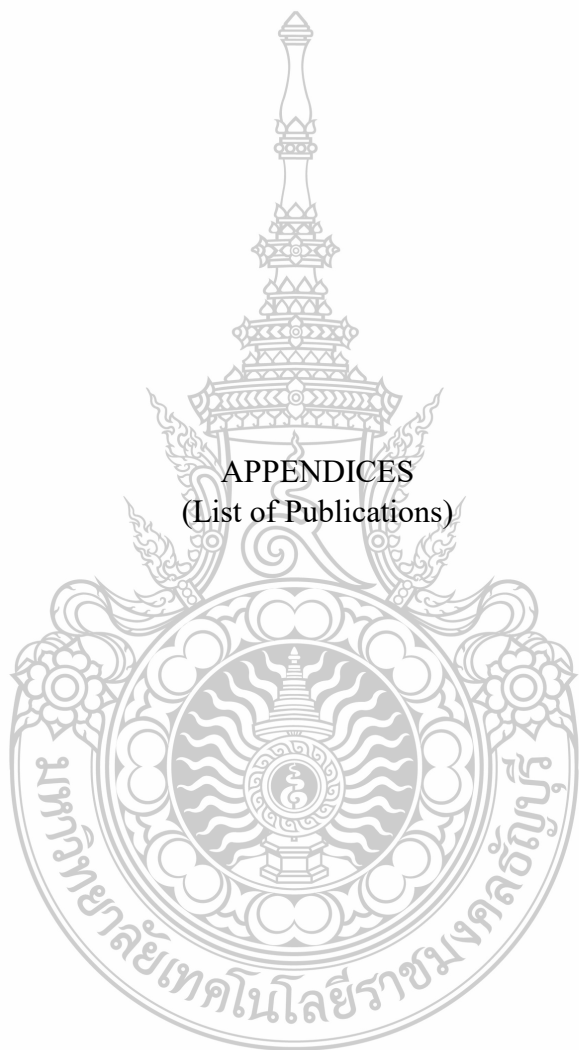
- [47] Furukawa, R., Shiosaka, Y., Kadota, K., Takagaki, K., Noguchi, T., Shimosaka, A., Shirakawa, Y. (2016). Size-induced segregation during pharmaceutical particle die filling assessed by response surface methodology using discrete element method. **Journal of Drug Delivery Science and Technology**, 35, 284-293.
- [48] Rosato, D. V., Schott, N. R., Rosato, M. G. (2001). *Plastics Institute of America "Plastics Engineering, Manufacturing & Data Handbook"*: Springer Science & Business Media.
- [49] Igathinathane, C., Pordesimo, L., Columbus, E., Batchelor, W., Methuku, S. (2008). Shape identification and particles size distribution from basic shape parameters using ImageJ. **Computers and electronics in agriculture**, 63(2), 168-182. Crawford EC, Mortensen JK. *Comput. Geosci.* 2009, 35, 347-359.
- [50] Crawford, E. C., Mortensen, J. K. (2009). An ImageJ plugin for the rapid morphological characterization of separated particles and an initial application to placer gold analysis. **Computers & Geosciences**, 35(2), 347-359.
- [51] Rodriguez, J., Edeskär, T., Knutsson, S. (2013). Particle shape quantities and measurement techniques: a review. **The Electronic journal of geotechnical engineering**, 18, 169-198.
- [52] Ortega-Rivas, E., Juliano, P., Yan, H. (2006). "Food powders: physical properties, processing, and functionality". Springer Science & Business Media.
- [53] Cumberland, D. J., & Crawford, R. J. (1987). "The packing of particles": Elsevier.
- [54] Aissa, A. A., Duchesne, C., Rodrigue, D. (2012). Characterization of polymer powder motion in a spherical mold in biaxial rotation. **Polymer Engineering & Science**, 52(5), 953-963.
- [55] Chinga, G., Gregersen, O., Dougherty, B. (2003). Paper surface characterisation by laser profilometry and image analysis. **Microscopy and Analysis**, 96, 21-24.
- [56] Jiang, H., Browning, R., Fincher, J., Gasbarro, A., Jones, S., Sue, H.-J. (2008). Influence of surface roughness and contact load on friction coefficient and scratch behavior of thermoplastic olefins. **Applied Surface Science**, 254(15), 4494-4499.

List of Bibliography (Continued)

- [57] Kontopoulou, M., Vlachopoulos, J. (1999). Bubble dissolution in molten polymers and its role in rotational molding. **Polymer Engineering & Science**, 39(7), 1189-1198.
- [58] Salih, S. E., Hamood, A. F., Alsalam, A. H. A. (2013). Comparison of the Characteristics of LDPE: PP and HDPE: PP Polymer Blends. **Modern Applied Science**, 7(3), 33.



APPENDICES
(List of Publications)



List of Publications

International Journal

Jansri, E. & O-Charoen, N. (2018). Polypropylene/polyethylene two-layered by one-step rotational molding. *Journal of Polymer Engineering*, 0(0), pp. -. Retrieved 27 Mar. 2018, from doi: 10.1515/polyeng-2017-0367
<https://doi.org/10.1515/polyeng-2017-0367>.

International Conferences

E. Jansri, N. O-Charoen and H. Hamada, “Polypropylene / Polyethylene hybrid in Rotational molding.” Proceeding, Oral presentation, Eco-Energy and Materials Science and Engineering Symposium (EMSES 2015), Krabi, Thailand, June 11-14, 2015.



Biography

Name – Surname Ektinai Jansri

Date of Birth 24 August 1989

Address 3/1 Moo. 2, Tambon Wanghin, Amphur Banrai, Uthaithani 61180

Education Bachelor's Degree in Textile Chemistry-Synthetic Fiber Engineering, Faculty of Engineering, Rajamangala University of Technology Thanyaburi (RMUTT)
Master of Engineering (Material Engineering) Faculty of Engineering, Rajamangala University of Technology Thanyaburi (RMUTT)
Doctor of Engineering Program in Energy and Materials Engineering (International Program), Faculty of Engineering, Rajamangala University of Technology Thanyaburi (RMUTT)

Experience Work Research Assistant, Department of Materials and Metallurgical Engineering, Faculty of Engineering, Rajamangala University of Technology Thanyaburi (RMUTT) 2012- Present.

Telephone Number 086-34-35824

Email Address Ektinai_j@mail.rmutt.ac.th

